KoG

No. 16. (2012)
ISSN 1331-1611

SCIENTIFIC-PROFESSIONAL JOURNAL OF CROATIAN SOCIETY
FOR GEOMETRY AND GRAPHICS

Official publication of the Croatian Society for Geometry and Graphics publishes scientific and professional papers from the fields of geometry, applied geometry and computer graphics.

Founder and Publisher

Croatian Society for Geometry and Graphics

Design

Miroslav Ambruš-Kiš

Layout

Sonja Gorjanc, Ema Jurkin

Cover

HDGG on Lubenice beach ("written" by *Miklós Hoffmann*), photo *Georg Glaeser*

Print

"O-TISAK", d.o.o., Zagreb

URL address

http://www.hdgg.hr/kog
http://hrcak.srce.hr

Edition

250

Published annually

Guide for authors
Please, see the last page

KoG is cited in: Mathematical Reviews, MathSciNet, Zentralblatt für Mathematik

---

This issue has been financially supported by The Ministry of Science, Education and Sport of the Republic of Croatia.

ISSN 1331–1611

KoG

No. 16
Zagreb, 2012

SCIENTIFIC AND PROFESSIONAL JOURNAL OF
CROATIAN SOCIETY FOR GEOMETRY AND GRAPHICS

CONTENTS

ORIGINAL SCIENTIFIC PAPERS

PROFESSIONAL PAPERS

ISSN 1331–1611

KoG

BROJ 16
Zagreb, 2012

ZNANSTVENO-STRUČNI ČASOPIS
HRVATSKOG DRUŠTVA ZA GEOMETRIJU I GRAFIKU

SADRŽAJ

ORIGINALNI ZNANSTVENI RADOVI

STRUČNI RADOVI

Original scientific paper
Accepted 28. 9. 2012.

TEMEL ERMIŞ
ÖZCAN GELIŞGEN
RUSTEM KAYA

On Taxicab Incircle and Circumcircle of a Triangle

On Taxicab Incircle and Circumcircle of a Triangle

ABSTRACT

In this work, we study existence of taxicab incircle and circumcircle of a triangle in the taxicab plane and give the functional relationship between them in terms of slope of sides of the triangle. Finally, we show that the point of intersection of taxicab inside angle bisectors of a triangle is the center of taxicab incircle of the triangle.

Key words: taxicab distance, taxicab circle, taxicab incircle, taxicab circumcircle, taxicab plane and taxicab geometry

MSC 2010: 51K05, 51K99, 51N20

O taxicab upisanoj i opisanoj kružnici trokuta

SAŽETAK

U ovom radu promatramo postojanje taxicab upisane i opisane kružnice trokuta u taxicab ravnini i dajemo njihov odnos s obzirom na koeficijente smjera stranica trokuta. Naposljetku, pokazujemo da je sjecište taxicab unutarnjih simetrala kuta trokuta središte njegove taxicab upisane kružnice.

Ključne riječi: taxicab udaljenost, taxicab kružnica, taxicab upisana kružnica, taxicab opisana kružnica, taxicab ravnina and taxicab geometrija

1 Introduction

Taxicab plane geometry introduced by Menger and developed by Krause using the metric $d_T(P,Q) = |x_1 - x_2| + |y_1 - y_2|$ instead of the well-known Euclidean metric $d_E(P,Q) = \left((x_1 - x_2)^2 + (y_1 - y_2)^2\right)^{1/2}$ for the distance between any two points $P = (x_1, y_1)$, $Q = (x_2, y_2)$ in the analytical plane $\mathbb{R}^2$. According to definition of taxicab distance function, the path between two points in the plane is union of two line segments which each of line segments is parallel to one of coordinate axis. Thus, taxicab distance is the sum of Euclidean lengths of these two line segments. Taxicab geometry have studied and developed in different aspects by mathematicians. One can see for some of these in [2], [3], [5], [6], [7], [9]. The linear structure of the taxicab plane is almost the same as Euclidean plane. There is one different aspect. Euclidean and taxicab planes have different distance functions. So it seems interesting to study the taxicab analogues of topics that are related with the concept of distance.

It is well known that there exist a unique incircle and a unique circumcircle for a given triangle in the Euclidean geometry. Also the distance d between the centers of incircle and circumcircle of a triangle is $d = \sqrt{R(R-2r)}$ where r and R are radii of incircle and of circumcircle, respectively. Here, we study and extend these three properties to the taxicab plane.

2 Taxicab incircles and circumcircles of a given triangle

The **incircle** of a triangle is the circle contained in the triangle and touches to (*is tangent to*) each of the three sides at one point. A circle passing through all three vertices of a triangle is called **circumcircle** of the triangle.

Let C be a point in the taxicab plane, and r be a positive real number. The set of points $\{X : d_T(C,X) = r\}$ is called **taxicab circle**, the point C is called *center of the taxicab circle*, and r is called the *length of the radius* or simply *radius* of the taxicab circle. Every taxicab circle in the taxi-

cab plane is an Euclidean square having sides with slopes ± 1.

Let l be a line with slope m in the taxicab plane. l is called a **gradual line**, a **steep line,** a **separator** if $|m|<1$, $|m|>1$, $|m|=1$, respectively (see Figure 1). In particularly, a gradual line is called **horizontal** if it is parallel to x-axis, and a steep line is called **vertical** if it is parallel to y-axis.

The isometry group of taxicab plane is the semi direct product of $D(4)$ and $T(2)$ where $D(4)$ is the symmetry group of Euclidean square and $T(2)$ is the group of all translations in the plane. That is, the rotations $\theta = k\pi/2$, $k \in \mathbb{Z}$, the reflections by lines with horizontal, vertical and separators and all translations are isometries in the taxicab plane (see [5], [8]).

The distance from the point $P=(x_0,y_0)$ to a line l with the equation
$ax+by+c=0$ is $d_T(P,l)=|ax_0+by_0+c| \diagup \max\{|a|,|b|\}$ (see [6]).

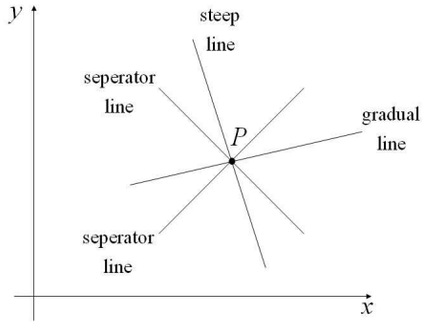

Figure 1

In the taxicab plane, the triangles can be classified as eight groups according to slopes of the sides of triangles:

i) All sides of the triangle lie on gradual (*steep*) lines.

ii) Two sides of the triangle lie on gradual (*steep*) lines, the other side lies on a steep (*gradual*) line.

iii) Two sides of the triangle lie on separator lines, the other side lies on a gradual (*steep*) or a horizontal (*vertical*) line.

iv) A side of the triangle lies on a separator line, two sides of the triangle lie on gradual (*steep*) lines.

v) A side of the triangle lies on a separator line, the other side lies on a gradual line and the third side lies on a steep line.

vi) A side of the triangle lies on a vertical line, the other side lies on a horizontal line and third side lies on a gradual (*steep*) line or separator line.

vii) A side of the triangle lies on a vertical (*horizontal*) line, two sides of the triangle lie on gradual (*steep*) lines.

viii) A side of the triangle lies on a vertical (*horizontal*) line, the other side lies on a gradual line and the third side lies on a steep line.

The next theorem gives an explanation about whether there exist an incircle and a circumcircle of a triangle or not.

Theorem 1 *A triangle has a taxicab circumcircle and incircle if and only if two sides of the triangle lie on gradual (steep) lines and remaining side lies on a steep (gradual) line.*

Proof. Let $\overset{\triangle}{ABC}$ be a triangle having a taxicab circumcircle and a taxicab incircle and let m_a, m_b and m_c denote the slopes of lines BC, AC and AB, respectively. A taxicab circumcircle compose of the line segments which are on lines with slopes ∓ 1, passing through the vertices of a triangle. That is, there is a line with slope 1 or -1 passing through every vertex of the triangle, and the triangle is completely inside the taxicab circumcircle. Every vertex of a triangle is a point intersection of two sides of this triangle. Since three vertices of the triangle are on different sides of the taxicab circle, vertices of two sides of the triangle are on neighbour sides of the taxicab circle. So two vertices of the triangle are on lines with same slope 1, and the third vertex is on a line with slope -1 or vice versa.

Suppose that vertices A, B, C of triangle are on lines with slopes -1, $+1$, -1, respectively. Thus $m_a<1$ and $m_a>-1$. That is, $|m_a|<1$.Similarly one can obtain $m_c<1$ and $m_c>-1$. That is, $|m_c|>1$. Third side AC is on a gradual or a steep line. Other cases can be proven similarly.

Since the triangle ABC has a taxicab incircle, three vertices of the circle are on sides of the triangle. Three vertices of the incircle are on lines slopes ∓ 1 and 0 or ∞. So there are two different cases (see Figure 2).

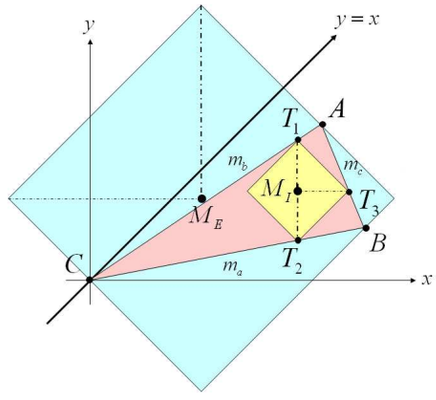

Figure 2

Case I: Let the vertices of the incircle be on lines with slopes -1, 1 and ∞. And let T_1, T_2, T_3 denote these points

such that T_1, T_2 and T_3 are on sides AC, BC and AB, respectively. If T_1 and T_2 are on a vertical line, then $|m_a| < 1$ and $|m_b| < 1$. Otherwise, a part of the sides of the incircle lie outside of the triangle. Also $|m_c| > 1$ since incircle must be inside the triangle.

Case II: Let the vertices of the incircle be on lines with slopes -1, 1 and 0. This case is proven similarly as case I.

Conversely, let two sides of the triangle be on gradual lines and other side be on a steep line. We may draw the lines of slopes 1 and -1 passing through vertices of the triangle. By the definition of the circumcircle, these lines must not pass through inner region of the triangle. Thus we may construct three sides of a taxicab circumcircle encircled the triangle. The fourth side of the taxicab circumcircle properly can be found.

Since three vertices of incircle of the triangle are on each sides of the triangle, we may construct incircle alike circumcircle case. □

In the rest of the article, we assume that the vertex C of a triangle $\overset{\triangle}{ABC}$ is the intersection point of gradual (*steep*) sides of the triangle. Without lose of generality, a vertex of the triangle can be taken at origin since all translations of the analytical plane are isometries of the taxicab plane. So we take the vertex C is at origin. Notice that this assumption about the position of the triangle does not loose the generality. If the role of vertices A and B of the triangle replace with each other, then the slopes m_a and m_b must be replaced with each other in all functional relations through the article.

The following theorem gives a relation between diameters of the circumcircle and incircle and the slopes of sides of a triangle in the taxicab plane.

Theorem 2 *Let slopes of sides AB, BC, CA of a triangle $\overset{\triangle}{ABC}$ be m_c, m_a and m_b, respectively and a, b, c be the taxicab lengths of sides of BC, CA, AB of the triangle $\overset{\triangle}{ABC}$. If the triangle has a taxicab incircle with radius $\mathbf{r}$ and a circumcircle with radius $\mathbf{R}$ then*

$$\frac{\mathbf{r}}{2\mathbf{R}} = \begin{cases} \rho(m_a, m_b, m_c), & |m_a|<1,\ |m_b|<1 \text{ and } |m_c|>1 \\ \rho\left(-m_a^{-1}, -m_b^{-1}, -m_c^{-1}\right), & |m_a|>1,\ |m_b|>1 \text{ and } |m_c|<1 \end{cases}$$

where $\rho(m_a, m_b, m_c) =$

$$\frac{|m_b - m_a|\,|\delta(m_a, m_b) - m_c|}{\max\{|1+\delta(m_a,m_b)|, |1-\delta(m_a,m_b)|\}\,|\max\{m_a,m_b\}(1-m_c) + \min\{m_a,m_b\}(1+m_c) - 2m_c|}$$

with

$$\delta(m_a, m_b) = \begin{cases} m_a, & a > b \\ m_b, & a < b \end{cases}.$$

Proof. Let $\overset{\triangle}{ABC}$ be a triangle such that $|m_a| < 1$, $|m_b| < 1$ and $|m_c| > 1$ where m_a, m_b and m_c are slopes of sides BC, AC and AB, respectively (see Figure 2). There are two main positions of gradual sides of the triangle:

i) Gradual sides are on same quadrant of the plane (see Figure 2)

ii) Gradual sides are on neighbour quadrants of the plane (see Figure 3).

Suppose that $A=(x_a, y_a), B=(x_b, y_b)$ are points such that $x_b > x_a > 0$ and $y_a > y_b > 0$ (see Figure 2). Therefore, center and radius of the taxicab circumcircle of triangle $\overset{\triangle}{ABC}$ are

$M_E = \left(\frac{x_b - y_b}{2}, \frac{x_a - x_b + y_a + y_b}{2}\right)$ and

$\mathbf{R} = \frac{x_a + y_a}{2} = \frac{x_a(1+m_b)}{2}$.

Three vertices of the taxicab incircle are on lines $\overleftrightarrow{AB}$, $\overleftrightarrow{BC}$ and $\overleftrightarrow{AC}$ with the equations $y = m_c(x - x_a) + y_a$, $y = m_a x$ and $y = m_b x$, respectively. Let T_1 and T_2 be on lines $\overleftrightarrow{AC}$ and $\overleftrightarrow{BC}$, respectively. So $T_1 = (t, m_b t)$ and $T_2 = (t, m_a t)$ for $t \in \mathbb{R}^+$. Thus center and radius of the taxicab incircle of the triangle $\overset{\triangle}{ABC}$ are

$$M_I = \left(t, m_a t + \frac{(m_b - m_a)t}{2}\right) \text{ and } \mathbf{r} = \frac{(m_b - m_a)t}{2}.$$

Since $T_3 = \left(t + \frac{(m_b - m_a)t}{2}, m_a t + \frac{(m_b - m_a)t}{2}\right)$ and T_3 is on the line with the equation $y = m_c(x - x_a) + y_a$, one can easily compute that

$t = \frac{2x_a(m_b - m_c)}{m_a + m_b - 2m_c + m_c(m_a - m_b)}$. Thus the relation between $\mathbf{R}$ and $\mathbf{r}$ is

$$\mathbf{r} = \frac{2\mathbf{R}(m_b - m_c)(m_b - m_a)}{(1+m_b)[m_a(1+m_c) + m_b(1-m_c) - 2m_c]}$$

Similarly, let $\overset{\triangle}{ABC}$ be a triangle such that $|m_a| < 1, |m_b| < 1$ and $|m_c| > 1$ (see Figure 3a).

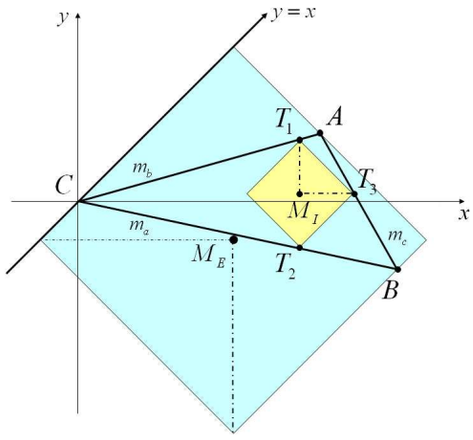

a

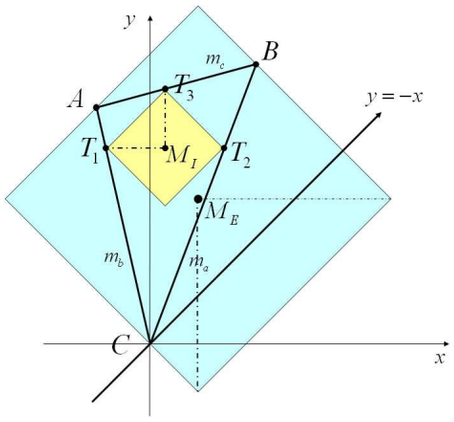

b

Figure 3

Suppose that $A=(x_a,y_a)$, $B=(x_b,y_b)$ are two points such that $x_b > x_a > 0$ and $y_a > 0 > y_b$ (see Figure 3a). Then, center and radius of the taxicab circumcircle of the triangle $\overset{\triangle}{ABC}$ are

$$M_E = \left(\frac{x_a+y_a}{2}, \frac{x_a-x_b+y_a+y_b}{2}\right)$$

and

$$\mathbf{R} = \frac{x_b-y_b}{2} = \frac{x_b(1-m_a)}{2}.$$

Three vertices of the taxicab incircle are on lines $\overleftrightarrow{AB}$, $\overleftrightarrow{BC}$ and $\overleftrightarrow{AC}$ with the equations $y=m_c(x-x_a)+y_a$, $y=m_ax$ and $y=m_bx$, respectively. Let T_1 and T_2 be on lines $\overleftrightarrow{AC}$ and $\overleftrightarrow{BC}$, respectively. So $T_1=(t,m_bt)$ and $T_2=(t,m_at)$ for $t\in\mathbb{R}^+$. Thus the center and the radius of the taxicab incircle of the triangle $\overset{\triangle}{ABC}$ are

$$M_I = \left(t, \frac{(m_a+m_b)t}{2}\right) \text{ and } \mathbf{r} = \frac{(m_b-m_a)t}{2}.$$

Since $T_3 = \left(t+\frac{(m_b-m_a)t}{2}, m_bt-\frac{(m_b-m_a)t}{2}\right)$ and point T_3 is on the line with the equation $y=m_c(x-x_b)+y_b$, one can easily compute that $t=\frac{2x_b(m_a-m_c)}{m_a+m_b-2m_c-m_c(-m_a+m_b)}$. Thus the relation between $\mathbf{R}$ and $\mathbf{r}$ is

$$\mathbf{r} = \frac{2\mathbf{R}(m_a-m_c)(m_b-m_a)}{(1-m_a)[m_a(1+m_c)+m_b(1-m_c)-2m_c]}. \qquad (2.1)$$

Notice that if the triangle $\overset{\triangle}{ABC}$ located as in Figure 3a is rotated with $\frac{\pi}{2}$ about the origin, then the triangle will be in the position in Figure 3b. In this case, the relation between $\mathbf{R}$ and $\mathbf{r}$ is

$$\mathbf{r} = \frac{2\mathbf{R}(m_a-m_c)(m_b-m_a)}{(1+m_a)[-m_a(1+m_c)+m_b(1-m_c)+2m_am_b]}. \qquad (2.2)$$

In fact, if m_a, m_b and m_c are replaced with $-m_a^{-1}$, $-m_b^{-1}$ and $-m_c^{-1}$, respectively, in equation (2.1), then we have relation (2.2). By this result, the rotation with $\frac{\pi}{2}$ is an isometry of the taxicab plane. Also the triangle $\overset{\triangle}{ABC}$ such that $|m_a|<1$, $|m_b|<1$ and $|m_c|>1$ is mapped to the triangle $\overset{\triangle}{ABC}$ with $|m_a|>1$, $|m_b|>1$ and $|m_c|<1$ under the rotation with $\frac{\pi}{2}$. Thus, one can find the relations about all positions of the triangle $\overset{\triangle}{ABC}$ if m_a, m_b and m_c are replaced with $-m_a^{-1}, -m_b^{-1}$ and $-m_c^{-1}$ in the relations for the triangles with $|m_a|<1$, $|m_b|<1$ and $|m_c|>1$. So the relations about all positions of the triangle can be easily generalized. □

The next theorem gives a relation about distance between centers of the incircle and circumcircle of the triangle in terms of $\mathbf{R}$, $\mathbf{r}$ and slopes of sides of the triangle.

Theorem 3 *Let slopes of sides AB, BC, CA of a triangle* $\overset{\triangle}{ABC}$ *be* m_c, m_a, m_b, *respectively. Let* M_I *and* M_E *be centers of the taxicab incircle with radius* $\mathbf{r}$ *and taxicab circumcircle with radius* $\mathbf{R}$ *of the triangle, respectively. Then*

$$d_T(M_I,M_E) = \begin{cases} \psi(m_a,m_b,m_c), & |m_a|<1,\ |m_b|<1,\ |m_c|>1 \\ \psi(-m_a^{-1},-m_b^{-1},-m_c^{-1}), & |m_a|>1,\ |m_b|>1,\ |m_c|<1 \end{cases}$$

where

$$\psi(m_a,m_b,m_c) = \min\left\{ \left| \frac{m_a+m_b-2sgn(m_c)}{(m_b-m_a)}\mathbf{r}-\mathbf{R} \right|, \right.$$

$$\left. \left| \frac{m_a+m_b-2sgn(m_c)}{(m_b-m_a)}\mathbf{r}-\left(1-\frac{2[(1-m_a)sgn(m_c)][m_b-m_c]}{[(1-m_b)sgn(m_c)][m_b-m_a]}\right)\mathbf{R} \right| \right\}.$$

Proof. Suppose that $\overset{\triangle}{ABC}$ is a triangle with vertices $A=(x_a,y_a)$, $B=(x_b,y_b)$ and $C=(0,0)$ such that $x_b > x_a > 0$ and $y_a > y_b$. If the triangle $\overset{\triangle}{ABC}$ has a taxicab circumcircle and incircle, then the two sides of the triangle are on gradual (*steep*) lines and third side is on a steep (*gradual*) line by Theorem 1 Therefore, there are two possible cases:

Case I : If $|m_c|>1$, $|m_a|<1$ and $|m_b|<1$, respectively (see Figure 2), then center and radius of the taxicab circumcircle of the triangle $\overset{\triangle}{ABC}$ are $M_E=\left(\frac{x_b-y_b}{2},\frac{x_a-x_b+y_a+y_b}{2}\right)$ and $\mathbf{R}=\frac{x_a+y_a}{2}$,respectively. Let vertices of the taxicab incircle on sides CA and CB be $T_1=(t,m_bt)$ and $T_2=(t,m_at)$ for $t\in\mathbb{R}^+$, respectively. Thus center and radius of the taxicab incircle of the triangle $\overset{\triangle}{ABC}$ are $M_I=\left(t,m_at+\frac{(m_b-m_a)t}{2}\right)$ and $\mathbf{r}=\frac{(m_b-m_a)t}{2}$, where $t=\frac{2x_a(m_b-m_c)}{m_a+m_b-2m_c+m_c(m_a-m_b)}$. Thus distance between centers of the taxicab incircle and circumcircle of the triangle $\overset{\triangle}{ABC}$ is

$$\begin{aligned} d &= d_T(M_E,M_I)\\ &= \left|t-\frac{x_b-y_b}{2}\right|+\left|m_at+\frac{(m_b-m_a)t}{2}-\frac{x_a-x_b+y_a+y_b}{2}\right|\\ &= \left|\frac{2}{m_b-m_a}\mathbf{r}-\frac{(1-m_a)(m_b-m_c)}{(1+m_b)(m_c-m_a)}\mathbf{R}\right|\\ &\quad+\left|\frac{m_a+m_b}{m_b-m_a}\mathbf{r}-\mathbf{R}+\frac{(1-m_a)(m_b-m_c)}{(1+m_b)(m_c-m_a)}\mathbf{R}\right| \end{aligned}$$

Similarly the relations about all positions of the triangle can be easily generalized. □

In Euclidean geometry it is well known that intersection point of inside angle bisectors of a triangle is the center of incircle of the triangle. Each point of an angle bisector is equidistant from the sides of the angle. Since taxicab distance is different from Euclidean distance, taxicab bisector of a angle is different from Euclidean bisector of the angle. Thus the intersection point of taxicab inside angle bisectors of a triangle is, generally different from the Euclidean case. The following theorem expresses that the above property is also valid in the taxicab plane.

Theorem 4 *The intersection point of the taxicab inside angle bisectors of a triangle with a taxicab incircle is the center of taxicab incircle of the triangle.*

Proof. A triangle $\overset{\triangle}{ABC}$ has a taxicab incircle if two sides of the triangle lie on gradual lines and the remaining side of its lies on a steep line by Theorem 1.

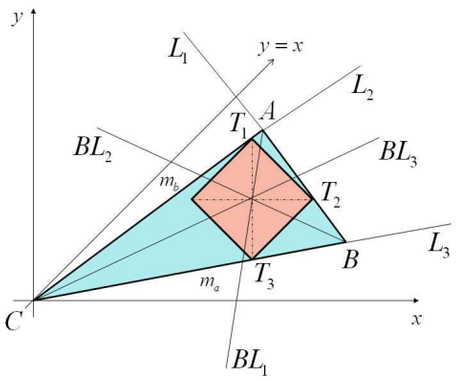

Figure 4

Equation of lines L_1, L_2 and L_3 containing the sides AB, AC and BC of the triangle are $y=m_c(x-x_a)+y_a$, $y=m_bx$ and $y=m_ax$, respectively. One can find the taxicab inside angle bisector lines BL_1, BL_2 and BL_3, by using definition of distance from a point to a line in the taxicab plane, as follows:

Since $BL_1=\{X=(x,y)\in\mathbb{R}^2 : d_T(X,L_1)=d_T(X,L_2)\}$; and

$$d_T(X,L_1)=\frac{|y+m_c(x_a-x)-y_a|}{\max\{|-m_c|,|1|\}}=\frac{y+m_c(x_a-x)-y_a}{m_c},$$

$$d_T(X,L_2)=\frac{|-m_bx+y|}{\max\{|-m_b|,|1|\}}=m_bx-y,$$

one can obtain the following equation:

$$d_T(X,L_1)=d_T(X,L_2)\Rightarrow\frac{y+m_c(x_a-x)-y_a}{m_c}=m_bx-y$$
$$\Rightarrow y=\frac{m_c(1+m_b)}{1+m_c}x+\frac{y_a-m_cx_a}{1+m_c}.$$

Thus, equation of line BL_1 is $y=\frac{m_c(1+m_b)}{1+m_c}x+\frac{y_a-m_cx_a}{1+m_c}$.

Similarly the equations of lines BL_2 and BL_3 are

$$y=\frac{m_c(1-m_a)}{1-m_c}x+\frac{y_a-m_cx_a}{1-m_c}\quad\text{and}\quad y=\frac{m_a+m_b}{2}x,$$

respectively. If the system of linear equations consisting of equations of BL_1, BL_2 and BL_3 is solved, then it is seen that there is a unique intersection point of lines BL_i, $i=1,2,3$. Also this point is the center of the taxicab incircle of the triangle $\overset{\triangle}{ABC}$. If two sides of the triangle lie on steep lines and the remaining side of its lies on a gradual line, the proof can be given, similarly. □

3 Taxicab incircles and circumcircles of a given triangle with at least a side on a separator line

In Euclidean geometry, it is well-known that the number of intersection points of a circle and a line is 0, 1 or 2. In the taxicab plane, this number is 0, 1, 2 or ∞. (see Figure 5)

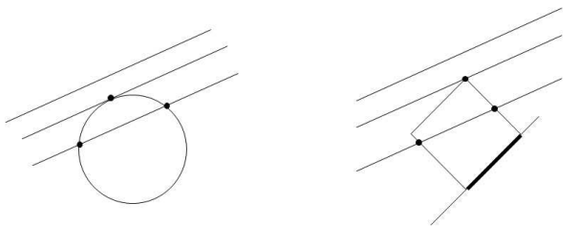

Figure 5

So far, we have considered that a incircle touches (is tangent to) each of the three sides of the triangle at only one point and circumcircle passes through all vertices of triangle. In this section we examine the incircle and circumcircle of a triangle by using following definition of concept of touching (tangent **!**). In the previous section, we have mentioned that a steep or a gradual line tangent to a taxicab circle if the taxicab circle and the steep or gradual line have common only one point. But sides of a taxicab circle always lie on separator lines. If slope of the a side of a triangle is $+1$ or -1 then that side coincides with a side of the taxicab incircle or circumcircle along a line segment. In this section, we consider the concept of **tangent along a line segment** if a line segment completely or partially lie on one side of the taxicab circle. This assumption increases the number of cases about existence of incircle and circumcircle for a given triangle in the taxicab plane. We only consider cases consisting infinite intersection points in this section. Because of this assumption, at least one side of the triangle must be on separator line. (see Figure 6).

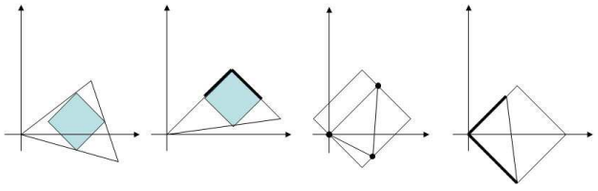

Figure 6

Next two theorems give some conditions about existence of incircle and circumcircle for a triangle with one or two sides on separator lines.

Theorem 5 *A triangle with at least one side on a separator line has always a taxicab circumcircle and incircle.*

Proof. Let $\overset{\triangle}{ABC}$ be a triangle which at least one side of it is on a separator line. Then there are two main cases:

1) A side of the triangle $\overset{\triangle}{ABC}$ is on a separator line. (see Figure 7).

2) Two sides of the triangle $\overset{\triangle}{ABC}$ are on separator lines. (see Figure 8).

Case 1: Let a side of the triangle $\overset{\triangle}{ABC}$ be on a separator line in the taxicab plane. Suppose that vertex C is at origin and m_a is -1 (or 1), that is, side BC lies on $y{=}{-}x$ (see Figure 7). A taxicab circumcircle composes of the line segments which are on lines with slopes ∓ 1, passing through the vertices of a triangle. Since $m_a{=}{-}1$, and the triangle is completely inside the taxicab circumcircle, side with slope -1 of the taxicab circumcircle coincides with the side BC of the triangle. So there are two subcases according to position of vertex A :

i) Vertex A is on opposite side of the circle according to side containing BC.

ii) Vertex A is on neighbour side of the circle according to side containing BC.

Infinite circumcircles can be drawn for both of cases. In subcase I, all circumcircles have the same radius. Note that the circumcircle moves along the line segment BC. In subcase II, all circumcircles have different radii. Note that the center of the circumcircle moves along a horizontal or a vertical line. Distance between centers of two of circumcircles is called as **quantity of change**, and it is shown by t (see Figure 7). If vertex A is on opposite side of the circle to side containing BC, then one of AC and AB is on a gradual line, and the other is on steep line. If vertex A is on neighbour side to side containing BC, then AC and AB are on gradual lines or steep lines.

A side of the taxicab incircle is on BC since the taxicab incircle is a taxicab circle, and it is tangent to all three sides. There are two subcases according to position of side of the taxicab incircle :

i) Side of the taxicab incircle doesn't pass through vertex B or C.

ii) Side of the taxicab incircle pass through vertex B or C.

In subcase I, two lines with slope 1 can be drawn at end point of side on BC. Since the incircle is completely inside the triangle, one of side of the triangle is on a steep line, and the other is on a gradual line.

In subcase II, side of the taxicab incircle on BC is tangent to two sides of the triangle. So sides of triangle are on gradual lines or steep lines (see Figure 7).

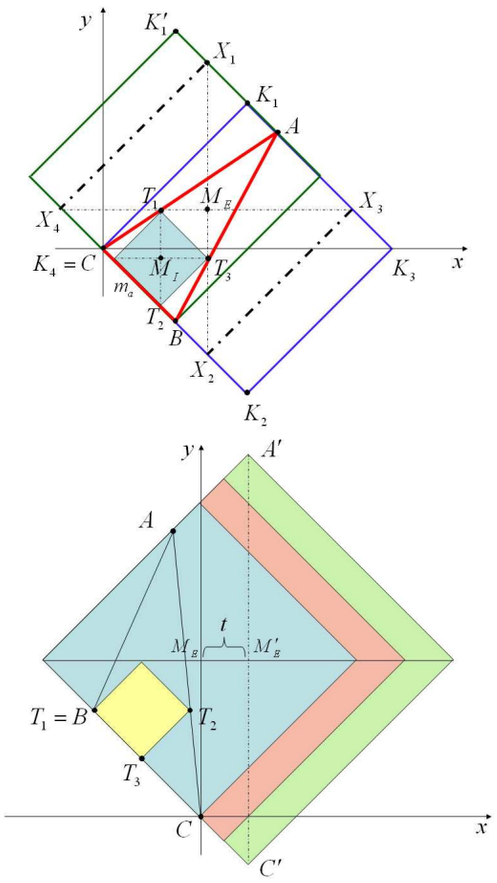

Figure 7

Case 2: The proof can be given as in Case 1.

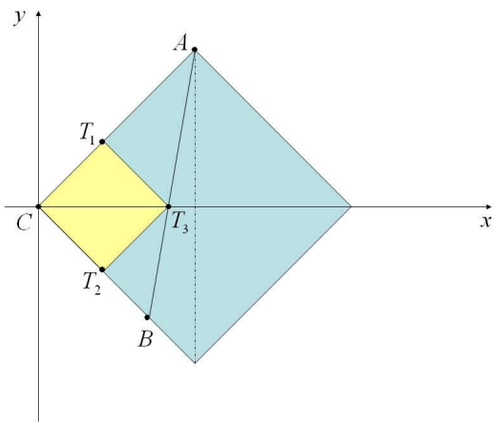

Figure 8

□

The following theorem gives the relations between radii of the incircle and circumcircle of a given triangle with one or two sides are on a separator line.

Theorem 6 *Let $\overset{\triangle}{ABC}$ be a triangle in the taxicab plane, m_a, m_b and m_c denote slopes of sides BC, AC and AB, respectively. If the triangle $\overset{\triangle}{ABC}$ has a taxicab incircle with radius* **r** *and circumcircle with radius* **R**, *and* **t** *is quantity of change, then*

$$\frac{\mathbf{r}}{2\mathbf{R}} = \begin{cases} \rho(m_a, m_b, m_c), & |m_a| \leq 1, |m_b| < 1 \text{ and } |m_c| > 1 \\ \rho\left(-m_a^{-1}, -m_b^{-1}, -m_c^{-1}\right), & |m_a| \geq 1, |m_b| > 1 \text{ and } |m_c| < 1. \end{cases}$$

and

$$\frac{\mathbf{r}}{2(\mathbf{R}-\mathbf{t})} = \begin{cases} \rho(m_c, m_b, m_a), & |m_a| = 1, |m_b| < 1 \text{ and } |m_c| < 1 \\ \rho\left(-m_c^{-1}, -m_b^{-1}, -m_a^{-1}\right), & |m_a| = 1, |m_b| > 1 \text{ and } |m_c| > 1 \\ \rho(m_a, m_b, m_c), & |m_a| = 1, |m_b| = 1 \text{ and } |m_c| > 1 \\ \rho\left(-m_a^{-1}, -m_b^{-1}, -m_c^{-1}\right), & |m_a| = 1, |m_b| = 1 \text{ and } |m_c| < 1 \end{cases}$$

where $\rho(m_a, m_b, m_c) =$

$$\frac{|m_b - m_a|\,|\delta(m_a, m_b) - m_c|}{\max\{|1+\delta(m_a,m_b)|, |1-\delta(m_a,m_b)|\}\,|\max\{m_a,m_b\}(1-m_c) + \min\{m_a,m_b\}(1+m_c) - 2m_c|}$$

with

$$\delta(m_a, m_b) = \begin{cases} m_a, & a > b \\ m_b, & a < b. \end{cases}$$

Proof. Let $\overset{\triangle}{ABC}$ be a triangle which at least one side of it on a separator line. One can easily see possible positions of the triangle from Theorem 5. Let $A = (x_a, y_a), B = (x_b, y_b)$ be two points such that $x_a > x_b > 0$, $y_a > 0 > y_b$, $m_a = -1$, $m_b < 1$ and $m_c > 1$.

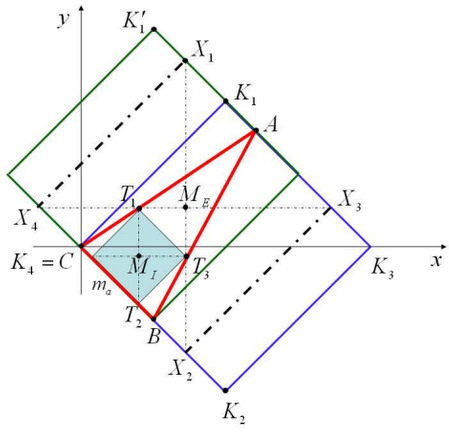

Figure 9

In this case a side of the circumcircle coincide with the side BC of the triangle, and vertex A is on opposite side of the circle to the side containing BC. So there are infinite taxicab circumcircles which of all have the same radius. $K_1 = \left(\frac{x_a+y_a}{2}, \frac{x_a+y_a}{2}\right)$ is the top vertex of the circumcircle that a vertex of it is C. Similarly, $K_1' = (x_b, -x_b+x_a+y_a)$ is the top vertex of the circumcircle such that a vertex of it is B. X_1 denotes the top vertex of all circumcircles. So $X_1 = \lambda K_1 + (1-\lambda)K_1'$ for all $\lambda \in [0,1]$ (see Figure 9). Therefore the vertices of circumcircles are

$$X_1 = (\lambda p + x_b, -\lambda p + (-x_b + x_a + y_a)),$$
$$X_2 = (\lambda p + x_b, -\lambda p - x_b),$$
$$X_3 = \left(\lambda p + \frac{x_a+y_a}{2} + x_b, (1-\lambda)p\right),$$
$$X_4 = ((1-\lambda)p, (1-\lambda)p),$$

where $p = \frac{x_a+y_a}{2} - x_b$. Thus, center and radius of the taxicab circumcircle having vertex X_i of the triangle $\overset{\triangle}{ABC}$ are

$$M_E = (\lambda p + x_b, (1-\lambda)p) \text{ and } \mathbf{R} = \frac{x_a+y_a}{2}.$$

Three vertices of the taxicab incircle are on lines $\overleftrightarrow{AB}$, $\overleftrightarrow{BC}$ and $\overleftrightarrow{AC}$ with the equations $y = m_c(x-x_a)+y_a$, $y=-x$ and $y=m_b x$, respectively. Let T_1 and T_2 be on lines $\overleftrightarrow{AC}$ and $\overleftrightarrow{BC}$ respectively. That is $T_1=(\gamma, m_b\gamma)$ and $T_2=(\gamma,-\gamma)$ for $\gamma \in \mathbb{R}^+$. Thus center and radius of the taxicab incircle of the triangle $\overset{\triangle}{ABC}$ are

$$M_I = \left(\gamma, \frac{(m_b-1)\gamma}{2}\right) \text{ and } \mathbf{r} = \frac{(m_b+1)\gamma}{2}.$$

Since $T_3=\left(\frac{(m_b+3)\gamma}{2}, \frac{(m_b-1)\gamma}{2}\right)$ and point T_3 is on $y = m_c(x-x_a)+y_a$, one can find as $\gamma = \frac{2x_a(m_b-m_c)}{m_b-3m_c-1-m_bm_c}$. Thus the relation between $\mathbf{R}$ and $\mathbf{r}$ is obtained as

$$\mathbf{r} = \frac{2\mathbf{R}(m_b-m_c)}{m_b-3m_c+m_a(1+m_bm_c)}.$$

m stand for slope of a line l. If l reflects with $y-$axis, then m changed to $-m$. So the above relation is valid for m_a=1, $m_b > -1$ and $m_c < -1$. The relation about other case for $|m_a|=1, |m_b|>1$ and $|m_c|<1$ can be found when m_a, m_b , m_c replace with $-m_a^{-1}, -m_b^{-1}$ and $-m_c^{-1}$ in the relations for $|m_a|$=1, $|m_b|<1$ and $|m_c|>1$. It is easily seen that all relations satisfy $\rho(m_a,m_b,m_c)$ for $|m_a|$=1, $|m_b|<1, |m_c|>1$ and $\rho\left(-m_a^{-1}, -m_b^{-1}, -m_c^{-1}\right)$ for $|m_a|$=1, $|m_b|>1$ and $|m_c|<1$.

Let $\overset{\triangle}{ABC}$ be a triangle such that $|m_a|=1, |m_b|>1$ and $|m_c|>1$ (see Figure 10). $A=(x_a,y_a), B=(x_b,y_b)$ and $C=(0,0)$ are three points such that $x_b < x_a < 0$ and $0 < y_b < y_a$.

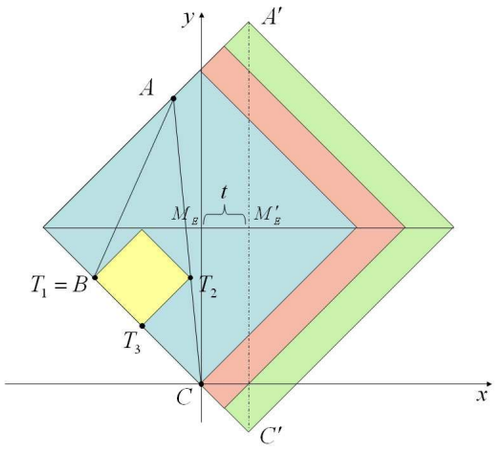

Figure 10

Therefore, center and radius of the taxicab circumcircle changing depend on parameter $\mathbf{t}$ of the triangle $\overset{\triangle}{ABC}$ are

$$M_E = \left(\mathbf{t}, \frac{-x_a+y_a}{2}\right) \text{ and } \mathbf{R} = \mathbf{t} + \frac{-x_a+y_a}{2}$$

where $\mathbf{t}$ is quantity of change. From last equation of $\mathbf{R}$, one can find that $x_a = \frac{2(\mathbf{R}-\mathbf{t})}{m_b-1}$. Three vertices of the taxicab incircle are on lines $\overleftrightarrow{AB}$, $\overleftrightarrow{BC}$ and $\overleftrightarrow{AC}$ with the equations $y = m_c(x-x_a)+y_a$, $y=-x$ and $y=m_bx$, respectively. Let T_1 and T_2 be on lines $\overleftrightarrow{AC}$ and $\overleftrightarrow{BC}$, respectively. So $T_1=(x_b,y_b)$ and $T_2=\left(\frac{y_b}{m_b}, y_b\right)$. Thus center and radius of the taxicab incircle of the triangle $\overset{\triangle}{ABC}$ are

$$M_I = \left(x_b + \frac{x_b(m_a-m_b)}{2m_b}, y_b\right) \text{ and } \mathbf{r} = \frac{x_b(m_a-m_b)}{2m_b}.$$

Since $m_c = \frac{y_a-y_b}{x_a-x_b}$, one can find as $x_b = \frac{x_a(m_c-m_b)}{m_c-m_a}$. Thus the relation between $\mathbf{R}$ and $\mathbf{r}$ is

$$\mathbf{r} = \frac{2(\mathbf{R}-\mathbf{t})(m_b-m_c)(m_b-m_a)}{2m_b(m_b+m_a)(m_c-m_a)}.$$

This relation is also valid if one can take $-m_a, -m_b, -m_c$ instead of m_a, m_b, m_c, respectively. The relation about other case for $|m_a|$=1, $|m_b|<1$ and $|m_c|<1$ can be found if m_a, m_b, m_c replace with $-m_a^{-1}, -m_b^{-1}, -m_c^{-1}$ in the relations for $|m_a|=1, |m_b|>1$ and $|m_c|>1$. It is easily seen that all relations satisfy $\rho(m_a,m_b,m_c)$ for

$|m_a| = 1, |m_b| < 1, |m_c| < 1$ and $\rho\left(-m_a^{-1}, -m_b^{-1}, -m_c^{-1}\right)$ for $|m_a| = 1, |m_b| > 1$ and $|m_c| > 1$.

Let $\overset{\triangle}{ABC}$ be a triangle with $|m_a|$=1, $|m_b|$=1 and $|m_c| > 1$ (see Figure 11). $A = (x_a, y_a)$, $B = (x_b, y_b)$ and $C = (0,0)$ are three points such that $x_a > x_b > 0$ and $y_a > 0 > y_b$.

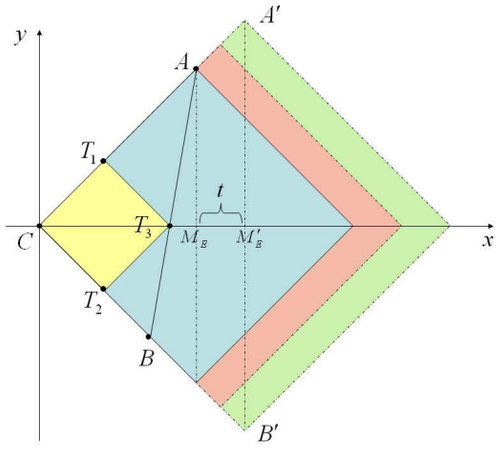

Figure 11

In this case, there are infinite taxicab circumcircles, and their centers move along a vertical or a horizontal line according to slope of side AB. So, the center and radius of the taxicab circumcircle changing depend on parameter $\mathbf{t}$ of the triangle $\overset{\triangle}{ABC}$ are

$$M_E = (x_a + \mathbf{t}, 0) \text{ and } \mathbf{R} = x_a + \mathbf{t}$$

where $\mathbf{t}$ is quantity of change. From last equation about $\mathbf{R}$ is obviously x_a=$\mathbf{R}$−$\mathbf{t}$.
Three vertices of the taxicab incircle are on lines $\overleftrightarrow{AB}$, $\overleftrightarrow{BC}$ and $\overleftrightarrow{AC}$ with the equations $y = m_c(x - x_a) + y_a$, $y = -x$ and $y = x$, respectively. Let T_1 and T_2 be on lines $\overleftrightarrow{AC}$ and $\overleftrightarrow{BC}$, respectively. So T_1=(γ, γ) and T_2=$(\gamma, -\gamma)$ for $\gamma \in \mathbb{R}^+$. Thus center and radius of the taxicab incircle of the triangle $\overset{\triangle}{ABC}$ are

$$M_I = (\gamma, 0) \text{ and } \mathbf{r} = \gamma.$$

Since $T_3 = (2\gamma, 0)$ and point T_3 is on $y = m_c(x - x_a) + y_a$, one can find as $\gamma = \dfrac{x_a(m_c - m_b)}{2m_c}$. Therefore the relation among $\mathbf{R}$, $\mathbf{r}$ and $\mathbf{t}$ is

$$\mathbf{r} = \frac{(\mathbf{R} - \mathbf{t})(|m_c| - 1)}{2|m_c|}.$$

This equation is also valid if m_c replace with $-m_c$.

The other case for $|m_a| = |m_b| = 1$ and $|m_c| < 1$ can be shown if m_a, m_b, m_c replace with $-m_a^{-1}$, $-m_b^{-1}$, $-m_c^{-1}$ in the relations for $|m_a| = |m_b|$=1 and $|m_c| > 1$. Thus, the proof of the theorem is completed. □

The next theorem gives relation between centers of the incircle and circumcircle.

Theorem 7 *Let $\overset{\triangle}{ABC}$ be a triangle which at least one side is on a separator line in the taxicab plane. If the triangle $\overset{\triangle}{ABC}$ has a taxicab incircle and circumcircle, then the distance between the center M_E of the taxicab circumcircle with radius $\mathbf{R}$, and the center M_I of the incircle with radius $\mathbf{r}$ is*

$$d_T(M_E, M_I) = \mathbf{R} - \mathbf{r}.$$

Proof. The proof is given by using the values of M_E and M_I in the Theorem 6. □

The following theorem shows that expression of the Theorem 7 is also valid for a triangle which at least one side is on a separator line.

Theorem 8 *Let $\overset{\triangle}{ABC}$ be a triangle with at least one side is on a separator line. If $\overset{\triangle}{ABC}$ has a taxicab incircle, then the center of incircle is the intersection point of the taxicab inside angle bisectors of the triangle $\overset{\triangle}{ABC}$.*

Proof. Let $\overset{\triangle}{ABC}$ be a triangle such that m_a, m_b and m_c are slopes of sides BC, AC and AB, respectively. If at least one side of a triangle $\overset{\triangle}{ABC}$ lies on a separator line, there are six different cases according to slopes of the sides of triangles;

i) $|m_a| = 1$, $|m_b| < 1$ and $|m_c| > 1$
ii) $|m_a| = 1$, $|m_b| > 1$ and $|m_c| < 1$
iii) $|m_a| = 1$, $|m_b| > 1$ and $|m_c| > 1$
iv) $|m_a| = 1$, $|m_b| < 1$ and $|m_c| < 1$
v) $|m_a| = 1$, $|m_b| = 1$ and $|m_c| > 1$
vi) $|m_a| = 1$, $|m_b| = 1$ and $|m_c| < 1$

Case i) Let $\overset{\triangle}{ABC}$ be a triangle with $|m_a|$=1, $|m_b| < 1$ and $|m_c| > 1$. Then A=(x_a, y_a), $B = (x_b, y_b)$ and $C = (0,0)$ are three points such that $x_a > x_b > 0$ and $y_b > 0 > y_a$ (see Figure 12).

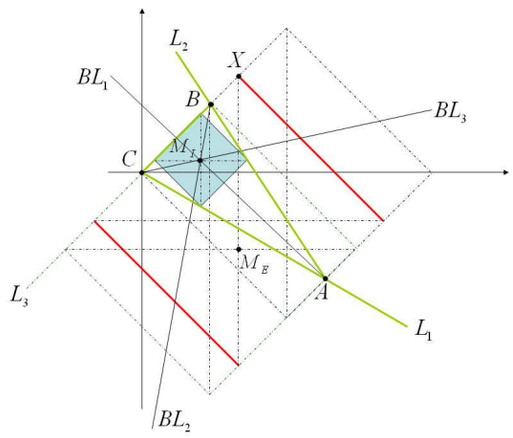

Figure 12

L_1, L_2 and L_3 denote the lines which lie on AC, AB and BC, respectively. These lines L_1, L_2 and L_3 are $y = m_b x$, $y = m_c(x - x_a) + y_a$, and $y=x$, respectively. Using definition of distance from a point to a line in the taxicab plane, the taxicab inside angle bisector lines BL_1, BL_2 and BL_3 are found as follow:

Since $BL_1 = \{X = (x,y) \in \mathbb{R}^2 : d_T(X,L_1) = d_T(X,L_2)\}$; and

$$d_T(X,L_1) = \frac{|y - m_b x|}{\max\{|-m_b|,|1|\}} = y - m_b x$$

$$d_T(X,L_2) = \frac{|y + m_c(x_a - x) - y_a|}{\max\{|-m_c|,|1|\}} = \frac{y + m_c(x_a - x) - y_a}{m_c},$$

one can obtain the following equation:

$$y = \frac{m_c(m_b - 1)}{m_c - 1}x + \frac{x_a(m_c - m_b)}{m_c - 1}.$$

Similarly the equations of lines BL_2 and BL_3 are

$$y = \frac{2m_c}{1 + m_c}x + \frac{x_a(m_b - m_c)}{1 + m_c} \quad \text{and} \quad y = \frac{1 + m_b}{2}x$$

respectively. If the system of linear equations consisting of equations of BL_1, BL_2 and BL_3 is solved, then the solution is found as

$$\left(\frac{2x_a(m_b - m_c)}{m_b - 3m_c - 1 - m_b m_c}, \frac{x_a(m_b - m_c)(m_b - 1)}{m_b - 3m_c - 1 - m_b m_c}\right).$$

That is, lines BL_1, BL_2 and BL_3 pass through the same point. Also this point is the center of taxicab incircle of the triangle $\overset{\triangle}{ABC}$.

The proof of the other cases can be given by similar ways.

□

References

[1] H. B. Çolakoğlu, R. Kaya, A synthetic approach to the taxicab circles, *Applied Sciences* **9** (2007), 67–77.

[2] H. B. Çolakoğlu, R. Kaya, Regular Polygons in the Taxicab Plane, *KoG* **12** (2008), 27–33.

[3] B. Divjak, Notes on Taxicab Geometry, *KoG* **5** (2000/01), 5–9.

[4] S. Ekmekçi, *Taksi Çemberleriyle İlgili Özellikler*, ESOGÜ, PhD, 2001.

[5] O. Gelisgen,R. Kaya, The Taxicab Space Group, *Acta Mathematica Hungarica* **122 (1–2)** (2009), 187–200.

[6] R. Kaya, Z. Akça, I. Gunaltili, M. Ozcan, General Equation for Taxicab Conics and Their Classification, *Mitt. Math. Ges. Hamburg* **19** (2000), 135–148.

[7] E. F. Krause, *Taxicab Geometry*, Addison-Wesley, Menlo Park, 1975.

[8] D. J. Schattschneider, The Taxicab Group, *Amer. Math. Monthly* **91** (1984), 423–428.

[9] S. S. So, Recent Developments in Taxicab Geometry, *Cubo Mat. Educ.* **4 (2)** (2002), 79–96.

[10] K. Thompson, Taxicab Triangle Incircles and Circumcircles, to appear in *The Pi Mu Epsilon Journal* (see author's home page).

Temel Ermiş
e-mail: termis@ogu.edu.tr

Özcan Gelişgen
e-mail: gelisgen@ogu.edu.tr

Rustem Kaya
e-mail: rkaya@ogu.edu.tr

Department of Mathematics and Computer Sciences
Faculty of Science and Arts
University of Eskişehir Osmangazi
26480 Eskişehir-Türkiye

Original scientific paper
Accepted 2. 11. 2012.

ANA SLIEPČEVIĆ
IVANA BOŽIĆ

Steiner Curve in a Pencil of Parabolas

Steiner Curve in a Pencil of Parabolas

ABSTRACT

Using the facts from the theory of conics, two theorems that are analogous to the theorems in triangle geometry are proved. If the pencil of parabolas is given by three lines a, b, c, it is proved that, the vertex tangents of all the parabolas in the pencil, envelop the Steiner deltoid curve δ, and the axes of all parabolas in the same pencil envelop further deltoid curve α. Furthermore, the deltoid curves are homeothetic. It is proved that all the vertices in the same pencil of parabolas are located at the 4th degree curve. The above mentioned curves are constructed and treated by synthetic methods.

Key words: Steiner deltoid curve, Wallace-Simson line, pencil of parabolas, vertex tangent

MSC 2010: 51M35, 51M15

Steinerova krivulja u pramenu parabola

SAŽETAK

Koristeći činjenice teorije konika, dokazuju se dva teorema koji su analogoni klasičnih teorema geometrije trokuta. Za pramen parabola zadan trima temeljnim tangentama a, b, c dokazuje se da tjemene tangente svih parabola omataju deltoidu δ, a osi parabola u istom pramenu deltoidu α. Pokazuje se da su deltoide homotetične. Još se dokazuje da sva tjemena parabola u istom pramenu leže na krivulji 4. reda. Spomenute krivulje se konstruiraju i istražuju metodama sintetičke geometrije.

Ključne riječi: Steinerova deltoida, Wallace-Simsonov pravac, pramen parabola, tjemena tangenta

1 Introduction

Some of the (numerous) classical theorems from the geometry of the triangle can be expressed in a different way in order to obtain new theorems in the theory of conics. In this article special attention will be given to the following two well known theorems:

Theorem 1 *If F is any point belonging to the circle k circumscribed to a triangle ABC, then three points W_a, W_b, W_c obtained by orthogonally projecting F, on the three sides of the triangle are collinear. The line thus obtained is called the Wallace-Simson line w of F, [1].*

See Figure 1.

In 1856 Jakob Steiner proved that the envelope of Wallace-Simson lines when F moves around the circumscribed circle to a triangle ABC is a special curve of third class and fourth degree. That curve which has the line at infinity as double ideal tangent, a curve that is tangent to the three sides and to the three altitudes of the triangle, and has three cuspidal points and the three tangent lines on them meet at a point is called the *Steiner deltoid*, [1].

Theorem 2 *The envelope of the Wallace-Simson lines of a triangle ABC is the Steiner deltoid curve, [2].*

See Figure 1.

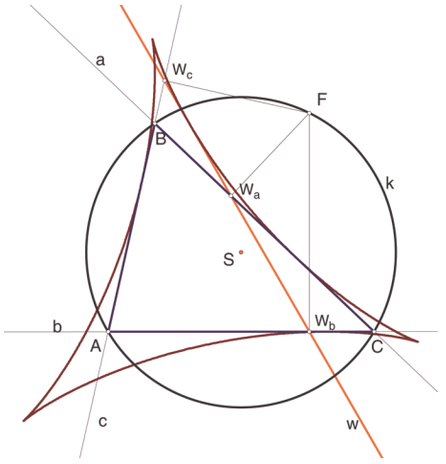

Figure 1

2 Deltoid curves in a pencil of parabolas

It is known for a fact that a pencil of parabolas can be set according to lines a, b, c. Therefore we can prove the following theorems.

Theorem 3 *Let $\{a,b,c\}$ be the pencil of parabolas touching three lines a, b, c. Let F be any point belonging to the circle k circumscribed to the triangle ABC given by the lines a, b, c. The Wallace-Simson line w of the point F is the vertex tangent of one parabola from the pencil.*

Proof. The focus points of all parabolas from the pencil lie on the circumscribed circle k, so the point F is the focus of one (certain) parabola, [3], [4].
It is known for a fact that the pedal curve of a parabola, with respect to pedal point O, is a circular cubic. If the pedal point O is the focus F of the parabola, the pedal curve degenerates into the isotropic lines of the focus F and the vertex tangent. In that case, the vertex tangent is the Wallace-Simson line w, [2]. □

It needs to be highlighted that:

Remark 1 *Each side of the triangle ABC is the Wallace-Simson line of the point antipodal to a vertex of triangle. The side a (b, c) of the triangle is the vertex tangent of the parabola from the pencil of parabolas, that as its focus has the antipodal point to the vertex A (B, C, respectively).*

Remark 2 *In the given pencil of parabolas there are three parabolas degenerated into three pairs of points, the vertex A (B, C) of the triangle and the point at infinite of the line a (b, c, respectively). The altitudes of the triangle ABC are the vertex tangents of three degenerated parabolas, from a pencil $\{a,b,c\}$, respectively they are Wallace-Simson lines of triangle vertices.*

The following theorem is the direct consequence of Theorems 2 and 3.

Theorem 4 *Let the pencil of parabolas touching three lines $\{a,b,c\}$ be given. The envelope of the vertex tangents of the parabolas from the pencil is the Steiner deltoid curve δ, (Figure 2).*

Theorem 5 *If $\{a,b,c\}$ is the pencil of parabolas touching three lines a, b, c, then the envelope of the axes of parabolas from the pencil $\{a,b,c\}$ is a deltoid curve α, that is the dilation image of the Steiner deltoid curve δ, with the center of dilation at the centroid T and a scale factor of -2.*

Proof. Let F be an arbitrary chosen point belonging to the circle k circumscribed to the triangle ABC, and w its associated vertex tangent. When F moves around circle k, the envelope of w is the Steiner deltoid curve denoted as δ. The perpendicular line from F to vertex tangent w is the axes o of the parabola with focus F, from the pencil $\{a,b,c\}$, (Figure 3). Let $A_1B_1C_1$ be the anti complementary triangle of ABC. The sides of the triangle $A_1B_1C_1$ coincide with the axes of the degenerated parabolas from the pencil $\{a,b,c\}$. Furthermore, the deltoid curve α of triangle ABC coincides with Steiner deltoid curve δ (vertex tangent deltoid curve) of anti complementary triangle $A_1B_1C_1$. The triangle ABC is the dilation image of the anti complementary triangle $A_1B_1C_1$ about the centroid T with the factor of $-1/2$. We can conclude that the deltoid curve α is the dilation image of the deltoid curve δ, with the scale factor of -2. □

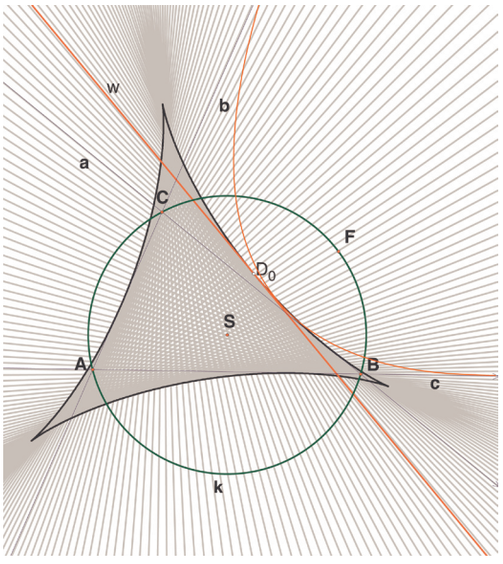

Figure 2

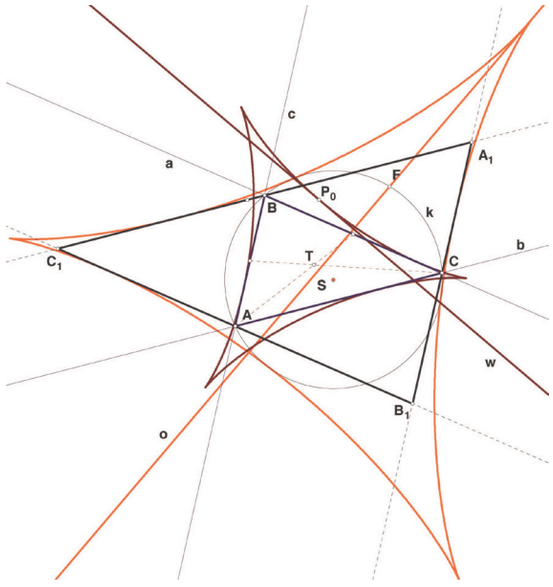

Figure 3

Theorem 6 *Let the pencil of parabolas touching three lines $\{a,b,c\}$ be given. All vertices in the pencil of parabolas $\{a,b,c\}$ lie on the 4^{th} order curve.*

Proof. Let the triangle *ABC* be determined by lines a, b, c, and let k be its circumscribe circle, $F \in k$. Let the intersection point of the vertex tangent w and the axis o be denoted as T_1. The point T_1 is the vertex of one parabola from the pencil $\{a,b,c\}$.
Let the envelop of the vertex tangent w, and the envelop of the axis o be denoted as δ and α, respectively. We will obtain a bijection between two 3^{rd} class pencils of lines, i.e. two deltoid curves δ and α. Each vertex tangent w of deltoid curve δ is corresponding to the (perpendicular) line o of deltoid curve α. According to Chasles's theorem, this correspondence will result in the 6^{th} order curve, [5]. Since the line at infinity as double tangent of one deltoid curve is corresponding to the line at infinity as double tangent of the other deltoid curve, the 6^{th} order curve degenerates into a quartic β and the line at infinity counted twice. The quartic β touches the line at infinity at the absolute points. Therefore, the line at infinity is an isolated double tangent of three mentioned quartics α, β, δ. □

Remark 3 *The quartic β passes through the vertices A, B, C of the triangle. Vertices A, B, C of the triangle are vertices of three degenerated parabolas from the pencil $\{a,b,c\}$. In Figure 4 focus points of parabolas with vertex tangents a, b, c are denoted as F_a, F_b, F_c. Vertex of the same parabolas are denoted as T_a, T_b, T_c. At these points the quartic β touches the sides of the triangle ABC.*

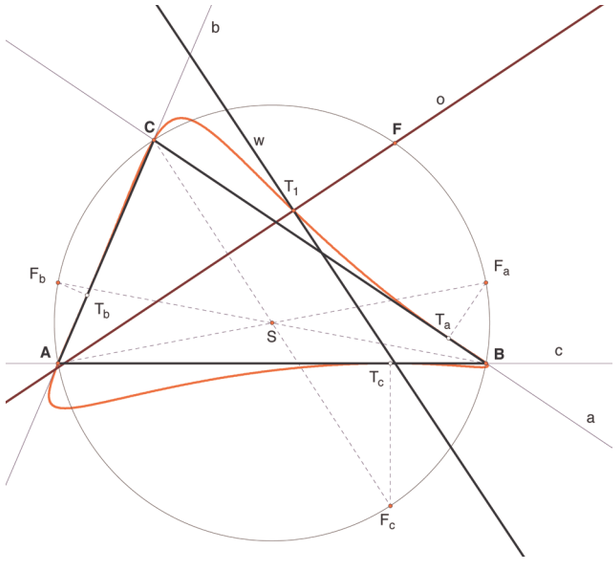

Figure 4

References

[1] M. DE GUZMAN, The envelope of the Wallace-Simson lines of a triangle. A simple proof of the Steiner theorem on the deltoid, *Rev. R. Acad. Cien. Serie A. Mat.* **95**(1), (2001), 57–64

[2] A. A. SAVELOV, *Ravninske krivulje*, Školska knjiga, Zagreb, 1979.

[3] A. SLIEPČEVIĆ, Isogonale Transformation und Fokalkurve einer Kegelschnittschar, *RAD HAZU* **470**(12) (1995), 157–166.

[4] A. SLIEPČEVIĆ, Über die zirkularen Kurven eines Viersets, *RAD HAZU* **491**(15) (2005), 169–174.

[5] H. WIELEITNER, *Spezielle Ebene Kurven*, G. J. Gäschen'sche Verlagshandlung, Leipzig, 1908.

Ana Sliepčević
e-mail: anas@grad.hr

Faculty of Civil Engineering, University of Zagreb
Kačićeva 26, 10000 Zagreb, Croatia

Ivana Božić
e-mail: ibozic4@tvz.hr

Tehničko veleučilište u Zagrebu
Avenija Većeslava Holjevca 15, 10000 Zagreb, Croatia

How to get KoG?

The easiest way to get your copy of KoG is by contacting the editor's office:

Marija Šimić Horvath
marija.simic@arhitekt.hr
Faculty of Architecture
Kačićeva 26, 10 000 Zagreb, Croatia
Tel: (+385 1) 4639 176
Fax: (+385 1) 4639 465

The price of the issue is €15 + mailing expenses €5 for European countries and €10 for other parts of the world.

The amount is payable to:

ACCOUNT NAME:	Hrvatsko društvo za geometriju i grafiku Kačićeva 26, 10000 Zagreb, Croatia
IBAN:	HR862360000-1101517436

Kako nabaviti KoG?

KoG je najbolje nabaviti u uredništvu časopisa:

Marija Šimić Horvath
marija.simic@arhitekt.hr
Arhitektonski fakultet
Kačićeva 26, 10 000 Zagreb
Tel: (01) 4639 176
Fax: (01) 4639 465

Za Hrvatsku je cijena primjerka 100 KN + 10 KN za poštarinu.

Nakon uplate za:

HDGG (za KoG), Kačićeva 26, 10000 Zagreb
žiro račun broj **2360000-1101517436**

poslat ćemo časopis na Vašu adresu.

Ako Vas zanima tematika časopisa i rad našeg društva, preporučamo Vam da postanete članom HDGG-a (godišnja članarina iznosi 150 KN). Za članove društva časopis je besplatan.

Original scientific paper
Accepted 5. 11. 2012.

HIROSHI OKUMURA

Ubiquitous Archimedean Circles of the Collinear Arbelos

Ubiquitous Archimedean Circles of the Collinear Arbelos

ABSTRACT

We generalize the arbelos and its Archimedean circles, and show the existence of the generalized Archimedean circles which cover the plane.

Key words: arbelos, collinear arbelos, ubiquitous Archimedean circles

MSC 2000: 51M04, 51M15, 51N10

Sveprisutne Arhimedove kružnice kolinearnog arbelosa

SAŽETAK

Generaliziramo arbelos i njegove Arhimedove kružnice te pokazujemo postojanje generaliziranih Arhimedovih kružnica koje pokrivaju ravninu.

Ključne riječi: arbelos, kolinearni arbelos, sveprisutne Arhimedove kružnice

1 Introduction

For a point O on the segment AB in the plane, the area surrounded by the three semicircles with diameters AO, BO and AB erected on the same side is called an arbelos. It has lots of unexpected but interesting properties (for an extensive reference see [1]). The radical axis of the inner semicircles divides the arbelos into two curvilinear triangles with congruent incircles called the twin circles of Archimedes. Circles congruent to those circles are said to be Archimedean. In this paper we generalize the arbelos and the Archimedean circles, and show the existence of the generalized Archimedean circles covering the plane, which is a generalization of the ubiquitous Archimedean circles of the arbelos in [4].

The arbelos is generalized in several ways, the generalized arbelos of intersecting type [7], the generalized arbelos of non-intersecting type [6] and the skewed arbelos [5], [8]. For the generalized arbelos of intersecting type and non-intersecting type, the twin circles of Archimedes are considered in a general way as Archimedean circles in aliquot parts. But Archimedean circles are still not given except them. In this paper we unify the two generalized arbeloi with one more additional generalized arbelos.

2 The collinear arbelos

In this section we generalize the arbelos and the twin circles of Archimedes to a generalized arbelos. For two points P and Q in the plane, (PQ) denotes the circle with diameter PQ. Let P and Q be point on the line AB, and let $\alpha = (AP)$, $\beta = (BQ)$ and $\gamma = (AB)$. Let O be the point of intersection of AB and the radical axis of the circles α and β and let $u = |AB|$, $s = |AQ|/2$ and $t = |BP|/2$. We use a rectangular coordinate system with origin O such that the points A, B have coordinate $(a,0)$, $(b,0)$ respectively with $a - b = u$. The configuration (α,β,γ) is called a collinear arbelos if the four points lie in the order (i) B, Q, P, A or (ii) B, P, Q, A, or (iii) P, B, A, Q. In each of the cases the configuration is explicitly denoted by $(BQPA)$, $(BPQA)$ and $(PBAQ)$ respectively. $(BQPA)$ and $(BPQA)$ are the generalized arbelos of non-intersecting type and the generalized arbelos of intersecting type respectively.

Let $(p,0)$ and $(q,0)$ be the coordinates of P and Q respectively. Since the point O lies on the radical axis of α and β, the powers of O with respect to α and β are equal, i.e., $ap = bq$ holds. Hence there is a real number $k < 0$ such that $b = ka$ and $p = kq$. Therefore we get

$$ta + sb = tq + sp = 0. \tag{1}$$

For points V and W on the line AB with x-coordinates v and w respectively, $V \leq W$ describes $v \leq w$, and $\mathcal{P}_W$ denotes the perpendicular to AB passing through W. The part (i) of the following lemma is proved in [3]. The proof of (ii) is similar and is omitted (see Figure 1).

Lemma 1 *The following circles have radii $|AW||BV|/(2u)$ for points V and W on the line AB.*

(i) *The circles touching the circles γ internally, (AV) externally and the line $\mathcal{P}_W$ from the side opposite to the point B in the case $B \leq V \leq A$ and $B \leq W \leq A$.*

(ii) *The circles touching γ externally, (AV) internally and $\mathcal{P}_W$ from the side opposite to the point A in the case $V \leq B \leq W \leq A$.*

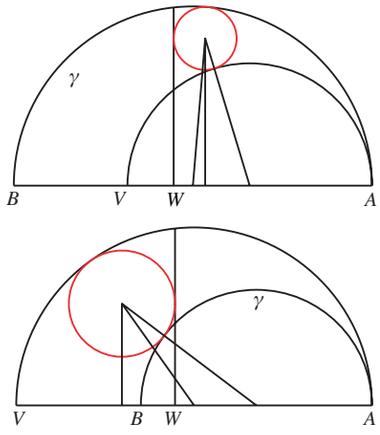

Figure 1: *Circles of radii $|AW||BV|/(2u)$.*

For collinear arbeloi $(BQPA)$ and $(BPQA)$, δ_α is the circle in the region $y > 0$ touching the circles γ internally, α externally and the line $\mathcal{P}_O$ from the side opposite to B. For a collinear arbelos $(PBAQ)$, δ_α is the circle in the region $y > 0$ touching γ externally, α internally and $\mathcal{P}_O$ from the side opposite to A. The circle δ_β is defined similarly (see Figure 2).

Theorem 1 *For a collinear arbelos (α,β,γ), the circles δ_α and δ_β are congruent with common radii $st/(s+t)$.*

Proof. If $(\alpha,\beta,\gamma) = (PBAQ)$, by (ii) of Lemma 1 and (1) the radius of δ_α is

$$\frac{|AO||BP|}{2u} = \frac{a(b-p)}{2(a-b)} = \frac{a(-ta/s+tq/s)}{2(a+ta/s)} = \frac{st}{s+t}.$$

Similarly the radius of δ_β is equal to $st/(s+t)$. The other cases are proved similarly. □

We now call the circles δ_α and δ_β the twin circles of Archimedes of the collinear arbelos. Circles congruent to the twin circles are called Archimedean circles of the collinear arbelos.

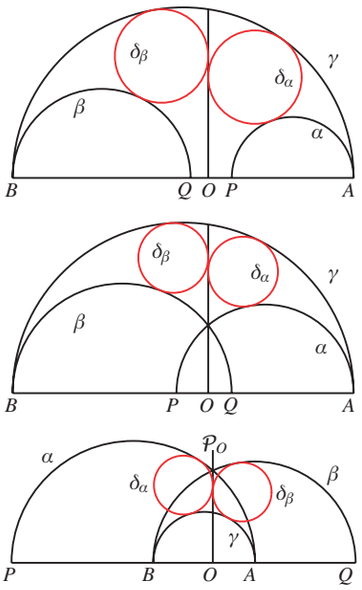

Figure 2: *The circles δ_α and δ_β.*

3 A pair of Archimedean circles generated by a point

We use the following lemma [4], which is easily proved by the properties of similar triangles.

Lemma 2 *For a triangle RGH with a point S on the segment GH, let E and F be points on the lines RG and RH respectively such that $SERF$ is a parallelogram. If T and U are points of intersection of RS with the lines parallel to GH passing through E and F respectively and $g = |GS|$, $h = |HS|$, then $|ET| = |FU| = gh/(g+h)$.*

Theorem 2 *For a collinear arbelos (α,β,γ), let R be a point which does not lie on the line AB, and let E and F be points on the line AR and BR respectively such that EP and FQ are parallel to BR and AR respectively. If the lines passing through E and F parallel to AB intersect the line OR at points T and U respectively, the circles (ET) and (FU) are Archimedean.*

Proof. Let EP and FQ intersect the line OR at points S and S' respectively (see Figures 3, 4, 5). The triangles RAO and $S'QO$ are similar. Also the triangles RBO and SPO are similar. While $|QO|/|AO| = |PO|/|BO|$ for O lies on the radical axis of the circles α and β. Therefore the ratios of the similarity of the two pairs of the similar triangles are the same. Hence $|S'O|/|RO| = |SO|/|RO|$, i.e.,

$S = S'$. Let A' and B' be the points of intersection of the line passing through S parallel to AB with the lines AR and BR respectively. Then $|A'S| = |AQ| = 2s$ and $|B'S| = |BP| = 2t$. Therefore $|ET| = |FU| = 2st/(s+t)$ by Lemma 2, i.e., the circles (ET) and (FU) are Archimedean. □

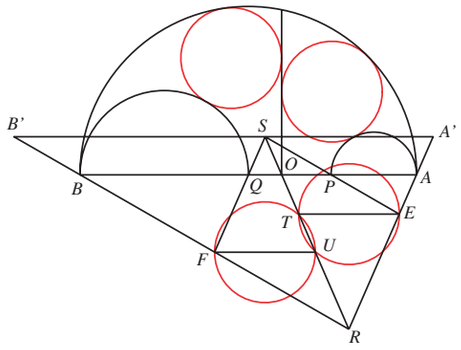

Figure 3

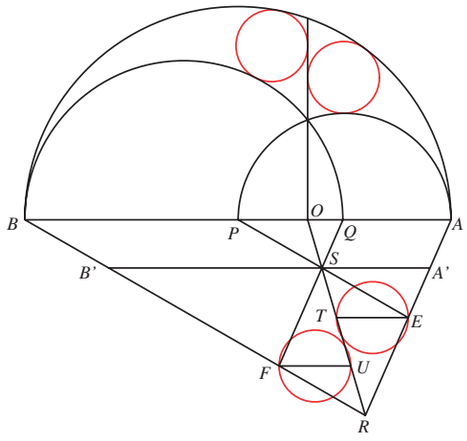

Figure 4

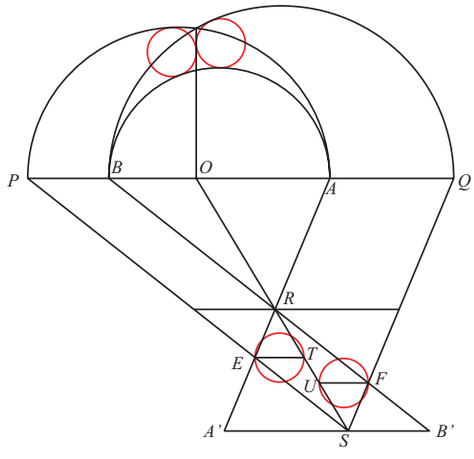

Figure 5

4 Ubiquitousness and parallelograms

However the word "ubiquitous" is used in the title of the paper [2], their Archimedean circles do not cover the plane. In this section, we show that our generalized Archimedean circles of the collinear arbelos cover the plane.

Let (α, β, γ) be a collinear arbelos. If a point X does not lie on the line AB, let Y and Z be points such that the midpoint of YZ is X, $\overrightarrow{YZ}$ and $\overrightarrow{AQ}$ are parallel with the same direction, and $|YZ| = 2r_A$. Let R be the point of intersection of the lines AY and OZ. Using the point R, let us construct a parallelogram $SERF$ and a point T as in Figures 3, 4, 5. Then (ET) is an Archimedean circle with center X.

If a point X lies on the line AB, we choose a point X' lying inside of the Archimedean circle with center X, so that X' does not lie on AB. If we use the point X' instead of X, and construct the parallelogram $SERF$ and the point T as in Figures 3, 4, 5 just as mentioned above, the Archimedean circle (ET) with center X' contains X. Therefore there is an Archimedean circle containing the point X in any case, i.e., the Archimedean circles cover the plane. In this sense our Archimedean circles are Ubiquitous.

However the five points A, B, P, Q and O are involved in the construction of the Archimedean circles, the three circles α, β and γ are not. Therefore it seems that the Archimedean circles are not so closely related to the collinear arbelos. But we can show that for a point R, which does not lie on the line AB, the parallelogram $SERF$ in Figures 3, 4, 5 are constructed by the circles α, β and γ (see Figure 6). Let the circle γ intersect the lines AR and BR at points I and J respectively, and let AJ intersect α at a point K and BI intersect β at a point L. Then KP and JB are parallel, also LQ and IA are parallel. Therefore if E, F, S are the points of intersection of the lines AR and KP, BR and LQ, KP and LQ respectively, then $SERF$ is a parallelogram.

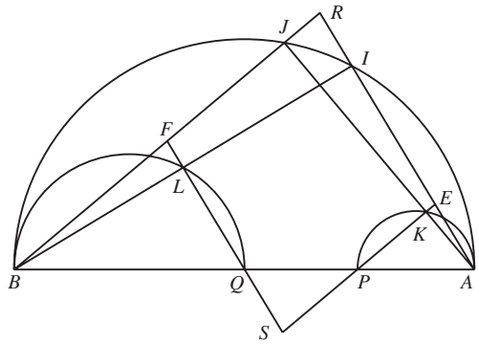

Figure 6

References

[1] H. P. BOAS, Reflections on the Arbelos, *Amer. Math. Monthly* **113** (2006), 236–249.

[2] C. W. DODGE, T. SCHOCH, P. Y. WOO, P. YIU, Those ubiquitous Archimedean circles, *Math. Mag.* **72** (1999), 202–213.

[3] R. NAKAJIMA, H. OKUMURA, Archimedean circles induced by skewed arbeloi, *Journal for Geometry and Graphics* **16** (2012), 13–17.

[4] H. OKUMURA, Ubiquitous Archimedean circles, *Mathematics and Informatics* **55** (2012), 308–311.

[5] H. OKUMURA, More on twin circles on the skewed arbelos, *Forum Geom.* **11** (2011), 139–144.

[6] H. OKUMURA, M. WATANABE, Generalized arbelos in aliquot parts: non-Intersecting case, *Journal for Geometry and Graphics* **13** (2009), 41–57.

[7] H. OKUMURA, M. WATANABE, Generalized Arbelos in aliquot parts: intersecting case, *Journal for Geometry and Graphics* **12** (2008), 53–62.

[8] H. OKUMURA, M. WATANABE, The twin circles of Archimedes in a skewed arbelos, *Forum Geom.* **4** (2004), 229–251.

Hiroshi Okumura
e-mail: hiroshiokmr@gmail.com
251 Moo 15 Ban Kesorn Tambol Sila
Amphur Muang Khonkaen 40000, Thailand

Original scientific paper
Accepted 30. 11. 2012.

NIKOLINA KOVAČEVIĆ
ANA SLIEPČEVIĆ

On the Certain Families of Triangles

On the Certain Families of Triangles

ABSTRACT

In the present paper, we study a set $\mathbf{T} = \{\mathcal{T}_{(r,d)} : d \in \mathbb{R}\}$ of the certain one-parameter families of triangles. The traces of some triangle points within the set are analyzed and described.

Key words: tangential triangle, hyperosculating circle, pencil of conics

MSC 2000: 51N20, 51N15

O nekim familijama trokuta

SAŽETAK

U ovom radu proučava se skup $\mathbf{T} = \{\mathcal{T}_{(r,d)} : d \in \mathbb{R}\}$ specijalnih jednoparametarskih familija trokuta. Analizirat će se i opisati krivulje mjesta nekih točaka trokuta unutar danog skupa.

Ključne riječi: tangencijalni trokut, hiperoskulacijska kružnica, pramen konika

1 Introduction

The study of triangles and their families even nowadays attracts many geometers. Various problems in connection to the triangles and their families are studied in [1], [2], [3]. Nowadays, the use of modern geometry softwares (*GeoGebra*, *Cinderella*, *The Geometer's Sketchpad* ...) enables the dynamic geometric constructions which, in general, facilitate the analysis of the movement of the triangles, or some triangle points, within the specified system.

When it comes to the families of triangles, there are many ways to associate triangles with each other. One such is defined in this paper generalizing the concept of the tangential triangles.

Generally, given a triangle $\Delta A_1A_2A_3$, the triangle $\Delta T_1T_2T_3$ is said to be the tangential triangle if it is formed by the lines tangent to the circumcircle of $\Delta A_1A_2A_3$ at its vertices. Hereafter, we will use the term a tangential triangle in connection to a circle. Hence, a triangle will be called a tangential triangle to a given circle $\mathcal{C}$ iff it is formed by the lines tangent to $\mathcal{C}$. Naturally, given the circle, there are ∞^3 such triangles. By adding some more elements into the specified family, a one–parameter family of triangles is defined in this paper. Furthermore, the connection between the added elements and the given circle–tangent configuration is studied.

Denoting by $PG(2,\mathbb{R})$ the projective closure of $\mathbb{R}^2$, we always assume that $PG(2,\mathbb{R})$ is embedded into its complexification $PG(2,\mathbb{R} \subset \mathbb{C})$. Choosing the line at infinity f as $x_3 = 0$, the interchange between homogeneous and Cartesian coordinates in $\mathbb{R}^2$ is realized.

1.1 The family of triangles $\mathcal{T}_{(r,d)}$

Let a circle $\Phi(S,r)$ with radius r and one of its tangents t be given. For $d \in \mathbb{R}$ a one–parameter family of triangles $\mathcal{T}_{(r,d)}$ is defined such that a triangle $\Delta ABC \in \mathcal{T}_{(r,d)}$ iff it satisfies the following two properties:

F1) a triangle ΔABC is tangential to the given circle $\Phi(S,r)$,

F2) $A, B \in t$ and $d = \pm|\overrightarrow{AB}|$.

Hence, as a segment of the fixed length d moves along the tangent t, a triangle ΔABC traversers a one–parameter family $\mathcal{T}_{(r,d)}$. This motion is continuous, but not rigid for the remaining two triangle sides which are therefore continuously changing.

Furthermore, by varying d a set $\mathbf{T} = \{\mathcal{T}_{(r,d)} : d \in \mathbb{R}\}$ of the triangle families is obtained in connection to the given circle and its fixed tangent.

Fig. 1 shows two triangles ΔABC and ΔBDE of the family $\mathcal{T}_{(r,d)}$ obtained for some d. The circle Φ is its ex– and incircle, and they share the side and one vertex lying on it. Altohough not necessary, it is convenient to introduce an orientation onto the tangent t to ensure that the position of only one vertex uniquely determines the remaining two vertices.

Obviously, given a configuration of a circle Φ and tangent t, the loci of many triangle points within two families $\mathcal{T}_{(r,d)}, \mathcal{T}_{(r,-d)} \in \mathbf{T}$ will coincide. This follows directly from the geometric construction, since the loci of the triangle centers within $\mathcal{T}_{(r,d)}$ are symmetric with respect to the circle diameter perpendicular to the given tangent t, as it will be shown later.

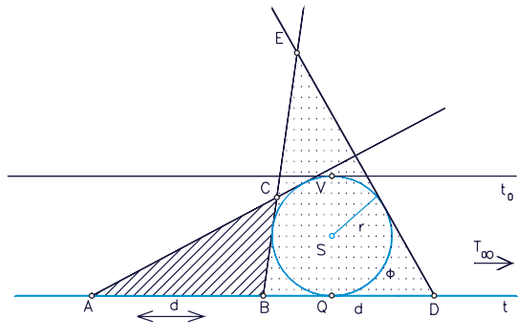

Figure 1

Before we continue with the traces of some points within triangle, let us focus onto some special triangles within a family $\mathcal{T}_{(r,d)} \in \mathbf{T}$. Following the similar approach as in [1], the position of those triangles with respect to Φ and t will play an important role in the determination of the traces of the triangle points within the family. The special triangles are degenerated triangle with one of the vertices lying on the given circle Φ or at the infinity. Hereafter, let Q be the contact point of Φ and t, and let t_1 be the tangent of Φ parallel to t. We distinguish the following three types of the special triangles within each family $\mathcal{T}_{(r,d)}$:

S1) If one of the vertices lying on t coincides with Q, the triangle degenerates into the segment of the length d. In each family there are two such triangles.

S2) Furthermore, it is possible that two triangle sides, having only one of the vertices on t, are parallel. Then their intersection point lies at infinity and determines the third vertex. The number of such triangles within each family depends on the relation between the given length d and the circle diameter $2r$.
For if $|d| > 2r$, we have two such triangles, if $|d| = 2r$ only one such triangle is possible, and for $|d| < 2r$ there are no real triangles satisfying this condition.

S3) If one of the points lying on t converges to the point at infinity T_∞ of the line t, then the intersection points of the tangents drawn to Φ converges to the point V, the contact point of the circle Φ and its tangent t_1 parallel to t.

Hence, in the first two cases we have the classes of special triangles obtained by varying d within the set $\mathbf{T}$. Interestingly, in the case S3 only one such triangle remains fixed within all families $\mathcal{T}_{(r,d)}$.

The aim of this paper is to examine the traces of some triangle points within the specified tangential families of triangles. The results will be presented analytically and their analysis will be provided by the use of the three classes of degenerated triangles. Furthermore, the connection between the given elements and obtained curves is studied.

The constructions in this work are done by *The Geometer's Sketchpad* and the computations with *Mathematica*.

In the section 2 it will be shown that the specified tangential families, which are subject to the present paper, belong to the special poristic families of triangles, [2]. The third triangle vertex lies on the conic which hyperosculates the given cirlce Φ at the point V. Since the triangle vertices are running on a singular cubic curve while the three lines spanned by the respective vertices envelope a circle, the triangles within a family $\mathcal{T}_{(r,d)}$ are triangles with a certain circumscribed degenerated cubic curve (a conic section and line t) tangential to the given circle Φ.

2 The locus of C

Naturally, we will start with the locus of the third triangle vertex, not lying on the tangent t. For $d \in \mathbb{R}$, let a familiy $\mathcal{T}_{(r,d)} \in \mathbf{T}$ be given.

Without loss of generality we can assume that the circle Φ and the tangent t are given by the equations

$$\Phi: \quad x^2+y^2=r^2, \qquad t: \quad y=-r. \tag{1}$$

Let $\Delta ABC \in \mathcal{T}_{(r,d)}$. Aiming at parametrization of the third vertex C, not lying on the given tangent t, let us denote the vertex A of ΔABC by A_λ given by $A_\lambda(\lambda,-r), \lambda \in \mathbb{R}$.

The third vertex C_λ is uniquely determined as the intersection point of the tangents drawn from A_λ and $B_\lambda = (\lambda+d,-r)$ to the given circle Φ. Its homogeneous coordinates depend on the the parameter λ and reads

$$C_\lambda = \Big(r^2(2\lambda+d) : r\big(\lambda(\lambda+d)-r^2\big) : \lambda(\lambda+d)+r^2\Big). \tag{2}$$

Thus, the one–parameter family of triangles $\mathcal{T}_{(r,d)}$ is described with λ as well, i.e. $\mathcal{T}_{(r,d)} = \{\Delta_\lambda ABC : \lambda \in \mathbb{R}\}$.

Our first goal is to describe the locus curve Γ_d of the vertex C which obviously lies on some conic. Note that Γ_d is symmetric with respect to the circle diameter perpendicular to t. For verifying that, let (T_∞) be the pencil of lines with vertex $T_\infty, T_\infty \in t$. Every line line $q_i \in (T_\infty)$ carries at most two triangle vertices of the family $\mathcal{T}_{(r,d)}$. For, if $C_\lambda \in q_i$, such that $\Delta_\lambda ABC \in \mathcal{T}_{(r,d)}$, then the triangle $\Delta_{-\lambda-d}ABC$ also lies in $\mathcal{T}_{(r,d)}$ having $C_{-\lambda-d} \in q_i$. Namely, if $\alpha_i := \angle A_\lambda C_\lambda B_\lambda$, then the locus of points where the circle Φ is seen under the same angle α_i is the concentric circle $\Phi_i(S,|SC|)$. The intersection points of q_i and Φ_i are the vertices C_λ and $C_{-\lambda-d}$. Furthermore, $\Delta_\lambda ABC \cong \Delta_{-\lambda-d}BCA$ and they are symmetric with respect to the axis $o_t \ni S$, $o_t \perp t$ (see Fig. 2).

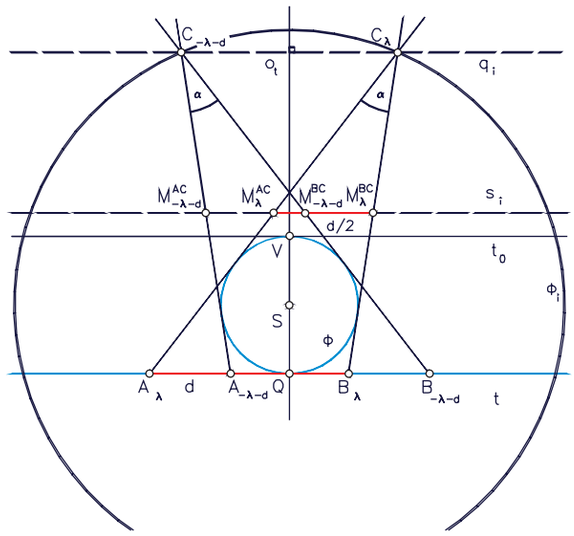

Figure 2

For $\lambda = -\frac{d}{2}$ the vertex C_λ lies on o_t, the both intersection points of the line $q_i \in (T_\infty)$ and Φ_i coincide and the line q_i is the tangent to the conic Γ_d with the vertex $C_{-\frac{d}{2}}$. The associated triangle $\Delta_{-\frac{d}{2}}ABC \in \mathcal{T}_{(r,d)}$ is an isosceles triangle. Especially, for $d = 2r$ such an isosceles triangle degenerates and one vertex coincides with the ideal point of the axis of symmetry o_t.

Before we derive an implicit equation of this curve let us determine the coordinates of the vertices of the special triangles given with S1–S3. Hence, we get for $\lambda \in \{0, -d\}$ the vertices $C_0 = (d, -r)$ and $C_{-d} = (-d, -r)$ lying on the tangent t. From (2) the coordinates of the vertices C_λ lying at infinity are given with $\lambda = \lambda_1$ or $\lambda = \lambda_2$, where

$$\lambda_{1,2} := \frac{-d \mp \tau}{2}, \quad \tau := \sqrt{d^2 - 4r^2}. \tag{3}$$

Thus, one distinguishes three cases depending on the number of triangles $\Delta ABC \in \mathcal{T}_{(r,d)}$ with the vertex C at infinity. They all depend on the relation between the circle diameter and given length d. Therefore, for the vertex C of the triangle $\Delta ABC \in \mathcal{T}_{(r,d)}$, we have:

i) if $d \geq 2r$, the two vertices $C_{\lambda_{1,2}} = (\tau : \mp 2r : 0)$ are lying on f and Γ_d is a hyperbola;

ii) if $d = 2r$, only one such vertex $C_{\lambda_1} = C_{\lambda_2} = (0 : 1 : 0)$ lies on f and Γ_d is a parabola;

iii) if $d < 2r$ there are no real vertices on f and Γ_d is an ellipse.

When $\lambda \to \pm\infty$, as a limiting point of (2) we get $C \to C_\infty = V = (0, r) \in \Phi \cap t_1$, and the circle tangent t_1 is given with

$$t_1 : \quad y = r, \quad t_1 || t. \tag{4}$$

The third case S3 determines one of the vertices V of the conic Γ_d lying on the axis o_t. The line t_1 given by (4) is then the common tangent of the conic Γ_d and given circle Φ. It remains fixed for all tangential families of triangles within the set $\mathbf{T}$. For $d \neq 0$, the point V is the only common point of the conics Φ and Γ_d. A one–parameter family of conics $\mathbf{P} = \{\Gamma_d : d \in \mathbb{R}\}$, obtained by varying d, belongs to the pencil of hyperosculating conics. We can see that this pencil is uniquely determined with two of its conics, the given circle Φ and the only degenerated conic within the pencil, two coinciding lines t_1.

Similar observations can be obtained by deriving the implicit equation of the required locus of the vertex $C(x, y)$ of the triangle $\Delta ABC \in \mathcal{T}_{(r,d)}$ from (2). It turns out to be a conic Γ_d given by

$$\Gamma_d : d^2(y - r)^2 - 4r^2(x^2 + y^2 - r^2) = 0. \tag{5}$$

For a given circle Φ and tangent t, all three types of hyperosculating conics Γ_d within the one–parameter family $\mathbf{P}$ obtained by varying d are shown in Fig. 3.

Thus we have:

Theorem 1 *Assume we are given a circle $\Phi(S, r)$, one of its tangents t, and a segment AB of length $d \in \mathbb{R}$ lying on t.*

The locus Γ_d of the vertex C such that $\Delta ABC \in \mathcal{T}_{(r,d)}$ is contained in the pencil of conics hyperosculating Φ at V, where $V \notin t$ and $o_t := VS \perp t$ is the focal axis of Γ_d. The length d serves as a parameter within the pencil.
The conic Γ_d is an ellipse, a parabola, or a hyperbola iff $|d| < 2r$, $|d| = 2r$, or $|d| > 2r$.

Let us conclude this section with another formulation of Theorem 1 which shows an interesting loci property of conic:

Proposition 1 *For given circle Φ the set of all points X such that the tangents drawn to Φ cut at one of its fixed tangent segments of equal length is a conic $\mathcal{C}$ that hyperosculates Φ.*

3 Some locus curves

As a result of the similarity of the triangles $\Delta_\lambda ABC$ and $\Delta_{-\lambda-d}ABC$ within the family $\mathcal{T}_{(r,d)} = \{\Delta ABC : \lambda \in \mathbb{R}\} \in \mathbf{T}$, the traces of the triangle centers lie on the symmetric curves with respect to the axis of symmetry o_t perpendicular to t. Many triangle points lie on the symmetric curves as well but their axis of symmetry may not coincide with o_t.

In what follows the traces of one such triangle point (the side midpoint) is analyzed, as well as the trace of one triangle center, the triangle circumcenter.

3.1 The midpoint M_{AC}

Let $d \in \mathbb{R}$ and a tangential family $\mathcal{T}_{(r,d)} \in \mathbf{T}$ be given. For $\Delta ABC \in \mathcal{T}_{(r,d)}$, let the vertices A and B lie onto t. The midpoints of the variable sides AC and BC trace the corresponding curves Ψ_d^{AC} and Ψ_d^{BC}. Since $\Gamma_d \equiv \Gamma_{-d}$ and $\Psi_d^{AC} \equiv \Psi_{-d}^{BC}$, the curves Ψ_d^{AC} and Ψ_d^{BC} are symmetric with respect to the axis o_t. Thus, in what follows only the the locus of the midpoints of the side variable side AC of the triangle ΔABC is given.

If the circle Φ and tangent t are given with (1), starting with the special triangles within the family $\mathcal{T}_{(r,d)}$ we can easily calculate the midpoints $M_{-d}^{AC} = (-d,-r)$ and $M_0^{AC} = (d/2,-r)$ in the case S1, the midpoints $M_{\lambda_{1,2}} = C_{\lambda_{1,2}} = (\tau : \mp 2r : 0)$ in the case S2, and the midpoint $M_\infty = T_\infty = (1:0:0)$ lying at infinity and obtained as the limiting point in the case S3.

Obviously, Ψ_d^{AC} is a symmetric cubic. For each line $q_i \in (T_\infty)$ let an involution in the pencil of lines (T_∞) having the lines t and q_i for its double lines be given. Then there is the line $s_i \in (T_\infty)$ associated to the line f at infinity such that the lines $(t,q_i;f,s_i)$ are harmonically related (see Fig. 2). Furthemore, in the previous section to the line q_i of the pencil (T_∞) two triangles $\Delta_\lambda ABC$ and $\Delta_{-\lambda-d}ABC$ are associated, if the vertices $C_\lambda, C_{-\lambda-d}$ are lying on it. Since the midpoints M_λ^{AC} and $M_{-\lambda-d}^{AC}$ are also symmetric with respect to the axis o_t, the midpoints $M_{-\lambda-d}^{AC}$ and $M_{-\lambda-d}^{BC}$ lying on $s_i \in (T_\infty)$ are at the distance $\frac{d}{2}$, the midsegment length of all tangential triangles within $\mathcal{T}_{(r,d)}$. Thus, the midpoints M_λ^{AC} and $M_{-\lambda-d}^{AC}$ are symmetric with respect to the axis o_M parallel to o_t and $d(o_t,o_M) = \frac{d}{4}$.

The obtained curve has a vertex lying on axis o_M associated to the isosceles triangle when $\lambda = -\frac{d}{2}$ and it coordiantes are given with $M_{-\frac{d}{2}} = \left(-\frac{d}{4}, \frac{4r^3}{\tau^2}\right) \in o_M$. The other intersection point with the axis o_M determines the double point of the midpoint trace and reads $M_{\lambda_{3,4}} = \left(-\frac{d}{4}, \frac{r}{2}\right)$ for $\lambda_{3,4} = \frac{-d \pm \sqrt{d^2-12r^2}}{2}$. Therefore, the cubic Ψ_{AC} has a cusp at $M_{\lambda_{3,4}}$ exactly if $d^2 = 12r^2$. If $d^2 < 12r^2$, $M_{\lambda_{3,4}}$ is an isolated double point.

Furthermore, since the midpoint M_∞ is the limiting point in S3 for all $d \in \mathbb{R}$ as $\lambda \to \pm\infty$, the line $t_0 \in (T_\infty)$ passing through M_∞ is the common asymptote for the curves Ψ_d^{AC} of the one–parameter family $\mathbf{G}^{AC} = \{\Psi_d^{AC} : d \in \mathbb{R}\}$ obtained by varying d. Since $(t,t_1;f,t_0)$ are harmonically related, it follows that t_0 passes through the circle center S.

Thus, we have shown:

Theorem 2 *The midpoint of the variable triangle side AC such that $\Delta ABC \in \mathcal{T}_{(r,d)}$ lies on a rational symmetric cubic Ψ_d^{AC} asymptotic to a line t_o which is parallel to the given tangent t and passes through the circle center S.*
It has a cusp at the double point if $d^2 = 12r^2$, a node if $d^2 > 12r^2$ and an isolated double point if $d^2 < 12r^2$.

An elementary computation using the equations of the triangle sides yields the homogenous coordinates of the triangle midpoints M_λ^{AC} as

$$M_\lambda^{AC}\left(\lambda^2(d+\lambda)+(d+3\lambda)r^2 : -2r^3 : 2\big(\lambda(\lambda+d)+r^2\big)\right) \tag{6}$$

if the circle Φ and the tangent t are given by (1). The equation of the cubic parameterized by (6) in terms of Cartesian coordinates reads

$$\Psi_d^{AC} : y^3(d^2-4r^2) = r\left(d^2y^2 + r\Big(2x(d+2x)-3r^2\Big)y + r^4\right). \tag{7}$$

The triangle family can be used for the parametrization of the locus and also for solving some complex problems whose computation cannot be done in an acceptable amount of time using computers. For example, the determination of the intersection points of the cubic Ψ^d and a circle Φ follows easily using the properties of the isosceles triangles. The midpoint M_λ^{AC} lies on the given circle Φ precisely when it coincides with one of the point of tangency of the inscribed (or escribed) circle Φ of the triangle ΔABC lying on the line AC. This is the case when $\det(S, M_\lambda^{AC}, B_\lambda) = 0$ where S is the center of Φ, i.e. when λ satisfies the following equality $\lambda^3 \cdot r + \lambda^2 \cdot dr + \lambda \cdot r^3 - dr^3 = 0$. Hence, the cubic Ψ_d^{AC} touches the given circle Φ once, or three times (see Fig. 3).

3.2 The circumcenter O

Again, for $d \in \mathbb{R}$, let a family $\mathcal{T}_{(r,d)} \in \mathbf{T}$ be given. Furthermore, let Υ_d be the locus of the circumcenter O_λ^d of a triangle $\Delta_\lambda ABC \in \mathcal{T}_{(r,d)}$. Since the circumcenter O_λ^d can be calculated as the intersection point of the perpendicular bisectors of the sides AC and AB, if the circle Φ and tangent t are given with (1), it yields

$$\begin{aligned} O_\lambda \;=\; & \Big(2r(d+2\lambda)\big(\lambda(\lambda+d)+r^2\big) : \lambda^2(\lambda+d)^2 - \\ & - r^2\Big((\lambda+d)^2+\lambda^2\Big) - 3r^4 : 4r\lambda\big((\lambda+d)+r^2\big)\Big) \end{aligned} \tag{8}$$

which parameterizes the rational symmetric quartic Υ_d with equation

$$\Upsilon_d : \left(4x^2 - 8r\cdot y - (d^2+4r^2)\right)^2 = 16r^2\left(d^2+4(r+y)^2\right) \tag{9}$$

Similar observations can be provided by the use of the tangential family $\mathcal{T}_{(r,d)}$ as well as the further analysis of the obtained curve.

Using the special triangles within the family we get the following. To the degenerated triangles $\Delta_{-d}ABC$ and $\Delta_0 ABC$ in S1 the circumcenters $O_0 = \left(\frac{d}{2}, -\frac{1}{4r}(d^2+3r^2)\right)$ and $O_{-d} = \left(-\frac{d}{2}, -\frac{1}{4r}(d^2+3r^2)\right)$ are associated lying at the perpendicular bisectors of the segment AB. They are symmetric with respect to the axis of symmetry o_t.

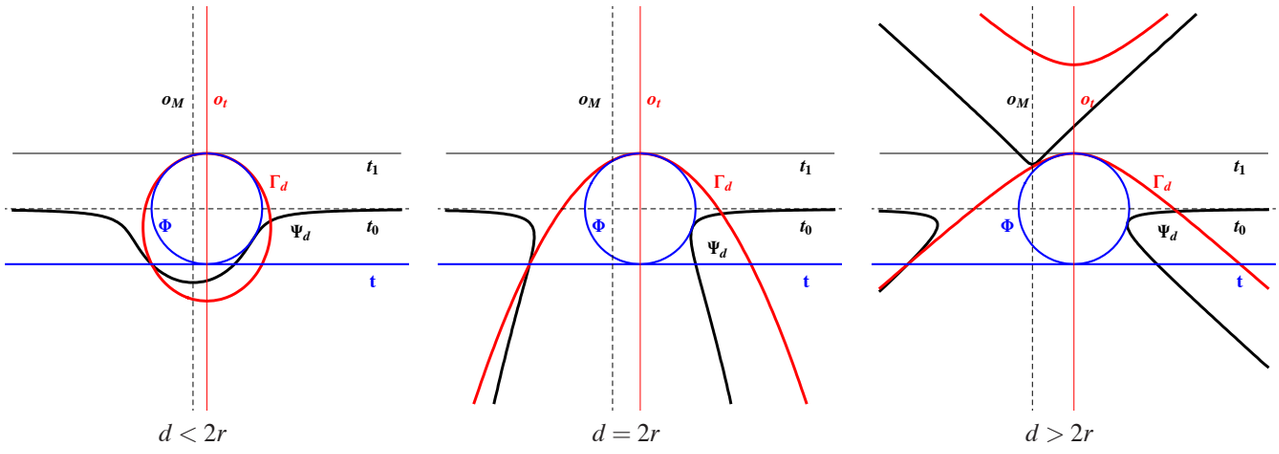

Figure 3

In S2, we get the circumcenters $O_{\lambda_1} = O_{\lambda_2} = O_\infty = (0:1:0)$, where λ_1 and λ_2 are given with (3), coinciding with the ideal point O_∞ of o_t. It is the cuspidal point of a quartic if $d^2 = 4r^2$, the nodal point if $d^2 > 4r^2$ and the isolated point if $d^2 < 4r^2$. In the case S3, as λ converges to the infinity, the circumcenter converges to the point O_∞ as well. Thus, it is actually the triple point of Υ_d belonging also to the circumcenter of the special triangle $\Delta_\infty ABC$ at which the line f touches the obtained symmetric quartic.

We can state:

Theorem 3 *The circumcenter O^d of the triangle $\Delta ABC \in \mathcal{T}_{(r,d)}$ lies on a rational symmetric quartic Υ_d with a triple point at infinity. It is the cuspidal point if $d^2 = 4r^2$, the nodal point if $d^2 > 4r^2$ and the isolated point if $d^2 < 4r^2$. One of the tangents at the quartic triple point is the infinity line, while the other two are perpendicular to the given tangent t.*

Fig. 4 displays some conics Γ_d of the one–parameter family $\mathbf{P} = \{\Gamma_d : d \in \mathbb{R}\}$ and associated quartics Υ_d belonging to the one–parameter family $\mathbf{O} = \{\Upsilon_d : d \in \mathbb{R}\}$. Those curve appear as traces of a circumcenter and vertex of a tangential triangle ΔABC within the family $\mathcal{T}_{(r,d)}$ associated to the given circle Φ and its tangent t for some real number d.

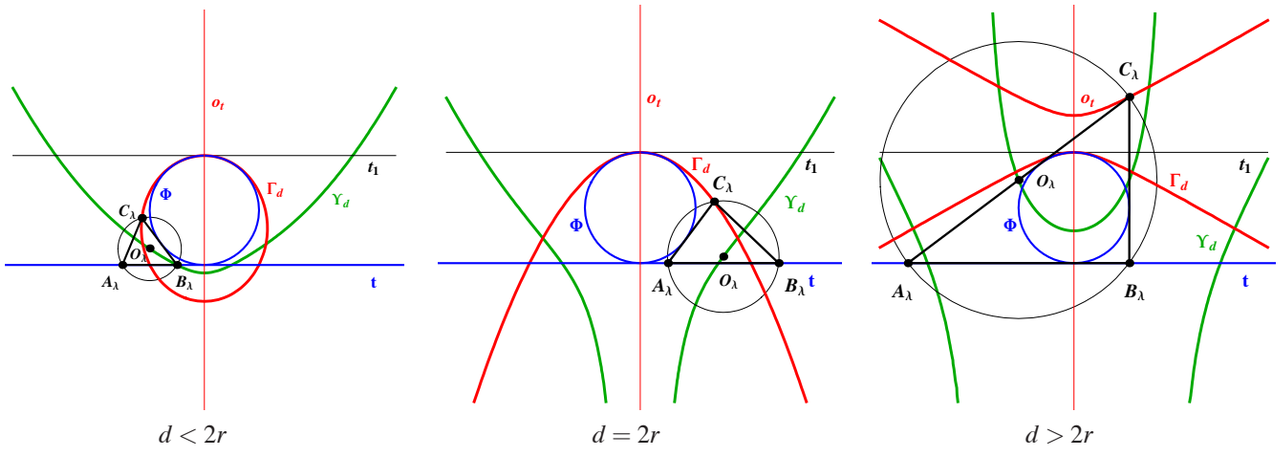

Figure 4

References

[1] A. SLIEPČEVIĆ, H. HALAS, Family of triangles and related curves, *Rad HAZU* (to apear)

[2] B. ODENHAL, Poristic Loci of Triangle Centers, *Journal for Geometry and Graphics* **15 (1)** (2011), 45–67

[3] P. PAMFILOS, Triangles with Given Incircle and Centroid, *Forum Geometricorum* **11** (2011), 27–51

Nikolina Kovačević
e-mail: nkovacev@rgn.hr
Faculty of Mining, Geology and Petroleum Engineering, University of Zagreb
Pierottijeva 6, 10000 Zagreb, Croatia

Ana Sliepčević
e-mail: anas@grad.hr
Faculty of Civil Engineering, University of Zagreb
Kačićeva 26, 10000 Zagreb, Croatia

Original scientific paper
Accepted 18. 12. 2012.

MARIJANA BABIĆ
SRĐAN VUKMIROVIĆ

Central Projection of Hyperbolic Space onto a Horosphere

Central Projection of Hyperbolic Space onto a Horosphere

ABSTRACT

Horosphere is surface in hyperbolic space that is isometric to the Euclidean plane. In order to correctly visualize hyperbolic space we embed flat computer screen as horosphere and investigate geometry of central projection of hyperbolic space onto horosphere. We also discuss realization of hyperbolic isometries. Corresponding algorithms are implemented in Mathematica package *L3toHorospere*. We briefly present the package and obtain some interesting pictures of hyperbolic polyhedra.

Key words: hyperbolic space, horosphere, central projection

MSC 2000: 00A66, 51M10

Centralna projekcija hiperboličkog prostora na horosferu

SAŽETAK

Horosfera je ploha u hiperboličkom prostoru izometrična euklidskoj ravnini. Kako bismo vjerno prikazali hiperbolički prostor, ravni ekran smjestili smo kao horosferu, a zatim istraživali geometriju centralnog projiciranja hiperboličkog prostora na horosferu. Također smo proučavali realizaciju izometrija hiperboličkog prostora. Odgovarajući su algoritmi implementirani u Mathematica paketu *L3toHorospere*. Dan je kratak prikaz tog paketa i dobivene su zanimljive slike hiperboličkih poliedara.

Ključne riječi: hiperbolički prostor, horosfera, centralna projekcija

Introduction

Hyperbolic geometry (or geometry of Bolyai - Lobachevskii) is together with spherical geometry the simplest "curved" geometry. Hyperbolic plane, usually denoted by H^2, is usually visualized using various models of hyperbolic plane. Poincaré disk, Klein disk and half-plane model are the best known models of hyperbolic plane.

In the Figure 1, obtained using Mathematica package [10], the red triangle, together with three triangles obtained by reflection with respect to its edges are shown in those three models. Note, that in all pictures, all four triangles are mutually congruent in hyperbolic plane. A region of hyperbolic plane is not isometric to a region of "flat", Euclidean plane. This means that it is not possible to represent, without distortions, a region of hyperbolic plane on a flat computer screen.

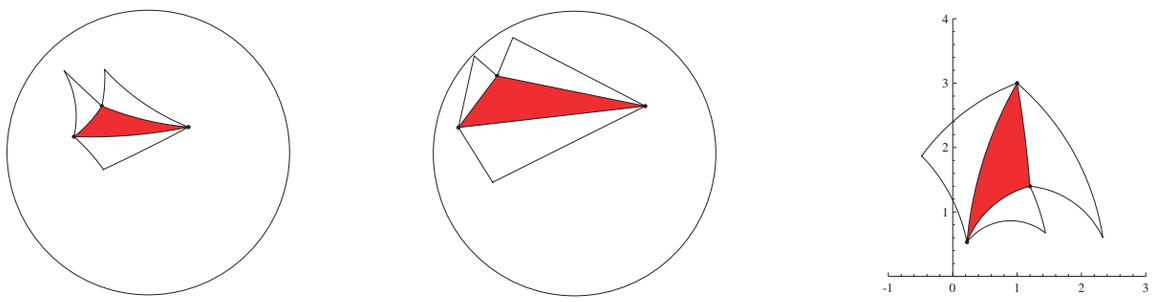

Figure 1: *The same objects in various models of hyperbolic plane*

Therefore, hyperbolic metric of model is not inherited from the Euclidean plane: distances become infinitely big near absolute (unit circle in the first two models and x-axis in the third model). Although to our eyes the absolute is finite, it represents infinity of the hyperbolic plane.

For hyperbolic space H^3 there exist analogous models: Poincaré ball, Klein ball and half-space model. Two approaches for visualization of the hyperbolic space have been used so far, and both approaches at least in one instance use some model.

The first is to represent a geometrical object in some model of hyperbolic space in $\mathbb{R}^3$ and then to project it onto computer screen by standard central projection of $\mathbb{R}^3$. This approach was used in the famous movie *Not knot* ([6]). This is also used a popular way of visualizing large graph objects and the structure of world wide web (see [7] and others). Probably the most famous visualizations of hyperbolic space so far are done by J. R. Weeks ([11, 12]) and use this approach.

The second approach is to fix a hyperbolic plane H^2 in hyperbolic space L^3, project the space onto H^2 by means of central projection in L^3 and finally visualize the plane H^2 using some model on the computer screen. In the master thesis [1] the author develops ray tracing algorithm for hyperbolic space and uses this approach for visualization.

In this paper we take a different approach. We wonder: how would hyperbolic space look like to us, if we were there? Equivalently, in terms of computer graphics: how would the picture look like if we isometrically embed our flat computer screen into H^3, project the hyperbolic space on the screen by means of central projection in H^3 and then watch the picture on the screen without any distortions and models?

The mathematical answer was well known to very founders of hyperbolic geometry: there is a peculiar surface in H^3, called horosphere, which is isometric to Euclidean plane. Therefore, if we isometrically embed a flat, Euclidean screen in hyperbolic space it may become a part of horosphere. In this paper we discuss necessary mathematical background regarding central projection of hyperbolic space onto horosphere, as well as, isometric transformations of the hyperbolic space. The final result is Mathematica package L3toHorosphere that allows visualization of H^3 by means of central projection onto horosphere and also visualization of hyperbolic motions. Using this package many interesting pictures and animations are obtained (see [3]).

On our request, Prof. Emil Molnár informed us that Prof. Imre Juhász (the head of Department of Descriptive Geometry of the University of Miskolc) dealt with a similar topic in his awarded Scientific Student Circle (OTDK) paper (in 1979) and in his diploma work (1978) at the Debrecen University, without any scientific publication on this topic, later on.

It is also worth mentioning that methods of Descriptive geometry in hyperbolic space have also been investigated (see [8, 9]).

Description of hyperbolic isometries is mathematically simple and found in many classical books, but when it comes to practical implementation the paper [5] is usually used. In this work we briefly cover this topic using slightly different approach that someone may find easier to understand.

The paper is organized as follows. In the first section we give a brief overview of models of hyperbolic space. In the second section we study horosphere and central projection onto horosphere. The third section is devoted to implementation of isometries of hyperbolic space. In the fourth section we give some examples of projections and animations obtained using package L3toHorosphere. In the last section we compare various approaches in visualizing hyperbolic geometry and give some ideas for future work.

Authors would like to thank Prof. Emil Molnár for useful discussions and for careful reading which significantly improved the final version of the paper.

1 Models of hyperbolic space

1.1 Klein ball and projective model

Klein ball model $\{P(x,y,z)\,|\,x^2+y^2+z^2<1\}$ is interior of unit sphere in $\mathbb{R}^3$. The unit sphere is absolute of this model. This means that points of unit sphere represent points in infinity of the hyperbolic space. Hyperbolic lines and planes are parts of Euclidean lines and planes. The distance between points P and Q is given by the formula

$$d(P,Q)=\frac{1}{2}\log\frac{|QA||PB|}{|PA|QB|}, \tag{1}$$

where A and B are endpoints of the chord containing P and Q and $|\cdot|$ denotes the Euclidean distance.

Klein ball model is closely related to Klein projective model or pseudosphere model. Namely for point $P(x,y,z)$ from the Klein model, one can consider homogenous coordinates $P(x:y:z:1)$. There are unique coordinates $\bar{P}(x_1,x_2,x_3,x_4)$ representing the same point and satisfying the relation

$$-x_1^2-x_2^2-x_3^2+x_4^2=1, x_4>0. \tag{2}$$

This means that one can regard hyperbolic space as pseudosphere (2) in Minkowski vector space $\mathbb{R}^{(3,1)}$, with inner product $\cdot$ given by matrix $J=diag(-1,-1,-1,1)$.

It is interesting that formula (1) for distance translates into

$$d(P,Q) = \cosh^{-1}(\bar{P}\cdot\bar{Q}),$$

where $\bar{P}(x_1,x_2,x_3,x_4)$ and $\bar{Q}(y_1,y_2,y_3,y_4)$ are coordinates of these points. Therefore, the isometries of Klein projective model are those projective transformations that preserve the pseudosphere, i.e. the inner product given by matrix J. The importance or this model is its linear nature: the lines and planes are linear and isometries are represented as multiplication of vectors by 4×4 matrices that belong to classical linear group $SO(3,1)$.

1.2 Half-space model

Half-space model consists of all points $P(x,y,z)$ from $\mathbb{R}^3$ satisfying the relation $z>0$. The plane $z=0$ is absolute of this model. Hyperbolic lines are half-circles orthogonal to the absolute (i.e. with center on the absolute and lying in a plane orthogonal to the absolute) and Euclidean rays orthogonal to the absolute. Planes of this model are half-spheres and half-planes orthogonal to the absolute. To be mathematically correct, we add single infinite point P_∞ to $\mathbb{R}^3$. This point compactifies $\mathbb{R}^3$ to sphere S^3 whereas the absolute $z=0$ becomes two-dimensional sphere, like absolute in the other two models. Each plane and each line in $\mathbb{R}^3$ can be regarded as sphere and circle, containing P_∞. The distance in this model is best described using the metric tensor

$$ds^2 = \frac{dx^2+dy^2+dz^2}{z^2}. \tag{3}$$

The isometries are compositions of reflections and inversions with respect to hyperbolic planes. We are interested in half-space model since the horosphere has its simplest representation in this model, as we show in the sequel.

1.3 Poincaré ball model

Poincaré ball model $\{P(x,y,z)\,|\,x^2+y^2+z^2<1\}$ is the interior of unit sphere in $\mathbb{R}^3$. The unit sphere is absolute of this model. Hyperbolic Lines are parts of circles orthogonal to the absolute and parts of lines orthogonal to the absolute (i.e. passing through the origin). Hyperbolic planes are parts of spheres orthogonal to the absolute and parts of planes orthogonal to absolute. The metric tensor reads

$$ds^2 = \frac{dx^2+dy^2+dz^2}{(1-x^2-y^2-z^2)^2}.$$

The isometries are compositions of reflections and inversions with respect to hyperbolic planes. The mapping

$$f(x,y,z) = (2(x,y,z))/(1+x^2+y^2+z^2) \tag{4}$$

is isometry that maps point $P(x,y,z)$ from Poincaré to Klein model. Isometry between Poincaré ball model and half-space model is simple composition of translations and spherical inversion

$$g(x,y,z) = \frac{1}{x^2+y^2+(z-1)^2}(4x,4y,2(1-x^2-y^2-z^2)). \tag{5}$$

2 Horosphere and the related central projection

2.1 Horosphere

Fix a point O on absolute and point $M\in H^3$. Horosphere (with center O containing point M) is set of images of point M in reflections with respect to all planes containing O. Note that, if O is finite point and M' is image of M then OM is congruent to OM' and the horosphere is hyperbolic sphere with center O. Therefore, one may think of horosphere as of sphere with center in infinity.

From construction of horosphere it follows that all horospheres are mutually congruent in H^3. We want to find the the simplest one in some model. Consider point P_∞ of the half-plane model as center of horosphere, and any finite point $M(x_0,y_0,z_0)$ of that model. All hyperbolic planes through P_∞ are exactly all Euclidean half-planes orthogonal to the absolute $z=0$. Therefore, all images M' of M have the same $z-$coordinate and the horosphere is the plane $z=z_0$. Note that this special horosphere touches the absolute in point P_∞. Since isometries are compositions of inversions and reflections, all horospheres of half-space model are Euclidean spheres that touch the absolute in its center, or planes parallel to the absolute.

From the isometries (4) and (5) between models we conclude that horospheres in Poincaré ball model are spheres touching the absolute in their center and in Klein ball model ellipsoids touching the absolute. The most simple horosphere $z=z_0$ in half-space model has restriction of the metric tensor (3) equal to

$$ds^2 = \frac{dx^2+dy^2}{z_0^2},$$

showing that the horosphere is isometric to the Euclidean plane, up to a scale. Since in this case the isometry between horosphere and Euclidean plane is given by the imbedding itself, the setup consisting of half-space model and horosphere $z=z_0$ is the one we use for implementation of the central projection.

Reparameterizing, one can write metric (3) in the form:

$$ds^2 = e^{\frac{2t}{k}}\left(dx^2+dy^2\right)+dt^2,$$

where $k > 0$ is the the curvature constant (in our case $k = 1$). This is so called horospherical coordinate system of the hyperbolic space H^3 , which consists of "concentric" horospheres, parameterized by the real line, $t \in \mathbb{R}$. In each horosphere we have Euclidean plane coordinates (x, y). This was the basic idea for distance measure of János Bolyai in his absolute geometry (in nowadays formulation, Lobachevskii distinguished the non-Euclidean case from the beginning), introduced without any model.

2.2 Central projection onto horosphere

We have shown that we can embed flat computer screen into hyperbolic space as a part of horosphere. What would an observer see on the screen if he is in the hyperbolic space? In any geometry, light ray carrying visual information from the object to the eye of the observer travels along geodesic, i.e. along straight line of that geometry. Klein model is the the easiest to sketch, since the hyperbolic lines of that model are parts of Euclidean lines. If we place the observer O outside the horosphere (see Figure 2, left) some points cannot be projected (point N) while others have two possible projections along the light ray (point M). On the other hand, if we place the observer inside the horosphere (see Figure 2, right) the projection is well defined for all points of hyperbolic space. For this reason, we chose that observer is inside the horosphere, although it is possible to consider the other case.

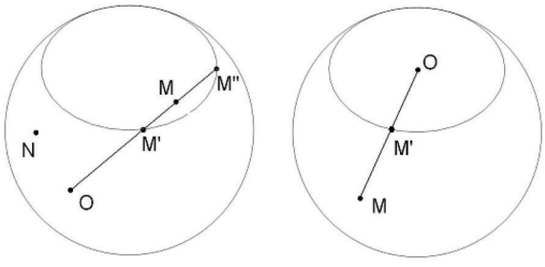

Figure 2: *Observer outside and inside the horosphere.*

In the half-space model, the point $O(x, y, z)$ is inside the horosphere $z = z_0$ if the condition $z > z_0$ holds. Particular coordinates of point O doesn't matter, so we can chose $O(0, 0, \omega)$, $\omega > z_0$.

Note that all points of half-space model are projected into finite points of horosphere $z = z_0$, except points M of the form $M(0, 0, z), z > \omega$ that are projected into point P_∞, the infinite point of the horosphere (i.e. screen).

2.3 Central projection of hyperbolic line segment

In order to visualize polyhedra in hyperbolic space we have to understand the projection of hyperbolic line segment. The line segment is projected into intersection of horosphere and the hyperbolic plane determined by the center of projecection O and the segment. For our purposes it is sufficient to consider half-space model, horosphere $z = z_0$ and the point $O(0, 0, \omega), \omega > z_0$.

Recall that hyperbolic line segment is either Euclidean segment orthogonal to the absolute or circular arc orthogonal to the absolute. The following cases are possible:

1. If hyperbolic segment is circular arc AB then hyperbolic plane containing A, B and O is half-sphere. The projection of the segment belongs to intersection of the half-sphere and the horosphere. It is circular arc $A'B'$ in horosphere $z = z_0$ (see Figure 3).

2. If hyperbolic segment is an Euclidean segment AB orthogonal to absolute then the hyperbolic plane OAB is Euclidean half-plane. The central projection of segment AB is

   a) Euclidean segment $A'B'$ if segment AB have no common point with $z-$axis above O (that is point $(0, 0, z), z > \omega$;

   b) Euclidean ray starting from A' if B is of form $B(0, 0, z), z > \omega$. This ray belongs to the intersection line of α and horosphere;

   c) Two disjoint Euclidean rays starting from A' and B' and belonging to the intersection line of α and horosphere. This happens if segment AB has one inner point of the form $(0, 0, z), z > \omega$;

   d) Empty set if segment AB is contained in the set $\{(0, 0, z) \mid z > \omega\}$.

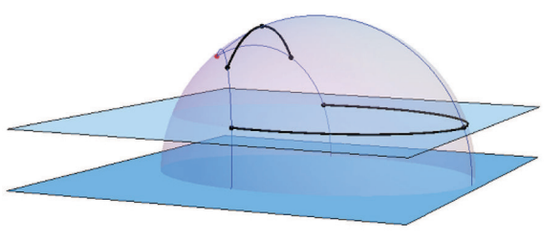

Figure 3: *Central projection of hyperbolic line segment.*

Note that that there are two circular arcs in horosphere $z = z_0$ with endpoints A' and B'. Therefore, to determine uniquely the projection of segment AB we need the projection C' of some point C belonging to the segment AB. Similar holds for Euclidean ray with the endpoint A'.

2.4 Visibility

We assume that polyhedra consists of faces that are not transparent. Therefore, not all vertices and edges are visible from the center of projection O. We may draw nonvisible edges as dashed lines to improve spacial understanding of the polyhedra (see for example Figure 5). Visibility in Klein ball model coincides with Euclidean visibility. Therefore, to determine the visibility one can use the standard algorithms from $\mathbb{R}^3$.

In reality, the human eye sees the part of scene that is inside the cone of vision. In computer graphics this translates into clipping. In this work we don't mind about cone of vision and consider mathematical central projection of polyhedra, i.e. we project points at the front, as well as, at the back of the observer. However, in our package [4] there is an option to draw the circle that separates front and back of the observer. That circle is the intersection of half-sphere with center $(0,0,0)$ and radius ω and horosphere $z = h < \omega$.

In Figure 11 (a) this is the black circle. The observer is inside the blue cube, so all its edges are visible, but some part of the cube is in the front and some part is in the back of the observer.

3 Isometries of hyperbolic space

The isometries of hyperbolic space are mathematically well known. The fastest and most elegant way to implement the isometries is to represent them as 4×4 matrices that are applied to column vectors of homogenous coordinates of points in Klein projective model. The homogenous coordinates are of the form $P(x_1 : x_2 : x_3 : x_4)$, where homogeneity means that coordinates $(\lambda x_1 : \lambda x_2 : \lambda x_3 : \lambda x_4)$, for each $\lambda \neq 0$ represent the same point.

As explained in Subsection 1.1 the isometries of Klein model belong to linear group $SO(3,1)$. They are linear mappings preserving Minkowski inner product, i.e. matrix A of an isometry satisfies $A^T J A = J$, where $J = diag(-1,-1,-1,1)$ is diagonal matrix of the inner product. Any hyperbolic isometry is composition of less than four reflections with respect to hyperbolic planes. In this review we don't want to exhaust all isometries, so we present only isometries that are composition at most two plane reflections.

3.1 Reflection with respect to plane (or point)

Plane in the Klein projective model is represented by hyperplane in the vector space $\mathbb{R}^{(3,1)}$, so it has an equation

$$\alpha_1 x_1 + \alpha_2 x_2 + \alpha_3 x_3 + \alpha_4 x_4 = 0$$

The plane has normal vector $n_\alpha = (\alpha_1 : \alpha_2 : \alpha_3 : -\alpha_4)^T$ with respect to the inner product given by matrix J. One can show that the reflection S_α with respect to the plane α has the matrix

$$S[n_\alpha] = I_4 - 2\frac{n_\alpha {n_\alpha}^T J}{{n_\alpha}^T J n_\alpha}, \tag{6}$$

where I_4 is 4×4 identity matrix. It is important to note that the numerator $n_\alpha n_\alpha^T J$ is 4×4 matrix, while denominator $n_\alpha^T J n_\alpha$ is squared norm of vector n_α and therefore a number. Vector n_α is considered column, while n_α^T is row vector.

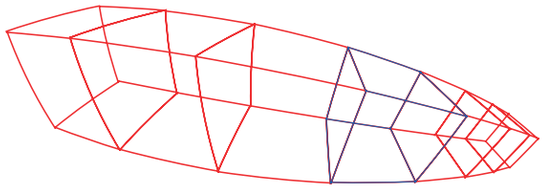

Figure 4: *Cube and its reflections*.

The Figure 4 shows consecutive reflections of the blue cube with respect to the opposite faces (red cubes).

One can show that reflection $S[P]$ with respect to point $P(x_1 : x_2 : x_3 : x_4)$ is given by the matrix

$$S[P] = I_4 - 2\frac{PP^T J}{P^T J P},$$

which uses the same formula as the reflection 6 with respect to hyperplane. The reflection $S[P]$ is formally defined as composition of three reflections $S[\gamma] \circ S[\beta] \circ S[\alpha]$ with respect to three mutually orthogonal planes α, β and γ that intersect in the point P.

The Figure 5 represents the red cube and its reflection with respect to its vertex.

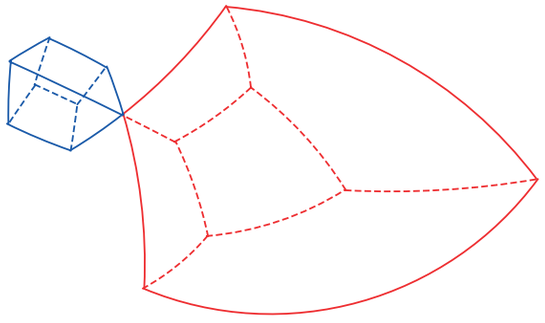

Figure 5: *Central reflection of a cube*.

3.2 Translation

Translation is composition $S[\beta] \circ S[\alpha]$ of two reflections with respect to hyperparallel planes α and β, i.e. the planes that have common normal line n, (that line is unique in hyperbolic geometry). If A and B are intersections of n with α and β, respectively, we call it translation from A to B and denote it $T[AB]$. Note that $T[AB]$ is not translation by vector AB, since the notion of vector is not possible to define in hyperbolic geometry. Many other properties of hyperbolic translation are quite different from its Euclidean counterpart. For example, we have $T[AB](A) = B$ and if $T[AB](M) = N$ then hyperbolic segments AB and MN are not congruent if $M \neq A$. Moreover, the relation $AB \leq MN$ always hold.

This is illustrated in Figure 6 which represent translation of a cube along its edge, i.e. form one vertex to another. Unlike in the Euclidean case, the face of the cube is not translated to the opposite face.

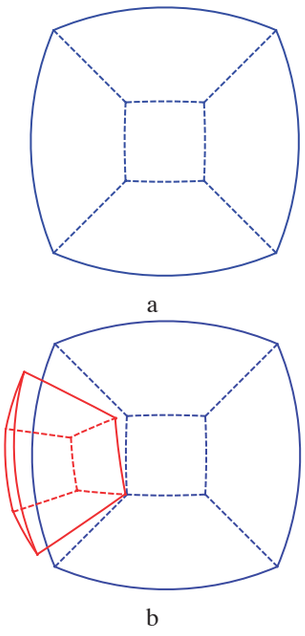

Figure 6: *Central projection of cube and its translate*.

To find matrix of translation denote by C the hyperbolic midpoint of segment AB. One can show that $T[AB] = S[\beta] \circ S[\alpha] = S[C] \circ S[A]$ and hence its matrix is product of known matrices:

$$T[AB] = S[C]S[A].$$

To find the hyperbolic midpoint C of the segment AB one can use the formula:

$$C = A\sqrt{(B^T JB)(A^T JB)} + B\sqrt{(A^T JA)(A^T JB)}.$$

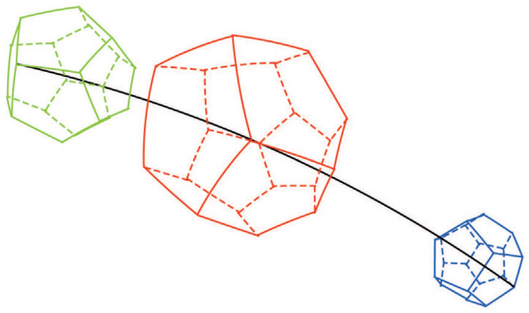

Figure 7: *Dodecahedron and its translates*.

3.3 Rotation

Hyperbolic rotation is composition $R[p,\phi] = S[\beta] \circ S[\alpha]$ of two reflections with respect to planes that intersect along axes of rotation, the line $p = \alpha \cap \beta$, and the angle between α and β equals $\frac{\phi}{2}$. From formula (1) it follows that Euclidean rotations that fix the origin $O(0,0,0)$ are also hyperbolic rotations. The consequence is that the angles in the origin of the Klein ball model are the same as Euclidean angles (this doesn't hold for any other point of Klein ball model). Therefore, to perform the rotation about line p, translate p to the origin, rotate around translated line p' as Euclidean rotation and finally translate back. To be more specific, if $Q \in p$ is any point of p, then $R[p,\phi]$ is given by the matrix:

$$R[p,\phi] = T[OQ] \circ R[p',\phi] \circ T[QO],$$

where homogenous coordinates of the origin are $O(0:0:0:1)$, $p' = T[QO][p]$, and $R[p',\phi]$ is 4×4 matrix

$$R[p',\phi] = \begin{pmatrix} R^E[p',\phi] & 0 \\ 0 & 1 \end{pmatrix}.$$

Here we denote by $R^E[p',\phi]$ the 3×3 Euclidean matrix of rotation around Euclidean line p' by angle ϕ.

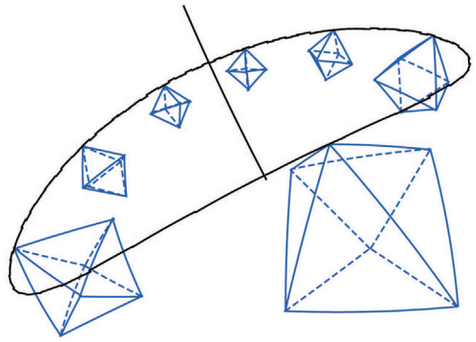

Figure 8: *Consecutive rotations of regular octahedron*.

3.4 Limit rotation

The limit or horocyclic rotation is probably the most intriguing isometry of hyperbolic plane, since it doesn't exist in Euclidean geometry. Limit rotation is composition $S[\beta] \circ S[\alpha]$ of two reflections with respect to parallel hyperbolic planes α and β, i.e. the planes with single common point on the absolute.

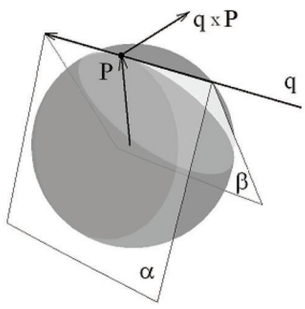

Figure 9: *Horocylic rotation in the Klein ball model.*

We now describe general formulas of limit rotation. Note that parallel planes α and β in Klein ball model are parts of Euclidean planes α and β that intersect along line q touching the absolute in point $P(x_0, y_0, z_0)$ (see Figure 9).

Planes α and β have normal vector of the form

$$P\cos\phi + (q \times P)\sin\phi = (a_1(\phi), a_2(\phi), a_3(\phi)),$$

for some $\phi = \phi_\alpha, \phi = \phi_\beta$. One can show that the normal vector of these planes in $\mathbb{R}^{(3,1)}$ in homogenous coordinates is given by:

$$n(\phi) = (a_1(\phi) : a_2(\phi) : a_3(\phi) : a_1(\phi)x_0 + a_2(\phi)y_0 + a_3(\phi)z_0).$$

Now, the 4×4 matrix of the limit rotation $S[\beta] \circ S[\alpha]$ is the product $S[n(\phi_\beta)]S[n(\phi_\alpha)]$ of their reflection matrices.

In the Figure 10 a horocyclic rotation is consecutive applied on the blue cube in both directions. One can imagine that "small" cubes converge to a single point in infinity - the center of horocyclic rotation. Of course, all the cubes are congruent but the cubes further from the observer appear smaller.

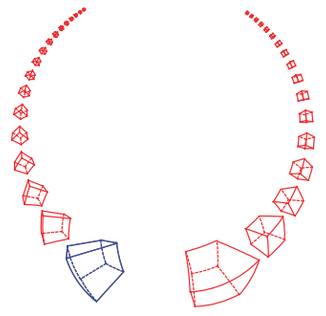

Figure 10: *Horocylic rotation applied on cube.*

4 *Mathematica* package L3toHorosphere

Mathematica package *L3toHorosphere* has three main features:

- central projection of hyperbolic polyhedra onto horosphere;
- visualization of the polyhedra and its projection in half-space model;
- realization of isometries of hyperbolic space.

Within the package, user can define any polyhedral surface in hyperbolic space by defining its faces (as lists of vertices) and vertices (using coordinates in any model). The polyhedral surface than can be repositioned using various hyperbolic isometries. Finally, the projection of the polyhedral surface onto horosphere can be obtained (see figures from Section 3).

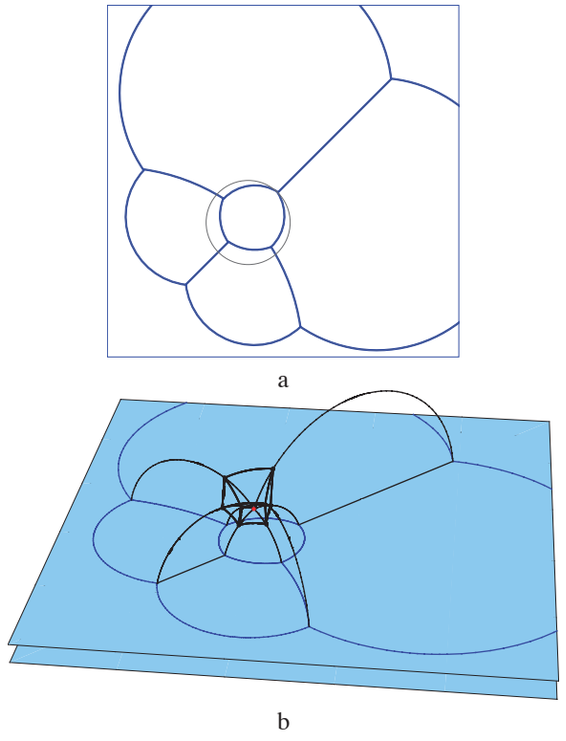

Figure 11: *Observer inside a cube: a) projection, b) situation in the half-space model.*

To achieve better understanding of what's going on, user can also visualize the polyhedral surface and its projection onto horosphere in the half-space model (see Figure 11). Visibility is implemented only for convex polyhedra without boundary.

Now we only list the functions implemented in the package. Some functions have options that can be obtained using command `Options[function]`. More details can be found in the user guide file that is delivered with the package [4].

`drawProjection[ω, k, vert, faces, options]` - project polyhedra given by `faces` and vertex coordinates `vert` from point $O(0,0,\omega)$ onto horosphere $z = k, \omega > k$.

`modelHS[ω, k, vert, faces, options]` - in half-space model draws polyhedra given by `faces` and vertex coordinates `vert` and its central projection from point $O(0,0,\omega)$ onto horosphere $z = k, \omega > k$).

`reflect[nVector]` - returns 4×4 matrix of reflection with respect to plane α with normal vector `nVector`. The normal vector is given in homogenous coordinates, i.e. is list of 4 numbers.

`reflect[P]` - returns 4×4 matrix of reflection with respect to point P given in homogenous coordinates.

`translate[A,B]` - returns 4×4 matrix of translation from A to B.

`rotate[A,B][ϕ]` - returns 4×4 matrix of rotation by angle ϕ around line AB.

`limitRotate[P][p][ϕ]` - returns 4×4 matrix of limit rotation by "angle" $\phi \neq \frac{\pi}{2} (\mathrm{mod}\, \pi)$ around line with direction p and containing unit point P (P orthogonal to p). The points P and p are given in the form (x,y,z).

`Klein2HS[pt]` - converts Klein projective point `pt` of form $(x_1 : x_2 : x_3 : x_4)$ to half-space model.

`HS2Klein[pt]` - converts half space point `pt` of the form $(x,y,z), z > 0$ to Klein projective point.

`m[A,B]` - returns midpoint of segment AB. All points are in Klein projective coordinates $(x_1 : x_2 : x_3 : x_4)$.

`normalVector[pt1, pt2, pt3]` - returns projective normal vector of plane determined by three points. All points are in Klein projective coordinates $(x_1 : x_2 : x_3 : x_4)$.

`edges[faces]` - returns edges of polyhedra with faces given by `faces`.

5 Conclusion and future work

The main advantage of our horosperical projection are realistic images of hyperbolic space. As in Euclidean central projection, closer objects appear larger. Furthermore, we don't use models of particular parameterizations - our projections are geometrically invariant and represent what flat Euclidean eye would really see in the hyperbolic space. All other approaches "cheat" in some way. The inevitable drawback of our approach is that projection of hyperbolic segment, in generic case, is circular arc that is complex to render. However, this is not heavy task for modern computers.

The sum of the angles in a hyperbolic triangle is strictly less than π. Therefore, when sketching hyperbolic objects we usually draw them to be curved concave. However, the projections we get in this paper are curved convex, what may bother someone's intuition. It is interesting that if the observer is placed outside the horosphere (first picture in Figure 2) the projections become curved concave. The Figure 12 (a) shows projection of a cube obtained using this approach.

It would be interesting to implement horosperical central projection of hyperbolic space in some more efficient programming language than Mathematica. This would allow us rendering of more complex hyperbolic scenes and probably lead to very interesting and unusual pictures. However, we are of opinion that even basic Mathematica package [4] we developed, can be very useful for better understanding of hyperbolic geometry and can be used as a good starting point for more complex visualizations.

One of classical scenes is Figure 12 (b), from video *Not knot* ([6]), used to cover many mathematical books. It represents tiling of hyperbolic space with regular dodecahedrons. This classic idea is common inspiration in mathematical art and jewelry making (see [2]). The natural question is to see regular hyperbolic tilings rendered using horospherical central projection.

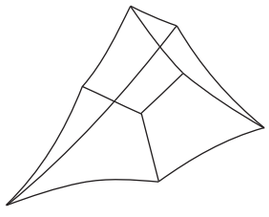

a

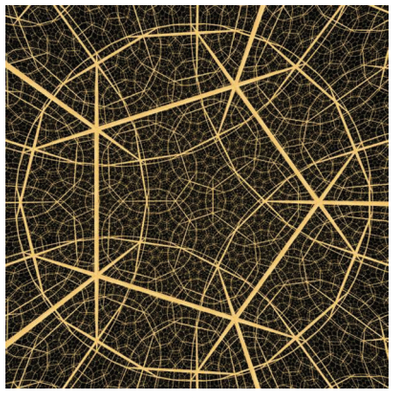

b

Figure 12

Another interesting topic is stereoscopic vision of hyperbolic scenes investigated in the paper [11]. Our preliminary testing, surprisingly, gave positive results, i.e. the human visual system seems to be able to "see" in hyperbolic space.

References

[1] B. AJDIN, *Rejtrejsing u Poenkareovom sfernom modelu hiperboličkog prostora,* master thesis, Faculty of Mathematics, Belgrade, 2010, (in Serbian, sort english version available at `http://www.mpi-inf.mpg.de/~bajdin/HRayTracing-eng.pdf`, acessed august 2012.)

[2] V. BULATOV, *Tilings of the hyperbolic space and their visualization*, Joint MAA/AMS meeting, New Orleans, 2011. (available at `//bulatov.org/math/1101/`, acessed august 2012.)

[3] M. BABIĆ, *Vizualizacija prostora Lobačevskog*, master thesis, Faculty of Mathematics, Belgrade, 2010, (in Serbian, available at `http://alas.matf.bg.ac.rs/~vsrdjan/files/marijana.pdf`, acessed august 2012.)

[4] M. BABIĆ, S. VUKMIROVIĆ, *L3toHorosphere - central projection of hyperbolic space onto horosphere*, Mathematica package 8335, Mathsource, 2012.

[5] M. PHILLIPS, C. GUNN, *Visualizing hyperbolic space: Unusual uses of* 4×4 *matrices*,, Proc. 1992. Symp. Interactive 3D Graphics, ACM Press, New York, 1992, 209–214.

[6] C. GUNN, D. MAXWELl, *Not knot*, video, 16 minutes, 1995.

[7] T. MUNZNER, Exploring Large Graphs in 3D Hyperbolic Space, *IEEE Computer Graphics and Applications* **18 (4)** (1998), 18–23.

[8] Z. A. SKOPEC, *"Foundations of Descriptive Geometry of Hyperbolic Space"* (Russian), series "Metods of Descrptive Geometry and its Applications", Moscow, 1955.

[9] Z. ŠNAJDER, Gemeinsame Eigenschaften der zentralen normalen, parallelen und berparallelen Projektionen im dreidimensionalen hyperbolischen Raum (German), *Mat. Vesnik* **9(24)** (1972), 27–37.

[10] S. VUKMIROVIC, *L2Primitives - basic drawing in the hyperbolic plane*, Mathematica package, 1998, `http://library.wolfram.com/infocenter/MathSource/4260/`

[11] J. R. WEEKS, Real-time rendering in curved spaces, *IEEE Computer Graphics and Applications* **22 (6)** (2002), 90–99.

[12] J. R. WEEKS, Real-time animation in hyperbolic, spherical, and product geometries, *Non-Euclidean Geometries*, János Bolyai Memorial Volume, (Ed. A. Prékopa and E. Molnár), *Mathematics and its Applications* **581**, Springer, 287–305, 2006.

Marijana Babić
e-mail: marijana@matf.bg.ac.rs

Srđan Vukmirović
e-mail: vsrdjan@matf.bg.ac.rs

Faculty of Mathematics, University Belgrade
Studentski trg 16, Belgrade, Serbia

Original scientific paper
Accepted 19. 12. 2012.

JÁNOS PALLAGI, BENEDEK SCHULTZ, JENÖ SZIRMAI

On Regular Square Prism Tilings in $\widetilde{\mathbf{SL}_2\mathbf{R}}$ Space

On Regular Square Prism Tilings in $\widetilde{\mathbf{SL}_2\mathbf{R}}$ Space

ABSTRACT

In [9] and [10] we have studied the regular prisms and prism tilings and their geodesic ball packings in $\widetilde{\mathbf{SL}_2\mathbf{R}}$ space that is one among the eight Thurston geometries. This geometry can be derived from the 3-dimensional Lie group of all 2×2 real matrices with determinant one.

In this paper we consider the regular infinite and bounded square prism tilings whose existence was proved in [9]. We determine the data of the above tilings and visualize them in the hyperboloid model of $\widetilde{\mathbf{SL}_2\mathbf{R}}$ space.

We use for the computations and visualization of the $\widetilde{\mathbf{SL}_2\mathbf{R}}$ space its projective model introduced by E. Molnár.

Key words: Thurston geometries, $\widetilde{\mathbf{SL}_2\mathbf{R}}$ geometry, tiling, prism tiling

MSC 2010: 52C17, 52C22, 53A35, 51M20

O popločavanju pravilnim kvadratskim prizmama u prostoru $\widetilde{\mathbf{SL}_2\mathbf{R}}$

SAŽETAK

U [9] i [10] smo proučavali pravilne prizme, popločavanje prizmama te njihovo popunjavanje geodetskim kuglama u prostoru $\widetilde{\mathbf{SL}_2\mathbf{R}}$, koji je jedan od osam Thurstonovih geometrija. Ova se geometrija može dobiti iz 3-dimenzionalne Lieve grupe svih 2×2 matrica s jediničnom determinantom.

U ovom članku promatramo popločavanje pravilnim beskonačnim i omeđenim kvadratskim prizmama čije je postojanje dokazano u [10]. Određujemo podatke gore spomenutog popločavanja i vizualiziramo ih u modelu hiperboloida u $\widetilde{\mathbf{SL}_2\mathbf{R}}$ prostoru.

Za računanje i vizualizaciju $\widetilde{\mathbf{SL}_2\mathbf{R}}$ prostora koristimo projektivni model koji je uveo E. Molnár.

Ključne riječi: Thurstonova geometrija, $\widetilde{\mathbf{SL}_2\mathbf{R}}$ geometrija, popločavanje, popločavanje prizmama

1 The $\widetilde{\mathbf{SL}_2\mathbf{R}}$ geometry

The $\mathbf{SL}_2\mathbf{R}$ Lie-group consists of the real 2×2 matrices $\begin{pmatrix} d & b \\ c & a \end{pmatrix}$ with unit determinant $ad-cb=1$. The $\widetilde{\mathbf{SL}_2\mathbf{R}}$ geometry is the universal covering group of this group, and is a Lie-group itself. Because of the 3 independent coordinates, $\widetilde{\mathbf{SL}_2\mathbf{R}}$ is a 3-dimensional manifold, with its usual neighbourhood topology. In order to model the above structure on the projective sphere $\mathcal{PS}^3$ and space $\mathcal{P}^3$ we introduce the new projective coordinates (x^0,x^1,x^2,x^3), where

$$a:=x^0+x^3, b:=x^1+x^2, c:=-x^1+x^2, d:=x^0-x^3, \quad (1)$$

with positive resp. non-zero multiplicative equivalence as projective freedom. Through the equivalence $\mathbf{SL}_2\mathbf{R}\sim\mathbf{PSL}_2\mathbf{R}$ it follows, that

$$0>bc-ad=-x^0x^0-x^1x^1+x^2x^2+x^3x^3 \quad (2)$$

describes the interior af the above one-sheeted hyperboloid solid $\mathcal{H}$ in the usual Euclidean coordinate simplex with the origin $E_0(1;0;0;0)$ and the ideal points of the axes $E_1^\infty(1;1;0;0), E_2^\infty(1;0;1;0), E_3^\infty(1;0;0;1)$. We shall consider the collineation group $\mathbf{G}_*$, which acts on the projective space $\mathcal{P}^3$ and preserves the polarity, ie. a scalar product of signature $(--++)$, moreover certain additional fibering structure. This group leaves the one sheeted hypeboloid $\mathcal{H}$ invariant. Choosing an appropriate subgroup $\mathbf{G}$ of $\mathbf{G}_*$ as isometry group, the universal covering space $\widetilde{\mathcal{H}}$ of $\mathcal{H}$ will be the hyperboloid model of $\widetilde{\mathbf{SL}_2\mathbf{R}}$. (See fig. 1.)

The specific isometries $\mathbf{S}(\phi)$ is a one parameter group given by the matrices:

$$\mathbf{S}(\phi)=\begin{pmatrix} \cos\phi & \sin\phi & 0 & 0 \\ -\sin\phi & \cos\phi & 0 & 0 \\ d & b & \cos\phi & -\sin\phi \\ d & b & \sin\phi & \cos\phi \end{pmatrix} \quad (3)$$

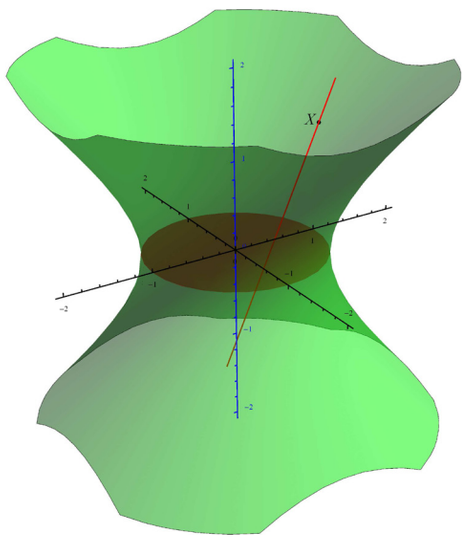

Figure 1: *The hypeboloid model of the* $\widetilde{\mathbf{SL}_2\mathbf{R}}$ *space with the "base plane" and the fibre line e.g. through the point* $X(1;1;\frac{1}{2};\frac{1}{3})$

The specific isometries $\mathbf{S}(\phi)$ is a one parameter group given by the matrices:

The elements of $\mathbf{S}(\phi)$ are the so-called "fibre translations" for $\phi \in \mathbb{R}$. We obtain an unique fibre-line to each $X(x^0;x^1;x^2;x^3) \in \widetilde{\mathcal{H}}$ as the orbit by right action of $\mathbf{S}(\phi)$ on X. The coordinates of points lying on the fibre line through X can be expressed as the images of X by $\mathbf{S}(\phi)$:

$$(x^0;x^1;x^2;x^3) \overset{\mathbf{S}(\phi)}{\to} (x^0\cos\phi - x^1\sin\phi; \\ x^0\sin\phi + x^1\cos\phi; x^2\cos\phi + x^3\sin\phi; -x^2\sin\phi + x^3\cos\phi) \tag{4}$$

The points of a fibre line through X by the usual inhomogeneous Euclidean coordinates $x = \frac{x^1}{x^0}, y = \frac{x^2}{x^0}, z = \frac{x^3}{x^0}$ are given by:

$$(1;x;y;z) \overset{\mathbf{S}(\phi)}{\to} (1; \frac{x+\tan\phi}{1-x\tan\phi}; \frac{y+z\tan\phi}{1-x\tan\phi}; \frac{z-y\tan\phi}{1-x\tan\phi}). \tag{5}$$

From formulas (4) and (5) we can see the π periodicity of the above maps.

The elements of the isometry group of $\widetilde{\mathbf{SL}_2\mathbf{R}}$ can be described in the above basis by the following matrix:

$$(a_i^j) = \begin{pmatrix} a_0^0 & a_0^1 & a_0^2 & a_0^3 \\ \mp a_0^1 & \pm a_0^0 & \pm a_0^3 & \mp a_0^2 \\ a_2^0 & a_2^1 & a_2^2 & a_2^3 \\ \pm a_2^1 & \mp a_2^0 & \mp a_2^3 & \pm a_2^2 \end{pmatrix} \tag{6}$$

where

$$-(a_0^0)^2 - (a_0^1)^2 + (a_0^2)^2 + (a_0^3)^2 = -1,$$
$$-(a_2^0)^2 - (a_2^1)^2 + (a_2^2)^2 + (a_2^3)^2 = -1,$$
$$-a_0^0a_2^0 - a_0^1a_2^1 + a_0^2a_2^2 + a_0^3a_2^3 = 0$$
$$-a_0^0a_2^1 - a_0^1a_2^0 + a_0^2a_2^3 + a_0^3a_2^2 = 0.$$

We define the translation group $\mathbf{G}_T$ as a subgroup of $\widetilde{\mathbf{SL}_2\mathbf{R}}$ isometry group acting transitively on the points of $\widetilde{\mathcal{H}}$ and mapping the origin $E_0(1;0;0;0)$ onto $X(x^0;x^1;x^2;x^3)$. These isometries and their inverses (up to a positive determinant factor) can be given by the following matrices:

$$\mathbf{T}: (t_i^j) = \begin{pmatrix} x^0 & x^1 & x^2 & x^3 \\ -x^1 & x^0 & x^3 & -x^2 \\ x^0 & x^1 & x^2 & x^3 \\ x^1 & -x^0 & -x^3 & x^2 \end{pmatrix} \tag{7}$$

$$\mathbf{T^{-1}}: (T_j^k) = \begin{pmatrix} x^0 & -x^1 & -x^2 & -x^3 \\ x^1 & x^0 & -x^3 & x^2 \\ -x^0 & -x^1 & x^2 & -x^3 \\ -x^1 & x^0 & x^3 & x^2 \end{pmatrix}$$

The rotation about the fibre line through the origin $E_0(1;0;0;0)$ by angle ω can be expressed by the following matrix:

$$\mathbf{R}_{E_0}(\omega) : (r_i^j(E_0,\omega)) = \begin{pmatrix} 0 & 0 & 0 & 0 \\ 0 & 0 & 0 & 0 \\ 0 & 0 & \cos\omega & \sin\omega \\ 0 & 0 & -\sin\omega & \cos\omega \end{pmatrix}, \tag{8}$$

while the rotation about the fibre line through point $X(x^0;x^1;x^2;x^3)$ by angle ω can be expressed by conjugation with the following formula: $(r_i^j(X,\omega)) = \mathbf{R}_X(\omega) = \mathbf{T}^{-1}\mathbf{R}_{E_0}(\omega)\mathbf{T}$.

We can introduce the so called hyperboloid parametrization as follows

$$x^0 = \cosh r\cos\phi,$$
$$x^1 = \cosh r\sin\phi,$$
$$x^2 = \sinh r\cos(\theta-\phi),$$
$$x^3 = \sinh r\sin(\theta-\phi), \tag{9}$$

where (r,θ) are the polar coordinates of the base plane, and ϕ is the fibre coordinate. We note, that

$$-x^0x^0 - x^1x^1 + x^2x^2 + x^3x^3 = -\cosh^2 r + \sinh^2 r = -1 < 0. \tag{10}$$

The inhomogeneous coordinates corresponding to (9), that play an important role in visualization, are given by

$$\begin{aligned} x &= \frac{x^1}{x^0} = \tan\phi, \\ y &= \frac{x^1}{x^0} = \tanh r \frac{\cos(\theta-\phi)}{\cos\phi}, \\ z &= \frac{x^1}{x^0} = \tanh r \frac{\sin(\theta-\phi)}{\cos\phi}. \end{aligned} \tag{11}$$

2 Geodesics and geodesic balls

In the following we are going to introduce the notion of the geodesic sphere and ball, using the concept of the metric tensor field and geodesic curve. After this we visualize the effects of the $\widetilde{\mathbf{SL}_2\mathbf{R}}$ isometries using geodesic balls.

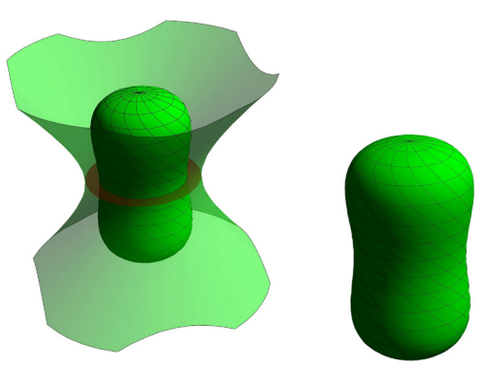

Figure 2: *Geodesic sphere of radius* 1 *centered at the origin*

The infinitesimal arc-length square can be derived by the standard method called pull back into the origin. By acting of (7) on the differentials $(dx^0;dx^1;dx^2;dx^3)$, we obtain by [2], [1] and [3] that in this parametrization the infinitesimal arc-length square at any point of $\widetilde{\mathbf{SL}_2\mathbf{R}}$ is the following:

$$(ds)^2 = (dr)^2 + \cosh^2 r \sinh^2 r (d\theta)^2 + [(d\phi) + \sinh^2 r (d\theta)]^2. \tag{12}$$

Hence we get the symmetric metric tensor field g_{ij} on $\widetilde{\mathbf{SL}_2\mathbf{R}}$ by components:

$$g_{ij} := \begin{pmatrix} 1 & 0 & 0 \\ 0 & \sinh^2 r(\sinh^2 r + \cosh^2 r) & \sinh^2 r \\ 0 & \sinh^2 r & 1 \end{pmatrix}, \tag{13}$$

The geodesic curves of $\widetilde{\mathbf{SL}_2\mathbf{R}}$ are generally defined as having locally minimal arc length between any two of their (close enough) points.

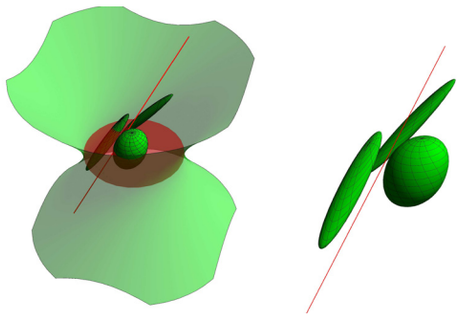

Figure 3: *Geodesic sphere rotated in 3rd order about a fibre line*

By (13) the second order differential equation system of the $\widetilde{\mathbf{SL}_2\mathbf{R}}$ geodesic curve of form (11) is the following:

$$\begin{aligned} \ddot{r} &= \sinh(2r)\,\dot\theta\,\dot\phi + \frac{1}{2}\big(\sinh(4r) - \sinh(2r)\big)\dot\theta\,\dot\theta, \\ \ddot\phi &= 2\dot r \tanh(r)(2\sinh^2(r)\,\dot\theta + \dot\phi), \\ \ddot\theta &= \frac{2\dot r}{\sinh(2r)}\big((3\cosh(2r) - 1)\dot\theta + 2\dot\phi\big). \end{aligned} \tag{14}$$

We can assume, that the starting point of a geodesic curve is $(1,0,0,0)$, because we can transform a curve into an arbitrary starting point. Moreover, $r(0) = 0$, $\phi(0) = 0$, $\theta(0) = 0$, $\dot r(0) = \cos\alpha$, $\dot\phi(0) = -\dot\theta(0) = \sin\alpha$ and so unit velocity can be assumed as follows in Table 1 from [1].

Table 1

Types	
$0 \le \alpha < \frac{\pi}{4}$ ($\mathbf{H}^2$ – like direction)	$r(s,\alpha) = \operatorname{arsinh}\Big(\frac{\cos\alpha}{\sqrt{\cos 2\alpha}}\sinh(\sqrt{\cos 2\alpha}s)\Big)$ $\theta(s,\alpha) = -\arctan\Big(\frac{\sin\alpha}{\sqrt{\cos 2\alpha}}\tanh(\sqrt{\cos 2\alpha}s)\Big)$ $\phi(s,\alpha) = 2\sin\alpha s + \theta(s,\alpha)$
$\alpha = \frac{\pi}{4}$ (light direction)	$r(s,\alpha) = \operatorname{arsinh}\Big(\frac{\sqrt{2}}{2}s\Big)$ $\theta(s,\alpha) = -\arctan\Big(\frac{\sqrt{2}}{2}s\Big)$ $\phi(s,\alpha) = \sqrt{2}s + \theta(s,\alpha)$
$\frac{\pi}{4} < \alpha \le \frac{\pi}{2}$ (fibre – like direction)	$r(s,\alpha) = \operatorname{arsinh}\Big(\frac{\cos\alpha}{\sqrt{-\cos 2\alpha}}\sin(\sqrt{-\cos 2\alpha}s)\Big)$ $\theta(s,\alpha) = -\arctan\Big(\frac{\sin\alpha}{\sqrt{-\cos 2\alpha}}\tan(\sqrt{-\cos 2\alpha}s)\Big)$ $\phi(s,\alpha) = 2\sin\alpha s + \theta(s,\alpha)$

The equation of the geodesic curve in the hyperboloid model – using the usual geographical coordiantes (λ,α), $(-\pi < \lambda \le \pi)$, as general longitude and altitude parameters for the later geodesic sphere $(-\frac{\pi}{2} \le \alpha \le \frac{\pi}{2})$, and the arc-length parameter $0 \le s \in \mathbf{R}$ – are determined in [1]. The Euclidean coordinates $X(s,\lambda,\alpha), Y(s,\lambda,\alpha), Z(s,\lambda,\alpha)$ of the geodesic curves can be determined by substituting

the results of Table 1 (see [1]) into the following equations by (11):

$$
\begin{aligned}
X(s,\lambda,\alpha) &= \tan\phi(s,\alpha),\\
Y(s,\lambda,\alpha) &= \tanh r(s,\alpha)\Big(\frac{\cos\left(\theta(s,\alpha)-\phi(s,\alpha)\right)}{\cos\phi(s,\alpha)}\cos\lambda-\\
&\quad-\frac{\sin\left(\theta(s,\alpha)-\phi(s,\alpha)\right)}{\cos\phi(s,\alpha)}\sin\lambda\Big)\\
&= \frac{\tanh r(s,\alpha)}{\cos\phi(s\alpha)}\cos[\theta(s,\alpha)-\phi(s,\alpha)+\lambda], \qquad (15)\\
Z(s,\lambda,\alpha) &= \tanh r(s,\alpha)\Big(\frac{\cos\left(\theta(s,\alpha)-\phi(s,\alpha)\right)}{\cos\phi(s,\alpha)}\sin\lambda+\\
&\quad\frac{\sin\left(\theta(s,\alpha)-\phi(s,\alpha)\right)}{\cos\phi(s,\alpha)}\cos\lambda\Big)\\
&= \frac{\tanh r(s,\alpha)}{\cos\phi(s\alpha)}\sin[\theta(s,\alpha)-\phi(s,\alpha)+\lambda].
\end{aligned}
$$

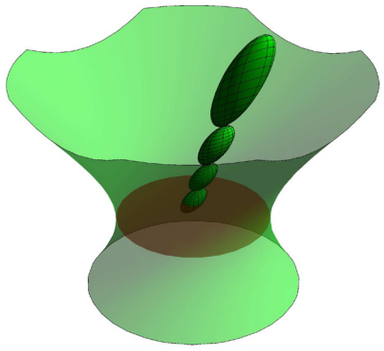

Figure 4: *Touching geodesic spheres of radius $\frac{1}{6}$ centered on a fibre line*

Definition 2.1 *The distance $d(P_1,P_2)$ between the points P_1 and P_2 is defined as the arc length of the geodesic curve from P_1 to P_2.*

In [10] the third author has investigated the notion of the geodesic spheres and balls, with the following definition:

Definition 2.2 *The geodesic sphere of radius ρ and center P is defined as the set of all points Q in the space with the additional condition $d(P,Q)=\rho\in\left[0,\frac{\pi}{2}\right)$.*

Remark 2.3 *The geodesic sphere above is a simply connected surface without self intersection in the space $\widetilde{\mathbf{SL}_2\mathbf{R}}$.*

Figure 2 shows a sphere with radius $\rho=1$ and the origin as its center.

3 Regular prisms in $\widetilde{\mathbf{SL}_2\mathbf{R}}$ space

In the paper [9] the third author has defined the prism and prism-like tilings in $\widetilde{\mathbf{SL}_2\mathbf{R}}$ space, and also classified the infinite and bounded regular prism tilings. Now, we study the square prisms and prism tilings in $\widetilde{\mathbf{SL}_2\mathbf{R}}$ space, review their most important properties and compute their metric data.

Definition 3.1 *Let $\mathcal{P}^i$ be a $\widetilde{\mathbf{SL}_2\mathbf{R}}$ infinite solid that is bounded by one-sheeted hyperbolid surfaces of the model space, generated by neighbouring "side fibre lines" passing through the vertices of a p-gon ($\mathcal{P}^b$) lying in the "base plane". The images of solids $\mathcal{P}^i$ by $\widetilde{\mathbf{SL}_2\mathbf{R}}$ isometry are called infinite p-sided $\widetilde{\mathbf{SL}_2\mathbf{R}}$ prisms.*

The common part of $\mathcal{P}^i$ with the base plane is called the *base figure* of $\mathcal{P}^i$ and is denoted by $\mathcal{P}$. Its vertices coincide with the vertices of $\mathcal{P}^b$.

Definition 3.2 *A p-sided prism is an isometric image of a solid, which is bounded by the side surfaces of a p-sided infinite prism $\mathcal{P}^i$, its base figure $\mathcal{P}$ and the translated copy $\mathcal{P}^t$ of $\mathcal{P}$ by a fibre translation.*

The side faces $\mathcal{P}$ and $\mathcal{P}^t$ are called *"cover faces"*, and are related by fibre translation along fibre lines joining their points.

Definition 3.3 *An infinite prism in $\widetilde{\mathbf{SL}_2\mathbf{R}}$ is regular if $\mathcal{P}^b$ is a regular p-gon with center at the origin in the "base plane" and the side surfaces are congruent to each other under an $\widetilde{\mathbf{SL}_2\mathbf{R}}$ isometry.*

Definition 3.4 *The regular p-sided prism in $\widetilde{\mathbf{SL}_2\mathbf{R}}$ space is a prism derived by Definition 3.2 from an infinite regular p-sided prism (see Definition 3.3).*

We consider a monohedral tessellation of the space $\widetilde{\mathbf{SL}_2\mathbf{R}}$ with congruent regular infinite or bounded prisms. A tiling is called face-to-face, if the intersection of any two tiles is either empty or a common face, edge or vertex of both tiles, otherwise it is non-face-to-face.

A regular infinite tiling $\mathcal{T}^i_p(q)$ in the $\widetilde{\mathbf{SL}_2\mathbf{R}}$ space is derived by a rotation subgroup $G^r_p(q)$ of the symmetry group $G_p(q)$ of $\mathcal{T}^i_p(q)$. $G^r_p(q)$ is generated by rotations $r_1,r_2,\ldots,r_p$ with angles $\omega=\frac{2\pi}{q}$ about the fibre lines $f_1,\ldots,f_p$ through the vertices of the given $\widetilde{\mathbf{SL}_2\mathbf{R}}$ p-gon $\mathcal{P}^b$, and let $\mathcal{P}^i_p(q)$ be one of its tiles, where we can suppose without the loss of generality, that its p-gonal base figure is centered at the origin.

The vertices $A_1, A_2, \ldots, A_p$ of the base figure $\mathcal{P}$ coincide with the vertices of a regular hyperbolic p-gon in the base plane with center at the origin, and we can introduce the following homogeneous coordinates to neighbouring vertices of the base figure of $\mathcal{P}_p^i(q)$ in the hyperboloid model of $\widetilde{\mathcal{H}} = \widetilde{\mathbf{SL}_2\mathbf{R}}$.

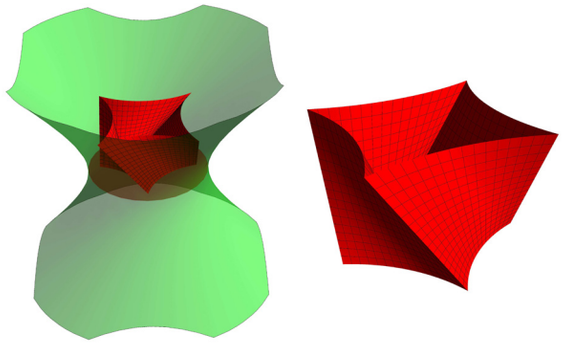

Figure 5: *The $\mathcal{P}_4^i(8)$ tile centered at the origin of the regular infinite tiling $\mathcal{T}_4^i(8)$*

$$A_1 = (1;0;0;x_3),$$
$$A_2 = (1;0;-x_3\sin(\frac{2\pi}{p});x_3\cos(\frac{2\pi}{p})),$$
$$A_3 = (1;0;-x_3\sin(\frac{4\pi}{p});x_3\cos(\frac{4\pi}{p})),$$
$$\ldots,$$
$$A_p = (1;0;-x_3\sin((p-1)\frac{2\pi}{p});x_3\cos((p-1)\frac{2\pi}{p})) \quad (16)$$

The side curves $c(A_iA_{i+1})(i = 1,\ldots,p; A_{p+1} \equiv A_1)$ of the base figure are derived from each other by $\frac{2\pi}{p}$ rotation about the x-axis, so they are congruent in $\widetilde{\mathbf{SL}_2\mathbf{R}}$ sense. The necessary requirement to the existence of $\mathcal{T}_p^i(q)$, that the surfaces of the neighbouring side faces of $\mathcal{P}_p^i(q)$ are derived from each other by $\frac{2\pi}{q}(\frac{2p}{p-2} < q \in \mathbb{N})$ rotation about the common fibre line.

We have the following theorem ([9]):

Theorem 3.5 *There exists regular infinite prism tiling $\mathcal{T}_p^i(q)$ for each $3 \leq p \in \mathbb{N}$, where $\frac{2p}{p-2} < q$.*

The coordinates of the $A_1, A_2, \ldots, A_p$ vertices of the base figure and thus the corresponding "fibre side lines" (the fibre lines through the vertices of the base figure) can be computed for any given (p,q) pair of parameters. Moreover the equation of the $c(A_2A_3)$ curve can be determined as follows.

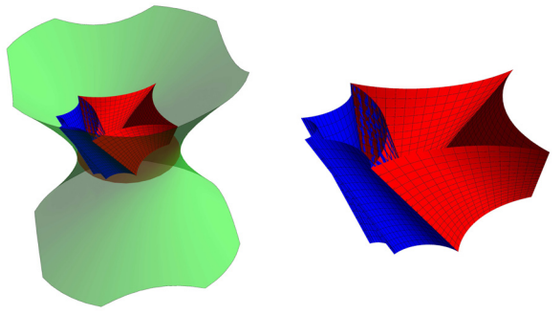

Figure 6: *Regular infinite prism tiling $\mathcal{T}_4^i(8)$*

Let $\mathcal{R}_{A_2}^{\frac{-2\pi}{q}}$ be the rotation matrix of the angle $\omega = -\frac{2\pi}{q}$ about the fibre line through A_2. Consider the half point F of the fibre line segment between the points A_3 and $A_1^{\mathcal{R}_{A_2}^{\frac{-2\pi}{q}}}$. The base curve $c(A_2A_3)$ will be the locus of common points of the fibre lines through the line segment A_2F with the "base plane" of the model. This also determines the side surfaces of $\mathcal{P}_p^i(q)$.

Using the above described method we can compute the x_3 parameter of the vertex coordinates, we obtain the following theorem (see [9]):

Theorem 3.6 *The vertices A_1, A_2, A_3 of the base figure $\mathcal{P}$ of $\mathcal{P}_3^i(q)$ are determined for parameters $p = 3$, and $7 \leq q \in \mathbb{N}$ by coordinates in (16) where*

$$x_3 = \sqrt{\frac{\sqrt{3}\cos\frac{2\pi}{q} - \sin\frac{2\pi}{q}}{2\sin\frac{2\pi}{q} + \sqrt{3}}}. \quad (17)$$

Therefore, the vertices of the prisms $\mathcal{P}_3^i(q)$ base figure $\mathcal{P}$ are the following:

$$A_1 = (1;0;0;\sqrt{\frac{\sqrt{3}\cos\frac{2\pi}{q} - \sin\frac{2\pi}{q}}{2\sin\frac{2\pi}{q} + \sqrt{3}}}),$$
$$A_2 = (1;0;-\frac{\sqrt{3}}{2}\sqrt{\frac{\sqrt{3}\cos\frac{2\pi}{q} - \sin\frac{2\pi}{q}}{2\sin\frac{2\pi}{q} + \sqrt{3}}};-\frac{1}{2}\sqrt{\frac{\sqrt{3}\cos\frac{2\pi}{q} - \sin\frac{2\pi}{q}}{2\sin\frac{2\pi}{q} + \sqrt{3}}}),$$
$$A_3 = (1;0;\frac{\sqrt{3}}{2}\sqrt{\frac{\sqrt{3}\cos\frac{2\pi}{q} - \sin\frac{2\pi}{q}}{2\sin\frac{2\pi}{q} + \sqrt{3}}};-\frac{1}{2}\sqrt{\frac{\sqrt{3}\cos\frac{2\pi}{q} - \sin\frac{2\pi}{q}}{2\sin\frac{2\pi}{q} + \sqrt{3}}}) \quad (18)$$

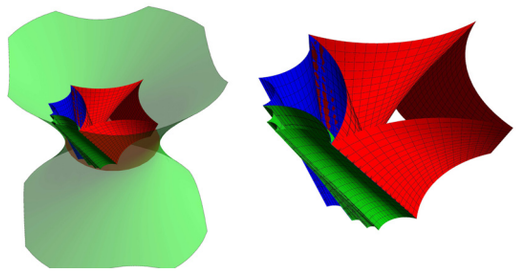

Figure 7: *Regular infinite prism tiling* $\mathcal{T}_4^i(8)$

With an analogous argument we also proved the following theorem, which seems to be a new, important result:

Theorem 3.7 *The vertices* A_1, A_2, A_3, A_4 *of the base figure* $\mathcal{P}$ *of* $\mathcal{P}_4^i(q)$ *are determined for parameters* $p = 4$, *and* $5 \leq q \in \mathbb{N}$ *by coordinates in (16) where*

$$x_3 = \sqrt{\frac{\cos\frac{\pi}{q} - \sin\frac{\pi}{q}}{\cos\frac{\pi}{q} + \sin\frac{\pi}{q}}}, \tag{19}$$

Using this, the vertices of the prisms $\mathcal{P}$ *base figure are:*

$$\begin{aligned}
A_1 &= (1;0;0;\sqrt{\frac{\cos\frac{\pi}{q} - \sin\frac{\pi}{q}}{\cos\frac{\pi}{q} + \sin\frac{\pi}{q}}}),\\
A_2 &= (1;0;-\sqrt{\frac{\cos\frac{\pi}{q} - \sin\frac{\pi}{q}}{\cos\frac{\pi}{q} + \sin\frac{\pi}{q}}};0),\\
A_3 &= (1;0;0;-\sqrt{\frac{\cos\frac{\pi}{q} - \sin\frac{\pi}{q}}{\cos\frac{\pi}{q} + \sin\frac{\pi}{q}}}),\\
A_4 &= (1;0;\sqrt{\frac{\cos\frac{\pi}{q} - \sin\frac{\pi}{q}}{\cos\frac{\pi}{q} + \sin\frac{\pi}{q}}};0).
\end{aligned} \tag{20}$$

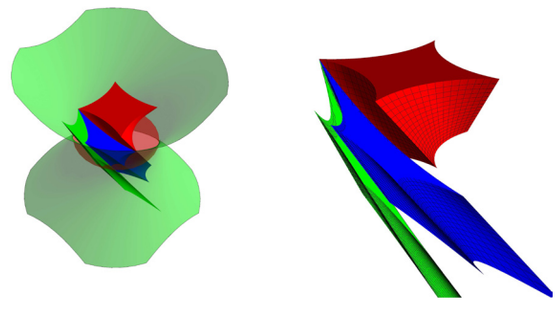

Figure 8: *Regular bounded prism tiling* $\mathcal{T}_4(8)$

Similarly to the regular infinite prism tilings we get the types of the regular bounded prism tilings which are classified in [9] where the third author has proved, that a regular bounded prism tiling are non-face-to-face one. In this paper we visualize in Fig. 8 only some neighbouring prisms of a bounded regular prism tiling $\mathcal{T}_4(8)$ where the height of the prisms are $\frac{3}{4}$. When visualizing prism tilings we use different colors to note the neighbourhooding prisms.

In this paper we have mentioned only some problems in discrete geometry of the $\widetilde{\mathbf{SL}_2\mathbf{R}}$ space, but we hope that from these it can be seen that our projective method suits to study and solve similar problems (see [4], [7], [8], [10]).

References

[1] B. Divjak, Z. Erjavec, B. Szabolcs, B. Szilgyi, Geodesics and geodesic spheres in $\widetilde{\mathbf{SL}}(\mathbf{2},\mathbb{R})$ geometry, *Mathematical Communications*, **Vol.14 No.2** 413-424.

[2] E. Molnár, The projective interpretation of the eight 3-dimensional homogeneous geometries. *Beitrge zur Algebra und Geometrie (Contributions to Algebra and Geometry)*, **38 No. 2** (1997), 261-288.

[3] E. Molnár, J. Szirmai, Symmetries in the 8 homogeneous 3-geometries, *Symmetry: Culture and Science*, Vol. **21 No. 1-3** (2010), 87-117.

[4] E. Molnár, J. Szirmai, Classification of **Sol** lattices. *Geometriae Dedicata,* **161/1** (2012), 251-275, DOI: 10.1007/s10711-012-9705-5.

[5] J. Pallagi, B. Schultz, J. Szirmai, Equidistant surfaces in $\mathbf{H}^2 \times \mathbf{R}$ space, *KoG* **15**, [2011], 3-6.

[6] P. Scott, The geometries of 3-manifolds. *Bull. London Math. Soc.*, **15** (1983) 401–487.

[7] J. Szirmai, Geodesic ball packing in $\mathbf{S}^2 \times \mathbf{R}$ space for generalized Coxeter space groups. *Beiträge zur Algebra und Geometrie (Contributions to Algebra and Geometry),* **52(2)** (2011), 413–430.

[8] J. Szirmai, Geodesic ball packing in $\mathbf{H}^2 \times \mathbf{R}$ space for generalized Coxeter space groups. *Mathematical Communications* **17/1** (2012), 151-170.

[9] J. Szirmai, Regular prism tilings in the $\widetilde{\mathbf{SL}_2\mathbf{R}}$ space. Manusript submitted to *Aequationes mathematicae* (2012)

[10] J. SZIRMAI, Volumes and geodesic ball packings to the regular prism tilings in $\widetilde{\mathbf{SL}_2\mathbf{R}}$ space. Manuscript (2012).

[11] J. SZIRMAI, A candidate to the densest packing with equal balls in the Thurston geometries. Manusript submitted to *Monatshefte für Mathematik* (2012).

[12] W. P. THURSTON, (and Levy, S. editor) (1997) Three-Dimensional Geometry and Topology, *Princeton University Press, Princeton, New Jersey*, **Vol 1.**

János Pallagi
e-mail: jpallagi@math.bme.hu
Benedek Schultz
e-mail: schultz.benedek@gmail.com
Jenö Szirmai
e-mail: szirmai@math.bme.hu
Budapest University of Technology and Economics,
Institute of Mathematics, Department of Geometry
H-1521 Budapest, Hungary

Acknowledgement: We thank Prof. Emil Molnár for helpful comments to this paper.

Original scientific paper
Accepted 21. 12. 2012.

NORMAN JOHN WILDBERGER
ALI ALKHALDI

Universal Hyperbolic Geometry IV: Sydpoints and Twin Circumcircles

Universal Hyperbolic Geometry IV: Sydpoints and Twin Circumcircles

ABSTRACT

We introduce the new notion of *sydpoints* into projective triangle geometry with respect to a general bilinear form. These are analogs of midpoints, and allow us to extend hyperbolic triangle geometry to non-classical triangles with points inside and outside of the null conic. Surprising analogs of circumcircles may be defined, involving the appearance of pairs of *twin circles*, yielding in general eight circles with interesting intersection properties.

Key words: universal hyperbolic geometry, triangle geometry, projective geometry, bilinear form, sydpoints, twin circumcircles

MSC 2000: 51M10, 14N99, 51E99

Univerzalna hiperbolička geometrija IV: sidtočke i kružnice blizanke

SAŽETAK

Uvodimo novi pojam sidtočaka u projektivnu geometriju trokuta s obzirom na opću bilinearnu formu. One su analogoni polovišta i dopuštaju nam proširiti hiperboličku geometriju trokuta ka neklasičnim trokutima s točkama unutar i van apsolutne konike. Mogu se definirati neočekivani analogoni opisanih kružnica koji uključuju pojavljivanje kružnica blizanki što vodi ka osam kružnica sa zanimljivim svojstvima presjeka.

Ključne riječi: univerzalna hiperbolička geometrija, geometrija trokuta, projektivna geometrija, bilinearna forma, sidtočka, kružnice blizanke

1 Introduction

In this paper we continue a study of hyperbolic triangle geometry, parallel to, but with different features to the Euclidean case laid out in [5] and [6], and in a related but different direction from [9], [10] and [11], using the framework of Universal hyperbolic geometry (UHG), developed by Wildberger in [13], [14], [15] and [16]. We study the new notion of *sydpoints* s of a side $\overline{ab}$—this is analogous and somewhat complementary to the more familiar notion of *midpoints* m; the related idea of *twin circumcircles* of a triangle; and introduce *circumlinear coordinates* to build up the Circumcenter hierarchy of a triangle, treating midpoints and sydpoints uniformly.

In [16] we saw that if each of the three sides of a triangle (in UHG) has midpoints m, then these six points lie three at a time on four circumlines C, whose duals are the four *circumcenters* c. These are the centers of the four *circumcircles* which pass through the three points of the triangle.

This is shown for a classical triangle in Figure 1, where the larger blue circle is the *null circle* defining the metrical structure, together with the *midlines* M—traditionally called perpendicular bisectors. While the red circumcircle is a classical circle in the Cayley Beltrami Klein model of hyperbolic geometry, the other three are usually described as *curves of constant width*, but for us they are *all just circles*. This is the start of the Circumcenter hierarchy in UHG.

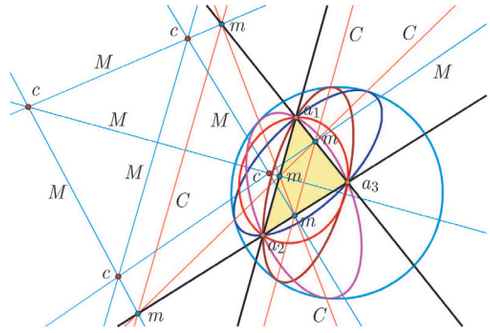

Figure 1: *Midpoints, Midlines, Circumlines, Circumcenters and Circumcircles*

Remarkably, much of this extends also to triangles with points both interior and exterior to the null circle, but we also find new phenomenon relating to circumcircles, that suggest a reconsideration of the classical case above.

The fundamental metrical notion between points in UHG is the *quadrance* q, and a midpoint of $\overline{ab}$ is a point m on ab satisfying $q(a,m) = q(b,m)$. Our key new concept is the following: a **sydpoint** of $\overline{ab}$ is a point s on ab satisfying

$$q(a,s) = -q(b,s).$$

While the existence of midpoints is equivalent to $1 - q(a,b)$ being a square in the field, the existence of sydpoints is equivalent to $q(a,b) - 1$ being a square. As with midpoints, if sydpoints exist there are generally two of them.

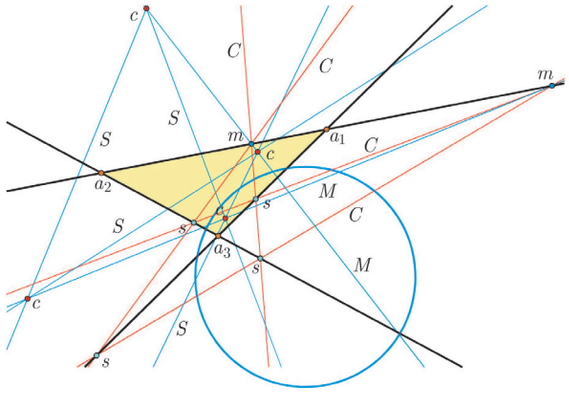

Figure 2: *A non-classical triangle with both midpoints and sydpoints*

In Figure 2, the non-classical triangle $\overline{a_1a_2a_3}$ has one side $\overline{a_1a_2}$ with midpoints m whose duals are *midlines* M, and two sides $\overline{a_1a_3}$ and $\overline{a_2a_3}$ with sydpoints s whose duals are *sydlines* S. The six midpoints and sydpoints lie three at a time on four *circumlines* C, whose duals are the four *circumcenters* c. The connection between these new circumcenters and the idea of circumcircles is particularly interesting, since in this case it is impossible to find *any* circles which pass through all three points of the triangle $\overline{a_1a_2a_3}$.

In UHG circles can often be paired: two circles are **twins** if they share the same center and their quadrances sum to 2. The circumcenters c are the centers of *twin circumcircles* passing through collectively the three points of the triangle. This notion extends our understanding even in the classical case. The four pairs of twin circumcircles give eight *generalized circumcircles* (even for the classical case), and these meet in a surprising way in the *CircumMeet points*, some of which pleasantly depend only the side of the triangle on which they lie.

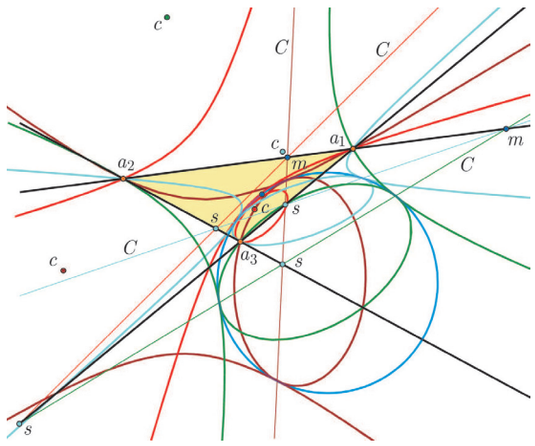

Figure 3: *Four twin circumcircles of a non-classical triangle*

In Figure 3 we see the twin circumcircles of the triangle of the previous Figure; some of these appear in this model as hyperbolas tangent to the null circle—these are invisible in classical hyperbolic geometry, but have a natural interpretation in terms of hyperboloids of one sheet in three-dimensional space (DeSitter space).

The other main contribution of this paper is in setting up *circumlinear coordinates*. UHG is more algebraic than the classical theory ([2], [1], [3], [4], [8]), emphasizing a projective metrical formulation without transcendental functions for Cayley-Klein geometries, valid both inside and outside the usual null circle (or absolute), and working over a general field, generally not of characteristic two. In [16], triangle geometry was studied in the more general setting of a projective plane over a field, with a metrical structure induced by a symmetric bilinear form on the associated three-dimensional vector space, or equivalently a general conic playing the role of the null circle or absolute. That paper focussed on *ortholinear coordinates*, and gave derivations for many initial constructions in the Incenter hierarchy, and only dual statements for the corresponding results for the Circumcenter hierarchy.

In this paper we introduce the complementary *circumlinear coordinates*, which are well suited for studying midpoints and sydpoints simultaneously. Finding formulas for key points and lines is, as always, a main aim. If the triangle $\overline{a_1a_2a_3}$ has either midpoints or sydpoints for each of its sides, a change of coordinates allows us to write $a_1 = [1:0:0]$, $a_2 = [0:1:0]$ and $a_3 = [0:0:1]$, with the bilinear form given by a matrix

$$C = \begin{bmatrix} 1 & a & b \\ a & 1 & c \\ b & c & \varepsilon \end{bmatrix} \tag{1}$$

where $\varepsilon^2 = \pm 1$. We reformulate formulas of the Orthocenter hierarchy of ([16]) using circumlinear coordinates,

including the *Orthoaxis A* with the five important points h, s, b, x and z, and then turn to the Circumcenter hierarchy, studying *Medians*, *Centroids*, *CircumCentroids*, *CircumDual points*, *Tangent lines*, *Jay lines*, *Wren lines*, *CircumMeet points* and some new associated points and lines, and finish with a nice correspondence between the Circumcenters and four *Sound conics* passing two at a time through the twelve *Sound points*. Note that when we study a particular triangle, we adopt the convention of Capitalizing major points and lines of that Triangle. Although the paper is one of a series, we have tried to make it largely self-contained.

1.1 Projective duality and midpoint constructions

One can approach Universal Hyperbolic Geometry from either a synthetic projective geometry or an analytic linear algebra point of view; both are useful, and they shed light on each other. In this section we give a synthetic introduction useful for dynamic geometry packages such as GSP, C.a.R., Cabri, GeoGebra and Cinderella. We work in the projective plane over a field, which in our pictures will be the rational numbers, with a distinguished conic, called the **null circle**, but elsewhere also the *absolute*. In our pictures, this will be the familiar unit circle, always in blue, with points lying on it called **null points**.

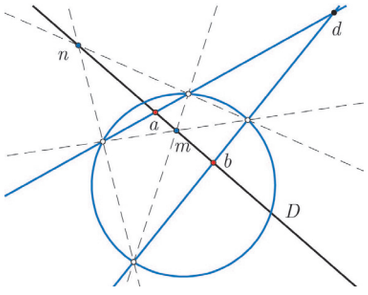

Figure 4: *Duals and perpendicularity*

The key duality, or polarity, between points and lines induced by the null circle allows a notion of perpendicularity: two points a and b are **perpendicular**, written $a \perp b$, precisely when b lies on the dual of a, or conversely a lies on the dual of b (these are equivalent), and similarly two lines L and M are **perpendicular**, written $L \perp M$, precisely when L passes through the dual of M, or conversely M passes through the dual of L.
In Figure 4 we see a construction for the *dual* of a point d; this is the line D formed by the other two diagonals n and m of any null quadrangle for which d is a diagonal point. Then d is perpendicular to any point on $D \equiv nm$, and any line through d is perpendicular to D. To construct the dual of a line L, take the meet of the duals of any two points on it.

The basic isometries in such a geometry are reflections in points (or reflections in lines—these two notions turn out to be the same). If m is not a null point, the reflection r_m in m interchanges the two null points on any line through m, should there be such. In Figure 5 for example, r_m interchanges x and w, and interchanges y and z. It is then a remarkable and fundamental fact that r_m extends to a projective transformation: to find the image of a point a, construct any line through a which meets the null circle at two points, say x and y, then find the images of x and y under r_m, namely w and z, and then define $r_m(a) = b \equiv (am)(wz)$ as shown. Perpendicularity of both points and lines is preserved by r_m.

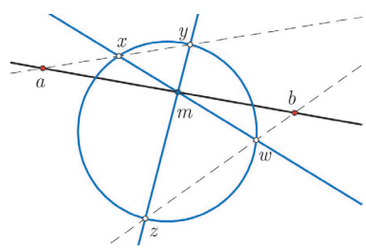

Figure 5: *Reflection r_m in m sends a to b*

The notion of reflection allows us to define midpoints without metrical measurements: if $r_m(a) = b$ then we may say that m is a **midpoint** of the side $\overline{ab}$. To construct the midpoints of a side $\overline{ab}$, when they exist (this is essentially a quadratic condition), we essentially invert the above construction.

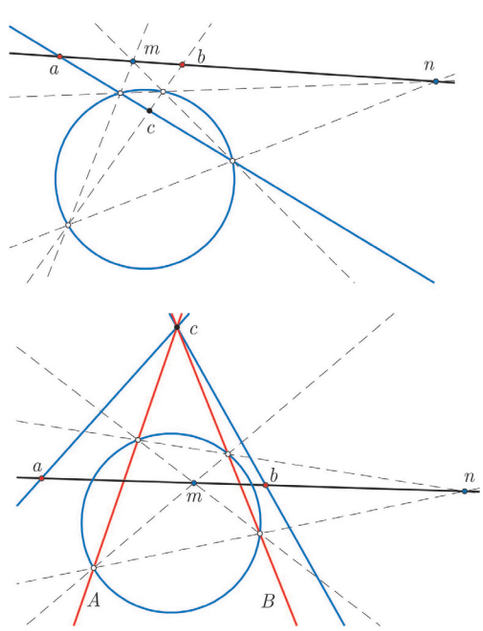

Figure 6: *Constructing midpoints m and n of the side $\overline{ab}$*

Figure 6 shows two situations where we can construct midpoints m and n of the side $\overline{ab}$, at least approximately over the rational numbers, which is the orientation of Geometer's Sketchpad and other dynamic geometry packages. In the top diagram, we take the dual c of the line ab, and if the lines ac and bc meet the null circle we take the other two diagonal points of this null quadrangle. This is also the case in Figure 4. In the bottom diagram, the lines ac and bc do not meet the null circle, but the dual lines A and B of a and b, which necessarily pass through c, do meet the null circle in a quadrangle, whose other diagonal points are the required midpoints m and n.

To define a circle $\mathcal{C}$ in this projective setting, suppose that c and p are points; then the locus of the reflections $r_x(p)$ as x runs along the dual line of c is the **circle** with center c through p. This projective definition immediately gives a correspondence between a circle and a line. Of course there is also a metrical definition, once we have set up quadrance and spread.

2 Metrical projective linear algebra

While the synthetic framework is attractive, for explicit computations and formulas it is useful to work with analytic geometry in the context of (projective) linear algebra. Our strategy, as in [16], will be to set up coordinates so that our basic triangle is as simple as possible, and all the complexity resides in the bilinear form. We begin with establishing some notation and basic results in the affine setting, although the projective setting is the main interest.

The three-dimensional vector space V over a field $\mathbb{F}$, of characteristic not two, consists of row vectors $v = (x,y,z)$ or equivalently 1×3 matrices $\begin{pmatrix} x & y & z \end{pmatrix}$. A metrical structure is determined by a *symmetric bilinear form*

$$v \cdot u = vu \equiv vCu^T$$

where C is an invertible symmetric 3×3 matrix. Note in particular our use of the algebraic notation vu. The dual vector space V^* may be viewed as column vectors $f = (l,m,n)^T$ or equivalently 3×1 matrices.

Vectors v, u are **perpendicular** precisely when $v\cdot u = vu = 0$. The **quadrance** of a vector v is the number $Q_v \equiv v\cdot v = v^2$. A vector v is **null** precisely when $Q_v = v^2 = 0$.

A variant of the following also appears in [7].

Theorem 1 (Parallel vectors) *If vectors v and u are parallel then*

$$Q_v Q_u = (vu)^2. \tag{2}$$

Conversely if (2) holds then either v and u are parallel, or the bilinear form restricted to the span of u and v is degenerate.

Proof. Consider a two-dimensional space containing v and u and the bilinear form restricted to it, given by a matrix $\widetilde{C} = \begin{pmatrix} a & b \\ b & c \end{pmatrix}$ with respect to some basis. If in this basis $v = (x,y)$ and $u = (u,v)$, then we may calculate that

$$Q_v Q_u - (vu)^2 = -\frac{(xv-yu)^4 \left(ac-b^2\right)^2}{\left(au^2+2buv+cv^2\right)^2 \left(ax^2+2bxy+cy^2\right)^2}.$$

So if v and u are parallel, the left hand side is zero, and conversely if the left hand side is zero, then either $ac-b^2 \neq 0$ in which case the bilinear form restricted to the span of v and u is degenerate, or $xv-yu=0$, meaning that the vectors v and u are parallel. □

The previous result motivates the following measure of the non-parallelism of two vectors. The **(affine) spread** between non-null vectors v and u is the number

$$s(v,u) \equiv 1 - \frac{(vu)^2}{Q_v Q_u}.$$

The spread is unchanged if either v or u are multiplied by a non-zero number.

2.1 Basic notation and definitions

One-dimensional and two-dimensional subspaces of $V = \mathbb{F}^3$ may be viewed as the basic objects forming the projective plane, with metrical notions coming from the affine notions of quadrance and spread in the associated vector space, but we prefer to give independent definitions so that logically neither the affine nor projective settings have priority. In general our notation in the projective setting is *opposite* to that in the affine setting, in the sense that the roles of small and capital letters are reversed throughout.

A (**projective**) **point** is a proportion $a = [x:y:z]$ in square brackets, or equivalently a projective row vector $a = \begin{bmatrix} x & y & z \end{bmatrix}$ where the square brackets in the latter are interpreted projectively: unchanged if multiplied by a non-zero number. A (**projective**) **line** is a proportion $L = \langle l:m:n \rangle$ in pointed brackets, or equivalently a projective column vector

$$L = \begin{bmatrix} l \\ m \\ n \end{bmatrix}.$$

When the context is clear, we refer to projective points and projective lines simply as **points** and **lines**. The **incidence** between the point $a = [x:y:z]$ and the line $L = \langle l:m:n \rangle$ is given by the relation

$$aL = \begin{bmatrix} x & y & z \end{bmatrix} \begin{bmatrix} l \\ m \\ n \end{bmatrix} = lx+my+nz = 0.$$

In such a case we say a **lies on** L, or L **passes through** a.

The **join** a_1a_2 of distinct points $a_1 \equiv [x_1 : y_1 : z_1]$ and $a_2 \equiv [x_2 : y_2 : z_2]$ is the line

$$\begin{aligned} a_1a_2 &\equiv [x_1 : y_1 : z_1] \times [x_2 : y_2 : z_2] \\ &\equiv \langle y_1z_2 - y_2z_1 : z_1x_2 - z_2x_1 : x_1y_2 - x_2y_1 \rangle . \end{aligned} \tag{3}$$

This is the unique line passing through a_1 and a_2. The **meet** L_1L_2 of distinct lines $L_1 \equiv \langle l_1 : m_1 : n_1 \rangle$ and $L_2 \equiv \langle l_2 : m_2 : n_2 \rangle$ is the point

$$\begin{aligned} L_1L_2 &\equiv \langle l_1 : m_1 : n_1 \rangle \times \langle l_2 : m_2 : n_2 \rangle \\ &\equiv [m_1n_2 - m_2n_1 : n_1l_2 - n_2l_1 : l_1m_2 - l_2m_1] . \end{aligned} \tag{4}$$

This is the unique point lying on L_1 and L_2.

Three points a_1, a_2, a_3 are **collinear** precisely when they lie on a line L; in this case we will sometimes write $L = a_1a_2a_3$. Similarly three lines L_1, L_2, L_3 are **concurrent** precisely when they pass through a point a; in this case we will sometimes write $a = L_1L_2L_3$.

It will be convenient to connect the affine and projective frameworks by the following conventions. If $v = (x, y, z) = \begin{pmatrix} x & y & z \end{pmatrix}$ is a vector, then $a = [v] = [x : y : z] = \begin{bmatrix} x & y & z \end{bmatrix}$ is the **associated projective point**, and v is a **representative vector** for a. If $f = (l, m, n)^T$ is a dual vector, then $L = [f] = \langle l : m : n \rangle = \begin{bmatrix} l & m & n \end{bmatrix}^T$ is the **associated projective line**, and f is a **representative dual vector** for L.

2.2 Projective quadrance and spread

If C is a symmetric invertible 3×3 matrix, with entries in $\mathbb{F}$, and D is its adjugate matrix (the inverse, up to a multiple), then we denote by $\mathbf{C}$ and $\mathbf{D}$ the corresponding projective matrices, each defined up to a non-zero multiple. This pair of projective matrices determine a metrical structure on projective points and lines, as follows.

The (projective) points a_1 and a_2 are **perpendicular** precisely when $a_1\mathbf{C}a_2^T = 0$, written $a_1 \perp a_2$. This is a symmetric relation, and is well-defined. Similarly (projective) lines L_1 and L_2 are **perpendicular** precisely when $L_1^T\mathbf{D}L_2 = 0$, written $L_1 \perp L_2$. The point a and the line L are **dual** precisely when

$$L = a^\perp \equiv \mathbf{C}a^T \quad \text{or equivalently} \quad a = L^\perp \equiv L^T\mathbf{D}. \tag{5}$$

Then two points are perpendicular precisely when *one is incident with the dual of the other*, and similarly for two lines. So $a_1 \perp a_2$ precisely when $a_1^\perp \perp a_2^\perp$, because of the projective relation

$$\begin{aligned} \left(\mathbf{C}a_1^T\right)^T \mathbf{D} \left(\mathbf{C}a_2^T\right) &= \left(a_1\mathbf{C}^T\right) \mathbf{D} \left(\mathbf{C}a_2^T\right) = a_1 \left(\mathbf{CD}\right) \left(\mathbf{C}a_2^T\right) \\ &= a_1\mathbf{C}a_2^T . \end{aligned}$$

A point a is **null** precisely when it is perpendicular to itself, that is, when $a\mathbf{C}a^T = 0$, and a line L is **null** precisely when it is perpendicular to itself, that is, when $L^T\mathbf{D}L = 0$. The null points determine the **null conic**, sometimes also called the *absolute*.

Hyperbolic and *elliptic geometries* arise respectively from the special cases

$$C = J \equiv \begin{pmatrix} 1 & 0 & 0 \\ 0 & 1 & 0 \\ 0 & 0 & -1 \end{pmatrix} = D \qquad \text{and}$$

$$C = I \equiv \begin{pmatrix} 1 & 0 & 0 \\ 0 & 1 & 0 \\ 0 & 0 & 1 \end{pmatrix} = D. \tag{6}$$

In the hyperbolic case, which forms the basis for almost all examples in this paper, the point $a = [x : y : z]$ is null precisely when $x^2 + y^2 - z^2 = 0$, and dually the line $L = (l : m : n)$ is null precisely when $l^2 + m^2 - n^2 = 0$. This is the reason we can picture the null circle in affine coordinates $X \equiv x/z$ and $Y \equiv y/z$ as the (blue) circle $X^2 + Y^2 = 1$. Note that in the elliptic case the null circle, over the rational numbers, has no points lying on it. This is why visualizing hyperbolic geometry is often easier than elliptic geometry.

The bilinear forms determined by C and D can be used to define the metrical structure in the associated projective setting. The dual notions of (**projective**) **quadrance** $q(a_1, a_2)$ between points a_1 and a_2, and (**projective**) **spread** $S(L_1, L_2)$ between lines L_1 and L_2, are

$$q(a_1, a_2) \equiv 1 - \frac{\left(a_1\mathbf{C}a_2^T\right)^2}{\left(a_1\mathbf{C}a_1^T\right)\left(a_2\mathbf{C}a_2^T\right)} \qquad \text{and}$$

$$S(L_1, L_2) \equiv 1 - \frac{\left(L_1^T\mathbf{D}L_2\right)^2}{\left(L_1^T\mathbf{D}L_1\right)\left(L_2^T\mathbf{D}L_2\right)}. \tag{7}$$

While the numerators and denominators of these expressions depend on choices of representative vectors and matrices for $a_1, a_2, \mathbf{C}, L_1, L_2$ and $\mathbf{D}$, the *quotients are independent of scaling*, so the overall expressions are indeed well-defined projectively.If $a_1 = [v_1]$, $a_2 = [v_2]$, and $L_1 = [f_1]$, $L_2 = [f_2]$, then we may write

$$q(a_1, a_2) = 1 - \frac{(v_1 \cdot v_2)^2}{(v_1 \cdot v_1)(v_2 \cdot v_2)} \qquad \text{and}$$

$$S(L_1, L_2) = 1 - \frac{(f_1 \odot f_2)^2}{(f_1 \odot f_1)(f_2 \odot f_2)}$$

where we introduce the dual bilinear form on column vectors by $f_1 \odot f_2 \equiv f_1^T D f_2$.

Clearly $q(a, a) = 0$ and $S(L, L) = 0$, while $q(a_1, a_2) = 1$ precisely when $a_1 \perp a_2$, and dually $S(L_1, L_2) = 1$ precisely when $L_1 \perp L_2$. Then using (5)

$$S\left(a_1^\perp, a_2^\perp\right) = q(a_1, a_2) .$$

In [14], we showed that both these metrical notions can also be reformulated projectively and rationally using suitable cross ratios (and no transcendental functions!)
The following formula, introduced in [12], is is given in a more general setting in [13].

Theorem 2 (Hyperbolic Triple quad formula) *Suppose that a_1,a_2,a_3 are collinear points, with quadrances $q_1 \equiv q(a_2,a_3)$, $q_2 \equiv q(a_1,a_3)$ and $q_3 \equiv q(a_1,a_2)$. Then*

$$(q_1+q_2+q_3)^2 = 2\left(q_1^2+q_2^2+q_3^2\right)+4q_1q_2q_3. \tag{8}$$

Proof. We may assume at least two of the points distinct, as otherwise the relation is trivial. Suppose that representative vectors are then v_1,v_2 and $v_3 \equiv kv_1+lv_2$, with v_1 and v_2 linearly independent. Consider just the two-dimensional subspace spanned by v_1 and v_2. The bilinear form restricted to the subspace spanned by the ordered basis v_1,v_2 is given by some symmetric matrix $\widetilde{C} = \begin{pmatrix} a & b \\ b & c \end{pmatrix}$. Then in this basis $v_1 = (1,0)$, $v_2 = (0,1)$ and $v_3 = (k,l)$, and we may compute that

$$q_3 = s(v_1,v_2) = \frac{ac-b^2}{ac}$$

$$q_2 = s(v_1,v_3) = \frac{l^2\left(ac-b^2\right)}{a\left(ak^2+2bkl+cl^2\right)}$$

$$q_1 = s(v_2,v_3) = \frac{k^2\left(ac-b^2\right)}{c\left(ak^2+2bkl+cl^2\right)}.$$

Then (8) is an identity. □

Here are a few useful consequences of the Triple quad formula. If one of the quadrances is $q_3 = 1$, then $q_1+q_2 = 1$; this is a consequence of the identity

$$(q_1+q_2+1)^2-2q_1^2-2q_2^2-2-4q_1q_2 = -(q_1+q_2-1)^2.$$

Also if two of the quadrances are equal, say $q_1 = q_2 = r$, then $q_3 = 0$ or $q_3 = 4r(1-r)$; this follows from the identity

$$(2r+q_3)^2-4r^2-2q_3^2-4r^2q_3 = -q_3\left(q_3-4r+4r^2\right).$$

2.3 Midpoints of a side

Midpoints are defined very simply using the metrical structure.

Definition 1 *A **midpoint** of a non-null side $\overline{ab}$ is a point m lying on ab which satisfies*

$$q(a,m) = q(b,m).$$

We exclude null sides because every two points on such a side have quadrance 0.

Theorem 3 (Side midpoints) *Suppose that a and b are distinct non-null points and $\overline{ab}$ is a non-null side. Then $\overline{ab}$ has a midpoint precisely when the quantity $1-q(a,b)$ is a square number. In this case, we may find representative vectors v and u for a and b respectively satisfying $v^2 = u^2$, and then there are exactly two midpoints of $\overline{ab}$, namely $m = [u+v]$ and $n = [u-v]$. These two midpoints are perpendicular. Furthermore a,m,b,n form a harmonic range.*

Proof. Suppose that $a = [v]$ and $b = [u]$ so that

$$1-q(a,b) = \frac{(vu)^2}{Q_vQ_u}.$$

A general point m on ab has representative non-zero vector $w = kv+lu$. The condition $q(a,m) = q(b,m)$ amounts to

$$\begin{aligned}\frac{(vw)^2}{Q_vQ_w} = \frac{(uw)^2}{Q_uQ_w} &\Leftrightarrow u^2\left(kv^2+l(vu)\right)^2 = v^2\left(k(vu)+lu^2\right)^2 \\ &\Leftrightarrow k^2u^2\left(v^2\right)^2+l^2(vu)^2u^2 = k^2v^2(vu)^2+l^2v^2\left(u^2\right)^2 \\ &\Leftrightarrow \left(v^2u^2-(vu)^2\right)\left(k^2v^2-l^2u^2\right) = 0.\end{aligned}$$

If $v^2u^2 = (vu)^2$ then by the Parallel vectors theorem either v and u are parallel, which is impossible since a and b are distinct, or the bilinear form restricted to $[v,u]$ is degenerate, which implies that the side $\overline{ab}$ is null. So a midpoint m exists precisely when $k^2v^2 = l^2u^2$.
In this case since a and b are non-null, v^2 and u^2 are non-zero, so k and l are also, since by assumption $w = kv+lu$ is non-zero, and we may renormalize v and u so that $v^2 = u^2$ (by for example setting $\widetilde{v} = kv$ and $\widetilde{u} = lu$, and then replacing $\widetilde{v}$,$\widetilde{u}$ by v,u again).
After this renormalization $1-q(a,b) = (vu)^2/\left(v^2\right)^2$ is then a square, and there are two midpoints $[v+u]$ and $[v-u]$. Since $(v+u)(v-u) = v^2-u^2 = 0$, the two midpoints are perpendicular. It is well known that for any two vectors v and u, the four lines $[v]$,$[v+u]$,$[u]$,$[v-u]$ form a harmonic range.
Conversely suppose that $1-q(a,b) = (vu)^2/\left(v^2u^2\right)$ is a square, say r^2. Then the ratio of v^2 to u^2 is a square, so v and u can be renormalized so that $v^2 = u^2$, at which point the above calculations show that $[v+u]$ and $[v-u]$ are both midpoints. □

We can also relate this to hyperbolic trigonometry as in [14]. If $q(a,b) = r \neq 0$, and m is a midpoint of the side $\overline{ab}$ with $q(a,m) = q(b,m) = q$, then $\{r,q,q\}$ satisfies the Triple quad formula. So as we observed earlier, $r = 4q(1-q)$, and in particular $1-r = 1-4q(1-q) = (2q-1)^2$ is a square number.
The dual lines M and N of the midpoints m and n of a side are called the **midlines** of the side. Since m and n are perpendicular, these each pass through the other midpoint, and

so might also be called the *perpendicular bisectors* of the side.
The dual concept of a midpoint of a side is the following.

Definition 2 *A **biline** of a non-null vertex $\overline{AB}$ is a line L passing through AB which satisfies*

$$S(A,L) = S(B,L).$$

From duality the vertex $\overline{AB}$ has a biline precisely when the quantity $1 - S(A,B)$ is a square number, and in this case we have exactly two bilines which are perpendicular. The symmetry between midpoints and bilines is reflected in the duality between the Incenter and Circumcenter hierarchies in UHG. This notion of symmetry is absent in classical hyperbolic geometry, since there we always have only one midpoint of a side and two bilines (usually called angle bisectors); the number-theoretic considerations with the existence of these are generally invisible—the price of working over the "real numbers"!

2.4 Sydpoints of a side

Definition 3 *A **sydpoint** of a non-null side $\overline{ab}$ is a point s lying on ab which satisfies*

$$q(a,s) = -q(b,s).$$

Note both the similarities and differences between the following theorem and the Side midpoints theorem.

Theorem 4 (Side sydpoints) *Suppose that a and b are distinct non-null points and $\overline{ab}$ is a non-null side. Then $\overline{ab}$ has a sydpoint precisely when $q(a,b) - 1$ is a square number. In this case we can find representative vectors v and u for a and b respectively satisfying $v^2 = -u^2$, and then there are exactly two sydpoints of $\overline{ab}$, namely $s = [v+u]$ and $r = [v-u]$. In such a case, a and b are also sydpoints of the side $\overline{sr}$, and while s and r are not in general perpendicular, we do have*

$$q(a,s) = q(b,r) \qquad \text{and} \qquad q(a,r) = q(b,s).$$

Furthermore a, s, b, r form a harmonic range.

Proof. Suppose that $a = [v]$ and $b = [u]$ so that a general point $s = [w]$ on ab has representative vector $w = kv + lu$. Then the relation $q(a,s) = -q(b,s)$ amounts to

$$\begin{aligned}
&1 - \frac{(vw)^2}{Q_v Q_w} = -1 + \frac{(uw)^2}{Q_u Q_w} \\
\Leftrightarrow\ & 2u^2v^2\left(kv+lu\right)^2 - u^2\left(kv^2 + l\left(vu\right)\right)^2 = v^2\left(k\left(vu\right) + lu^2\right)^2 \\
\Leftrightarrow\ & k^2u^2\left(v^2\right)^2 + l^2\left(u^2\right)^2 v^2 - \left(k^2v^2 + l^2u^2\right)(vu)^2 = 0 \\
\Leftrightarrow\ & \left(v^2u^2 - (vu)^2\right)\left(k^2v^2 + l^2u^2\right) = 0.
\end{aligned}$$

If $v^2u^2 = (vu)^2$ then by the Parallel vectors theorem either v and u are parallel, which is impossible since a and b are distinct, or the bilinear form restricted to $[v,u]$ is degenerate, which implies that the side $\overline{ab}$ is null. So a sydpoint s exists precisely when $k^2v^2 = -l^2u^2$. In this case we may renormalize v and u so that $v^2 = -u^2$, so that $s \equiv [v+u]$ and $r \equiv [v-u]$ are sydpoints. If $q(a,s) = -q(b,s) = d$, $q(a,r) = -q(b,r) = e$ and also $q(r,s) = f$, then the Triple quad formula applied to $\{a,r,s\}$ and $\{b,r,s\}$ implies that both

$$(f+d+e)^2 = 2\left(f^2+d^2+e^2\right) + 4fde \qquad \text{and}$$

$$(f-d-e)^2 = 2\left(f^2+d^2+e^2\right) + 4fde$$

which implies that $f+d+e = \pm(f-d-e)$. Since $f \neq 0$, we conclude that $d = -e$, which shows that

$$q(a,s) = q(b,r) \qquad \text{and} \qquad q(a,r) = q(b,s).$$

Now $(v+u)(v-u) = v^2 - u^2 = 2v^2$ so the two sydpoints s and r are *not* in general perpendicular. However

$$(v+u)^2 = v^2 + 2uv + u^2 = 2uv \qquad \text{and}$$

$$(v-u)^2 = v^2 - 2uv + u^2 = -2uv$$

so that $(v+u)^2 = -(v-u)^2$. By symmetry this implies that $[(v+u)+(v-u)] = [2v] = a$ and $[(v+u)-(v-u)] = [-2u] = b$ are sydpoints of $\overline{rs}$. □

For a fixed q there is at most one sydpoint s of $\overline{ab}$ for which $q(a,s) = q$; the other sydpoint r then satisfies $q(a,r) = -q \neq q$ since q is non-zero.

Example 1 *In the hyperbolic case, suppose that $a = [x:0:1]$ and $b = [y:0:1]$. Then from [14], Ex. 6*

$$q(a,b) = -\frac{(x-y)^2}{(1-x^2)(1-y^2)}$$

and so midpoints $m = [w:0:1]$ and sydpoints $s = [z:0:1]$ of $\overline{ab}$ exist precisely when $\left(x^2-1\right)\left(y^2-1\right) = r^2$ and $\left(x^2-1\right)\left(y^2-1\right) = -t^2$ respectively, in which cases

$$w = \frac{xy+1 \pm r}{x+y} \qquad \text{and} \qquad z = \frac{(1-xy)(x+y) \pm t(x-y)}{x^2+y^2-2}.$$

So we see that algebraically sydpoints are somewhat more complicated than midpoints in general.

Over the rational numbers, any non-null side either approximately has midpoints or sydpoints, since being a square is approximately the same as being positive.
There are a few related notions which are useful to define. The duals S and R of the sydpoints s and r of a side $\overline{ab}$ are the **sydlines** of the side $\overline{ab}$. They do not in general pass through the sydpoints themselves. There is also a dual notion to that of sydpoints of a side which applies to vertices.

Definition 4 *A **siline** of a vertex $\overline{AB}$ is a line L which passes through AB and satisfies $S(A,L) = -S(B,L)$.*

Again by duality we deduce that a vertex $\overline{AB}$ has a siline precisely when the quantity $S(A,B)-1$ is a square number, and in this case there are exactly two silines L and K of the vertex $\overline{AB}$. Then also A, B, L and K are a harmonic pencil of lines. The duals of the silines are the **sipoints** of a vertex $\overline{AB}$.

2.5 The construction of Sydpoints

The following theorem is helpful in constructing sydpoints using a dynamic geometry package.

Theorem 5 (Sydpoints null points) *Suppose that the non-null side $\overline{ab}$ has sydpoints s and r, and that $\overline{ac}$ has midpoints m and n, where $c = (ab)^{\perp}$. Then $x \equiv (mr)(bc) = (ns)(bc)$ and $y \equiv (ms)(bc) = (nr)(bc)$ are null points.*

Proof. Suppose that $a = [v]$, $b = [u]$ and $c = [w]$. Then $vw = uw = 0$, since $c = (ab)^{\perp}$, and also since ab is not null v, u and w are independent. If $\overline{ac}$ has midpoints, in which case we may assume that $v^2 = w^2$, these are $m \equiv [v+w]$ and $n \equiv [v-w]$. If also $\overline{ab}$ has sydpoints, in which case we may assume that $v^2 = -u^2$, these are $s = [v+u]$ and $r = [v-u]$. Note that this renormalization can be made independent of the previous one.
Now consider $x \equiv (mr)(bc)$. This is a point with a representative vector of the form $k(v+w)+l(v-u)$ for some numbers k and l. Since x has a representative vector which is also in the span of u and w, it must be a multiple of $(v+w)-(v-u) = u+w$. But then

$$(u+w)^2 = u^2 + 2uw + w^2 = 0$$

since $uw = 0$ and $u^2 = -w^2$. So x is a null point, and similarly for y. □

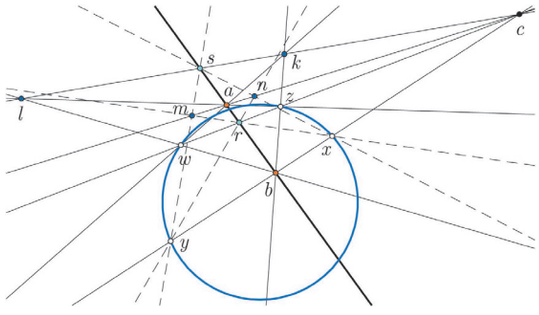

Figure 7: *Construction of sydpoints of $\overline{ab}$*

We make some remarks that are useful for practical constructions involving Geometer's Sketchpad, C.a.R., Cabri, GeoGebra or Cinderella etc. To approximately construct the sydpoints r and s of $\overline{ab}$ as in Figure 7, first construct the dual $c = (ab)^{\perp}$, then the midpoints m and n of $\overline{ac}$, and then use the null points x and y lying on bc as shown (we are assuming these exist—for a dynamic geometry package, approximately is sufficient!
The required points are $s = (nx)(ab) = (my)(ab)$ and $r = (ny)(ab) = (mx)(ab)$. Similarly, given the sydpoints r and s of $\overline{ab}$, a and b can be constructed as the sydpoints of $\overline{rs}$ using the null points w and z lying on rc and the midpoints k and l of $\overline{cs}$, the required points are $a = (lz)(rs) = (kw)(rs)$ and $b = (lw)(rs) = (kz)(rs)$. So the construction of sydpoints can be reduced, at least in this kind of situation, to computations of midpoints.
Once we establish the Circumlines theorem, it is interesting that Figure 7 can be viewed as a limiting case applied to the triangle $\overline{abc}$—the null points x and y act as midpoints of $\overline{bc}$, so mrx acts as a circumline.
Another useful construction is to find, given the point b and one of the sydpoints s, the other point a and the other sydpoint r as in Figure 8. First construct the dual $c = (bs)^{\perp}$, then find the midpoints k and l of $\overline{cs}$. Use the null points u,t lying on bk and the null points v,w lying on bl to construct $r = (cuv)(bs)$ and $a = (lu)(bs) = (kv)(bs)$.
However by symmetry there is a second solution: $\overline{r} = (cwt)(bs)$ and $\overline{a} = (lt)(bs) = (kw)(bs)$. Thus, we can think of s and r as being the sydpoints of the side $\overline{ab}$, and s and $\overline{r}$ as the sydpoints of the side $\overline{\overline{ab}}$. Notice also that b is a midpoint of the side $r\overline{r}$ and similarly s is a midpoint of the side $a\overline{a}$, and in fact $q(b,r) = q(b,\overline{r}) = q(s,a) = q(s,\overline{a})$.

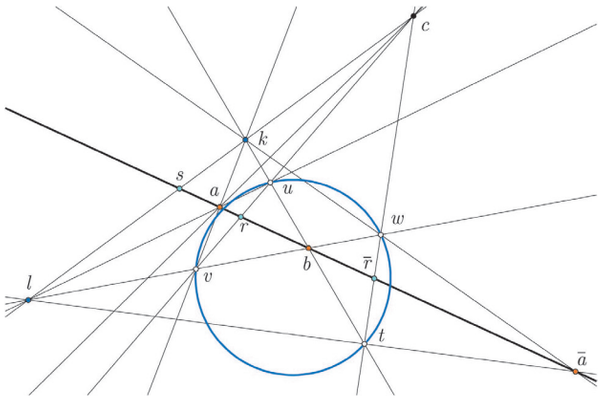

Figure 8: *Constructing r and a (or $\overline{r}$ and $\overline{a}$) from s and b*

2.6 Twin circles

In the geometry we are studying, a circle $\mathcal{C}$ may be defined as an equation of the form $q(c,x) = k$, for a fixed point c called the **center**, and a fixed number k called the **quadrance** of the circle. We also write $\mathcal{C}_c^k$ for this circle, and say that a point a **lies on** the circle precisely when $q(c,a) = k$. Since in this case the circle is also determined by c and a,

we write $\mathcal{C}_c^k = \mathcal{C}_c^{(a)}$. The bracket reminds us that a is not unique.

Definition 5 *Two circles $\mathcal{C}_1$ and $\mathcal{C}_2$ with the same center c and quadrances q_1 and q_2 are **twins** precisely when*

$$q_1 + q_2 = 2.$$

We now show that twin circles are naturally connected with sydpoints.

Theorem 6 (Sydpoint twin circle) *If s is a sydpoint of $\overline{ab}$, and c lies on $S \equiv s^\perp$, then the circles $\mathcal{C}_c^{(a)}$ and $\mathcal{C}_c^{(b)}$ are twins. Conversely if $\mathcal{C}_c^{(a)}$ and $\mathcal{C}_c^{(b)}$ are twins, then $s \equiv c^\perp(ab)$ is a sydpoint of $\overline{ab}$.*

Proof. If s is a sydpoint of $\overline{ab}$ then $q(a,s) = q = -q(b,s)$ for some q. Then since c and s are perpendicular, $q(c,s) = 1$. Let $d = s^\perp(ab)$. Then since d and s are perpendicular, $q(d,s) = 1$, and then $q(a,d) = 1 - q(a,s) = 1 - q$ and $q(b,d) = 1 - q(b,s) = 1 + q$. So $q(a,d) + q(b,d) = 2$. Now suppose that $q(c,d) = r$. Then by Pythagoras' theorem (see [13], [14]) in the right triangle $\overline{cda}$ we have

$$q(c,a) = r + (1-q) - r(1-q)$$

while in the right triangle $\overline{cdb}$ we have

$$q(c,b) = r + (1+q) - r(1+q).$$

Then

$$q(c,a) + q(c,b) =$$
$$= r + (1-q) - r(1-q) + r + (1+q) - r(1+q) = 2.$$

The argument can be reversed to show the converse. □

We note that the theorem has another possible interpretation: the locus of a point c such that $q(a,c) + q(b,c) = 2$ is a line.

2.7 Constructions of twin circles

The Sydpoint twin circle theorem assists us to construct twin circles; we generally expect this to reduce to finding midpoints, but there are also some simpler scenarios. Suppose we are given a circle $\mathcal{C}$ (in brown) with center c as in Figure 9. Choose an arbitrary point a on the circle $\mathcal{C}$ and construct $C \equiv c^\perp$, then let s be the meet of ac and C, and t the meet of $A \equiv a^\perp$ and C.

Now, we can apply the construction of Figure 8; suppose that the side $\overline{st}$ has midpoints m and n, and that x and y are null points on am, and z and w are null points on an. Then $b \equiv (mz)(ac) = (ny)(ac)$ and $e \equiv (mw)(ac) = (nx)(ac)$ lie on the twin circle $\mathcal{D}$ to $\mathcal{C}$. Symmetry implies that we could also use $d \equiv (mw)(ct) = (ny)(ct)$ and $f \equiv (mz)(ct) = (nx)(ct)$.

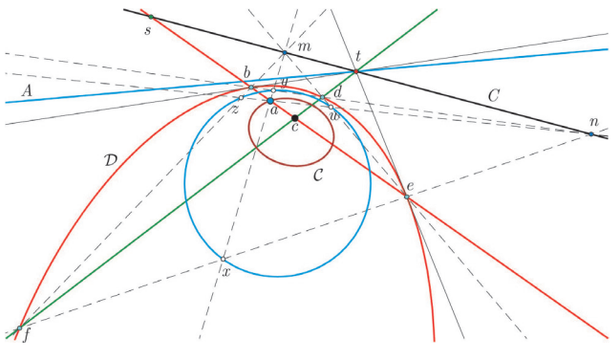

Figure 9: *Constructing the twin circle $\mathcal{D}$ of $\mathcal{C}$*

Figure 10 shows another example of constructing the twin $\mathcal{D}$ of a given circle $\mathcal{C}$ (in brown) with center c. In this case c is outside the null circle, so its dual line C passes through null points x and y (approximately—remember that a dynamic geometry package usually only deals with decimal approximations, so the number-theoretical subtlety is diminished). Choose a point a on $\mathcal{C}$ with dual line $A = a^\perp$. Then the twin circle $\mathcal{D}$ (in red) is the locus of the point $b = (ax)A$ or the point $d = (ay)A$ as a moves along $\mathcal{C}$.

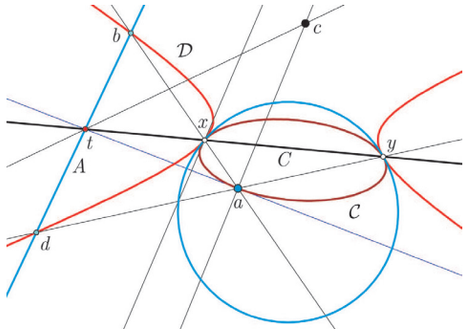

Figure 10: *Another construction of a twin circle*

The fact that $q(a,c) + q(b,c) = 2$ follows by applying either the Nil Cross law ([14, Thm 80]) or the Null subtended quadrance theorem ([14, Thm 90]) to the triangle $\overline{abc}$. Similarly, given the red circle $\mathcal{D}$, its twin circle $\mathcal{C}$ (in brown) can be constructed as the locus of the point $a = (bx)b^\perp$ when moving the point b on $\mathcal{D}$.

It should also be noted that we have *not at all established that the twin of any circle necessarily exists*. In fact over the rational numbers, the twin circle of a given circle does not always exist. For example over the rational numbers, if c is inside the null circle, then $q(c,a)$ never takes on values in the range $(0,1)$, but it can take on values in the range $(1,2)$.

3 Circumlinear coordinates and the Orthocenter hierarchy

In the paper ([16]) we focussed on ortholinear coordinates, as the Orthocenter is arguably the most important point in hyperbolic triangle geometry, and secondly on the Incenter hierarchy. In this paper we are primarily interested in the Circumcenter hierarchy, and we introduce *circumlinear coordinates* to work efficiently with both *midpoints* and *sydpoints* simultaneously. While triangle geometry involving sydpoints will be new and somewhat unfamiliar, the natural beauty and elegance of this theory is very compelling indeed.

Suppose the bilinear form $v \cdot u = vAu^T$ in the associated three-dimensional vector space $V = \mathbb{F}^3$ is given by a symmetric matrix A, and that $T : V \to V$ is a linear transformation given by an invertible 3×3 matrix M, so that $T(v) = vM = w$, with inverse matrix N, so that $wN = v$. The new bilinear form $\circ$ defined by

$$\begin{aligned} w_1 \circ w_2 &\equiv (w_1N) \cdot (w_2N) = (w_1N)A(w_2N)^T \\ &= w_1(NAN^T)w_2^T \end{aligned} \tag{9}$$

has matrix $C = NAN^T$.

So let us start with three (projective) points a_1, a_2 and a_3 such that *each of the three sides of the triangle* $\overline{a_1a_2a_3}$ *has either midpoints or sydpoints*. That means we can find representative vectors v_1, v_2 and v_3 in V so that for any i and j, $v_i^2 = \pm v_j^2$. There are two possibilities up to relabelling and re-scaling: 1) $v_1^2 = v_2^2 = v_3^2 = 1$ (this corresponds to three midsides) and 2) $v_1^2 = v_2^2 = -v_3^2 = 1$ (this corresponds to one midside and two sydsides). We can incorporate both situations at once by supposing that

$$v_1^2 = v_2^2 = \varepsilon v_3^2 = 1 \qquad \text{where} \qquad \varepsilon = \pm 1.$$

Now we can find a linear transformation to map v_1, v_2 and v_3 to the basis vectors $e_1 = (1,0,0)$, $e_2 = (0,1,0)$ and $e_3 = (0,0,1)$ respectively. With respect to this new basis, the bilinear form is then given by a new matrix of the form

$$C = \begin{pmatrix} 1 & a & b \\ a & 1 & c \\ b & c & \varepsilon \end{pmatrix} \qquad \text{with adjugate}$$

$$D = \begin{pmatrix} c^2 - \varepsilon & a\varepsilon - bc & b - ac \\ a\varepsilon - bc & b^2 - \varepsilon & c - ab \\ b - ac & c - ab & a^2 - 1 \end{pmatrix} \tag{10}$$

where the diagonal entries of C ensure that $e_1^2 = e_2^2 = 1$ and $e_3^2 = \varepsilon$, and otherwise $e_1e_2 = a$, $e_1e_3 = b$ and $e_2e_3 = c$ are arbitrary. So the metrical structure depends on the numbers a, b and c and (the sign of) ε. Note that

$$\det \begin{pmatrix} 1 & a & b \\ a & 1 & c \\ b & c & \varepsilon \end{pmatrix} = -a^2\varepsilon - b^2 - c^2 + \varepsilon + 2abc.$$

This quantity appears as a common factor in several of the derivations of proportions in the paper, and since it is by assumption non-zero, we simply cancel it without mention.

We now reformulate some of the formulas of the Orthocenter hierarchy of ([16]) using circumlinear coordinates, maintaining the convention of using capital letters for various constructions associated to a base triangle. The projective matrices corresponding to C and D are denoted **C** and **D** respectively.

Our starting point is that the basic Triangle $\overline{a_1a_2a_3}$ has been projectively transformed so that its **Points** are

$$a_1 = [1:0:0] \quad a_2 = [0:1:0] \quad a_3 = [0:0:1]. \tag{11}$$

The **Lines** of the Triangle are then

$$L_1 = \langle 1:0:0 \rangle \quad L_2 = \langle 0:1:0 \rangle \quad L_3 = \langle 0:0:1 \rangle.$$

The main assumption is that each of the three sides is either a midside or a sydside, or possibly both, which we have seen allows us to write the bilinear form using the projective matrices (10). The Triangle will have three midsides if $\varepsilon = 1$, and two sydsides and one midside if $\varepsilon = -1$. The computations are based on two basic operations: *finding joins and meets*, which essentially amounts to taking cross products as in (3) and (4); and *finding duals*, either by multiplying transposes of points by C on the left, or transposes of lines by D on the right as in (5).

Our goal is to establish formulas for important points and lines to facilitate determining relationships between them: the reader is encouraged to follow along and check our computations, which are mostly elementary. Occasionally we simplify a proportion by cancelling a common factor: naturally this factor should not be zero, so we state this as a condition.

3.1 Change of coordinates and the main example

Most of the diagrams in this paper deal with the particular triangle in Figure 11 created with GSP, with affine points $a_1 \approx [-0.03959, 0.15272]$, $a_2 \approx [-0.20363, 0.78056]$ and $a_3 \approx [-1.75344, 0.19797]$, and corresponding representative vectors $v_1 \approx (-0.237, 0.914, 5.985)$, $v_2 \approx (-2.036, 7.806, 10)$ and $v_3 \approx (-7.128, 0.805, 4.065)$. These have been normalized so that

$$Q_{v_1} = Q_{v_2} = -Q_{v_3}$$

with respect to the bilinear form $v \cdot u \equiv vJu^T$, where J is defined in (6).

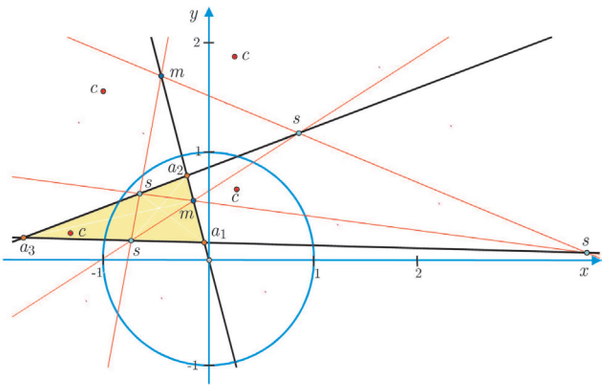

Figure 11: *Basic example triangle with coordinates*

We now show how to explicitly change coordinates, following Section 1.5 of [16]. The linear transformation $T(v) = vN$, where N is

$$N = \begin{pmatrix} -0.237 & 0.914 & 5.985 \\ -2.036 & 7.806 & 10 \\ -7.128 & 0.805 & 4.065 \end{pmatrix},$$

sends $e_1 = (1,0,0)$, $e_2 = (0,1,0)$ and $e_3 = (0,0,1)$ to v_1, v_2 and v_3 respectively. The inverse matrix $M = N^{-1}$ sends the vectors v_1, v_2 and v_3 to e_1, e_2 and e_3. Following (9), after we apply the linear transformation T, J is replaced by the matrix

$$C = NJN^T \approx \begin{pmatrix} 1.0 & 1.495 & 0.627 \\ 1.495 & 1 & 0.568 \\ 0.627 & 0.568 & -1 \end{pmatrix} \quad \text{with adjugate}$$

$$D = \begin{pmatrix} 1.327 & -1.851 & -0.222 \\ -1.851 & 1.393 & -0.369 \\ -0.222 & -0.369 & 1.235 \end{pmatrix}.$$

We get the constants

$$a = 1.495 \qquad b = 0.627 \qquad c = 0.568 \qquad \varepsilon = -1.$$

As an example of how to explicitly apply the theorems of this paper to our specific triangle, consider the midpoints of the side $\overline{a_1a_2}$ in standard coordinates which are $m = n_{1+} = [1:1:0]$ and $m = n_{1-} = [1:-1:0]$. Multiply by N and then renormalize so that $z = 1$, to find these midpoints in the original triangle to be

$$\begin{aligned} n_{1+} &= [1:1:0]N = \begin{bmatrix} -2.273 & 8.72 & 15.985 \end{bmatrix} \\ &= \begin{bmatrix} -0.142 & 0.546 & 1.0 \end{bmatrix} \\ n_{1-} &= [1:-1:0]N = \begin{bmatrix} 1.799 & -6.892 & -4.015 \end{bmatrix} \\ &= \begin{bmatrix} -0.448 & 1.72 & 1.0 \end{bmatrix}. \end{aligned}$$

As another example, using the formulas from the Circumlines/Circumcenter theorem, we may similarly compute that the circumcenters c, in agreement with Figure 11, are

$$\begin{aligned} c_0 &= \begin{bmatrix} 0.268 & 0.653 & 1.0 \end{bmatrix} \quad c_1 = \begin{bmatrix} -0.997 & 1.573 & 1.0 \end{bmatrix} \\ c_2 &= \begin{bmatrix} 0.249 & 1.898 & 1.0 \end{bmatrix} \quad c_3 = \begin{bmatrix} -1.308 & 0.241 & 1.0 \end{bmatrix}. \end{aligned}$$

3.2 Altitudes, Orthocenter and Orthic triangle

The **Dual lines** are

$$\begin{aligned} A_1 &\equiv a_1^\perp = \mathbf{C}a_1^T = \langle 1 : a : b \rangle \\ A_2 &\equiv a_2^\perp = \mathbf{C}a_2^T = \langle a : 1 : c \rangle \\ A_3 &\equiv a_3^\perp = \mathbf{C}a_3^T = \langle b : c : \varepsilon \rangle. \end{aligned}$$

The **Dual points** are

$$\begin{aligned} l_1 &\equiv L_1^T D = \begin{bmatrix} c^2 - \varepsilon : \varepsilon a - bc : b - ac \end{bmatrix} \\ l_2 &= \begin{bmatrix} \varepsilon a - bc : b^2 - \varepsilon : c - ab \end{bmatrix} \\ l_3 &= \begin{bmatrix} b - ac : c - ab : a^2 - 1 \end{bmatrix}. \end{aligned}$$

The **Altitudes** are

$$\begin{aligned} N_1 &\equiv a_1 l_1 = \langle 0 : ac - b : \varepsilon a - bc \rangle \\ N_2 &\equiv a_2 l_2 = \langle c - ab : 0 : bc - \varepsilon a \rangle \\ N_3 &\equiv a_3 l_3 = \langle ab - c : b - ac : 0 \rangle \end{aligned}$$

and the **Altitude dual points** are

$$\begin{aligned} n_1 &\equiv A_1 L_1 = \begin{bmatrix} 0 : -b : a \end{bmatrix} \\ n_2 &\equiv A_2 L_2 = \begin{bmatrix} c : 0 : -a \end{bmatrix} \\ n_3 &\equiv A_3 L_3 = \begin{bmatrix} -c : b : 0 \end{bmatrix}. \end{aligned}$$

The **Base points** are

$$\begin{aligned} b_1 &\equiv N_1 L_1 = \begin{bmatrix} 0 : \varepsilon a - bc : b - ac \end{bmatrix} \\ b_2 &\equiv N_2 L_2 = \begin{bmatrix} \varepsilon a - bc : 0 : c - ab \end{bmatrix} \\ b_3 &\equiv N_3 L_3 = \begin{bmatrix} b - ac : c - ab : 0 \end{bmatrix} \end{aligned}$$

and the **Base lines** are

$$\begin{aligned} B_1 &\equiv n_1 l_1 = \left\langle b^2 - 2abc + a^2\varepsilon : a\left(\varepsilon - c^2\right) : b\left(\varepsilon - c^2\right) \right\rangle \\ B_2 &\equiv n_2 l_2 = \left\langle a\left(\varepsilon - b^2\right) : c^2 - 2abc + a^2\varepsilon : c\left(\varepsilon - b^2\right) \right\rangle \\ B_3 &\equiv n_3 l_3 = \left\langle b\left(1 - a^2\right) : c\left(1 - a^2\right) : b^2 - 2abc + c^2 \right\rangle. \end{aligned}$$

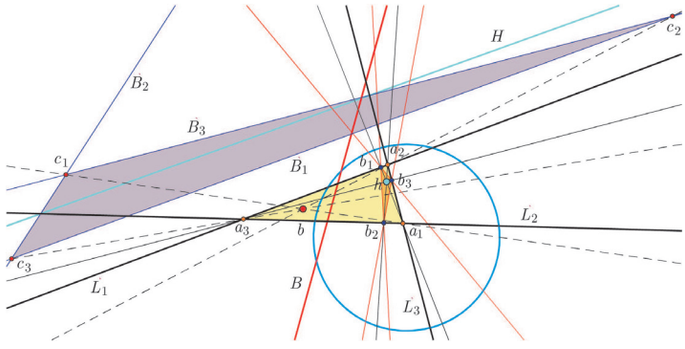

Figure 12: *Altitudes, Orthocenter, Orthic triangle and Base center b*

Assuming $a\varepsilon - bc \neq 0$, $b - ac \neq 0$ and $c - ab \neq 0$, the **Orthic lines** are

$$\begin{aligned} C_1 &\equiv b_2 b_3 = \langle ab - c : b - ac : \varepsilon a - bc \rangle \\ C_2 &\equiv b_1 b_3 = \langle c - ab : ac - b : \varepsilon a - bc \rangle \\ C_3 &\equiv b_1 b_2 = \langle c - ab : b - ac : bc - a\varepsilon \rangle. \end{aligned}$$

The **Orthic points** are

$$\begin{aligned}
c_1 \equiv B_2B_3 =&[\left(2ca^2-ba-c\right)\varepsilon+c\left(2b^2+c^2-3abc\right):\\
&:(ac-b)\left(b^2-\varepsilon\right):(bc-a\varepsilon)\left(a^2-1\right)]\\
c_2 \equiv B_1B_3 =&[(ab-c)\left(c^2-\varepsilon\right):\left(2ba^2-ca-b\right)\varepsilon+\\
&+b\left(b^2+2c^2-3abc\right):(bc-a\varepsilon)\left(a^2-1\right)]\\
c_3 \equiv B_1B_2 =&[(ab-c)\left(c^2-\varepsilon\right):(ac-b)\left(b^2-\varepsilon\right):\\
&:a\left(a^2-1\right)\varepsilon+\left(2ab^2-3a^2bc+2ac^2-bc\right)].
\end{aligned}$$

The **Orthocenter** is arguably the most important point in triangle geometry, it is

$$\begin{aligned}
&h \equiv N_1N_2 = N_2N_3 = N_1N_3\\
&= [(b-ac)(a\varepsilon-bc):(c-ab)(a\varepsilon-bc):(ac-b)(ab-c)].
\end{aligned}$$

The dual line is the **Ortholine**

$$H \equiv n_1n_2 = n_1n_3 = n_2n_3 = \langle ab : ac : bc\rangle.$$

The **Orthic triangle** $\overline{b_1b_2b_3}$ is perspective with the Triangle $\overline{a_1a_2a_3}$ with center of perspectivity the Orthocenter h.

The *Triangle Base center theorem* states that the **Orthic dual triangle** $\overline{c_1c_2c_3}$ is perspective with the Triangle $\overline{a_1a_2a_3}$. The center of perspectivity is the **Base center**

$$b = \left[(ab-c)\left(c^2-\varepsilon\right):(ac-b)\left(b^2-\varepsilon\right):(bc-\varepsilon a)\left(a^2-1\right)\right]$$

with dual line the **Base axis**

$$B = \langle c+ab : b+ac : \varepsilon a+bc\rangle.$$

In Figure 12 we see the Altitudes, Orthocenter h and the dual Ortholine H, the Orthic triangle $\overline{b_1b_2b_3}$, Orthic dual triangle $\overline{c_1c_2c_3}$, base center b and Base axis B.

3.3 Desargues points and the Orthoaxis

The **Desargues points** are the meets of corresponding Orthic lines and Lines:

$$\begin{aligned}
g_1 &\equiv C_1L_1 = [0 : bc-\varepsilon a : b-ac]\\
g_2 &\equiv C_2L_2 = [bc-\varepsilon a : 0 : c-ab]\\
g_3 &\equiv C_3L_3 = [b-ac : ab-c : 0]
\end{aligned}$$

and the dual **Desargues lines** are

$$\begin{aligned}
G_1 &= \left\langle b^2-a^2\varepsilon : 2bc-ac^2-a\varepsilon : bc^2+b\varepsilon-2ac\varepsilon\right\rangle\\
G_2 &= \left\langle 2bc-ab^2-a\varepsilon : c^2-a^2\varepsilon : b^2c+c\varepsilon-2ab\varepsilon\right\rangle\\
G_3 &= \left\langle b+a^2b-2ac : 2ab-c-a^2c : b^2-c^2\right\rangle.
\end{aligned}$$

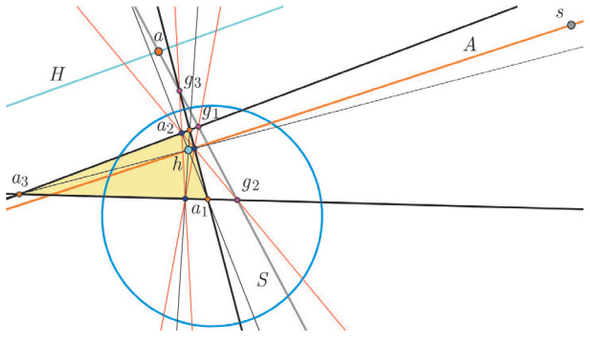

Figure 13: *Desargues points, Orthic axis S and Orthoaxis A*

Desargues' theorem implies that the Desargues points g_1, g_2, g_3 are collinear. They lie on the **Orthic axis**

$$S = \langle ab-c : ac-b : bc-a\varepsilon\rangle. \tag{12}$$

Dually the Desargues lines G_1, G_2, G_3 are concurrent, passing through the **Orthostar**

$$s = \begin{bmatrix} \left(2ca^2-3ba+c\right)\varepsilon+c\left(2b^2-c^2-abc\right):\\ \left(2ba^2-3ca+b\right)\varepsilon-b\left(b^2-2c^2+abc\right):\\ a\left(1-a^2\right)\varepsilon+\left(2ab^2-a^2bc+2ac^2-3bc\right)\end{bmatrix}.$$

The **Orthoaxis** A**,** introduced in [16], is arguably the most important line in hyperbolic triangle geometry; it and its dual the **Orthoaxis point** a are

$$\begin{aligned}
A \equiv sh =&\langle(ab-c)\left(a^2\varepsilon-b^2\right):(b-ac)\left(a^2\varepsilon-c^2\right):\\
&:(bc-a\varepsilon)\left(b^2-c^2\right)\rangle\\
a \equiv SH =&\left[c\left(a^2\varepsilon-b^2\right):b\left(c^2-\varepsilon a^2\right):a\left(b^2-c^2\right)\right].
\end{aligned}$$

The *Base center on Orthoaxis theorem* asserts that the Orthoaxis A passes through the Base center b.

3.4 Parallels and the Double triangle

Recall from [14] that the **parallel line** P **through a point** a **to a line** L is the line through a perpendicular to the altitude from a to L. This motivates the definition of the Double triangle of a Triangle. The **Parallel lines**

$$\begin{aligned}
P_1 &\equiv a_1n_1 = \langle 0 : a : b\rangle\\
P_2 &\equiv a_2n_2 = \langle a : 0 : c\rangle\\
P_3 &\equiv a_3n_3 = \langle b : c : 0\rangle
\end{aligned}$$

are the joins of corresponding Points a and Altitude points n, and their duals are the **Parallel points**

$$\begin{aligned}
p_1 &= \left[b^2-2abc+a^2\varepsilon : bc-a\varepsilon : ac-b\right]\\
p_2 &= \left[bc-a\varepsilon : c^2-2abc+a^2\varepsilon : ab-c\right]\\
p_3 &= \left[\varepsilon(ac-b) : \varepsilon(ab-c) : b^2-2abc+c^2\right].
\end{aligned}$$

Assuming $a \neq 0$, $b \neq 0$ and $c \neq 0$, the meets of Parallel lines are the **Double points**

$$d_1 \equiv P_2P_3 = [-c : b : a]$$
$$d_2 \equiv P_1P_3 = [c : -b : a]$$
$$d_3 \equiv P_1P_2 = [c : b : -a]$$

and their duals are the **Double lines**

$$D_1 \equiv p_2p_3 = \langle 2ab - c : b : \varepsilon a \rangle$$
$$D_2 \equiv p_1p_3 = \langle c : 2ac - b : \varepsilon a \rangle$$
$$D_3 \equiv p_1p_2 = \langle c : b : 2bc - \varepsilon a \rangle .$$

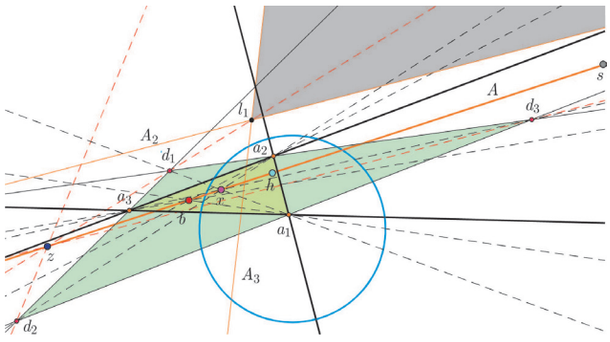

Figure 14: *The Double triangle, Orthoaxis A, and the points z, b, x, h and s*

We give here another proof of the following result, involving a simpler computation than in [16].

Theorem 7 (Double triangle midpoint) *The Points a_1, a_2, a_3 are midpoints of the Double triangle $\overline{d_1d_2d_3}$.*

Proof. We compute

$$q(d_1, a_3) = \frac{-b^2 - c^2 + 2abc}{a^2 - b^2 - c^2 + 2abc} = q(d_2, a_3).$$

Similarly, a_1 is a midpoint of $\overline{d_2d_3}$, and a_2 is a midpoint of $\overline{d_1d_3}$. □

The *Double triangle perspectivity theorem* states that the Double triangle $\overline{d_1d_2d_3}$ and the Triangle $\overline{a_1a_2a_3}$ are perspective from a point, the **Double point**, or x **point**

$$x = [c : b : a]$$

which lies on the Orthoaxis A. The proof is very simple in these coordinates: we compute that

$$a_1d_1 = \langle 0 : -a : b \rangle$$
$$a_2d_2 = \langle a : 0 : -c \rangle$$
$$a_3d_3 = \langle -b : c : 0 \rangle$$

and then observe that these lines meet at x.

The dual of the x point is the X **line**

$$X = \langle 2ab + c : 2ac + b : 2bc + a\varepsilon \rangle .$$

The *Double dual triangle perspectivity theorem* asserts that the Double triangle $\overline{d_1d_2d_3}$ and the Dual triangle $\overline{l_1l_2l_3}$ are perspective from a point, the **Double dual point**, or z **point**

$$z = \begin{bmatrix} (ca^2 - 2ba + c)\varepsilon + c(b^2 - c^2) : \\ (ba^2 - 2ca + b)\varepsilon - b(b^2 - c^2) : \\ a(1 - a^2)\varepsilon + ab^2 - 2bc + ac^2 \end{bmatrix}.$$

Its dual is the Z **line**

$$Z = \langle c : b : \varepsilon a \rangle .$$

The z point lies on the Orthoaxis A, or equivalently the Orthoaxis point a lies on the Z line.

4 The Circumcenter hierarchy

We now begin the study of the Circumcenter hierarchy. The basic assumption that we used to set up circumlinear coordinates was that each side of the triangle was either a midside or a sydside. We wish to treat both cases symmetrically, hence we introduce the notion that a **smydpoint** n of the side $\overline{ab}$ is either a midpoint or a sydpoint (or possibly both). Smydpoints exists precisely when $1 - q(a, b)$ is either a square or the negative of a square (or possibly both). Our diagrams will illustrate the situation when one side has midpoints and the other two sides have sydpoints. We introduce consistent labelling to bring out the four-fold symmetry in this situation.

4.1 Circumcenters, medians and centroids

By the Side midpoints and Side sydpoints theorems, in Circumlinear coordinates the smydpoints are

$$n_{1+} = [0 : 1 : 1] \text{ and } n_{1-} = [0 : -1 : 1] \quad \text{on } \overline{a_2a_3}$$
$$n_{2+} = [1 : 0 : 1] \text{ and } n_{2-} = [1 : 0 : -1] \quad \text{on } \overline{a_1a_3}$$
$$n_{3+} = [1 : 1 : 0] \text{ and } n_{3-} = [1 : -1 : 0] \quad \text{on } \overline{a_1a_2}.$$

Note that the indices of our labelling reflect the positions and relative signs of the non-zero entries.

Theorem 8 (Circumlines/Circumcenters) *The six Smydpoints lie three at a time on four* ***Circumlines***

$$C_0 \equiv n_{1-}n_{2-}n_{3-} = \langle 1 : 1 : 1 \rangle$$
$$C_1 \equiv n_{1-}n_{2+}n_{3+} = \langle -1 : 1 : 1 \rangle$$
$$C_2 \equiv n_{2-}n_{1+}n_{3+} = \langle 1 : -1 : 1 \rangle$$
$$C_3 \equiv n_{3-}n_{1+}n_{2+} = \langle 1 : 1 : -1 \rangle .$$

The duals are the ***Circumcenters***

$$c_0 = C_0^{\perp} = \begin{bmatrix} (a-1)\varepsilon - c(a+b-c)+b : \\ (a-1)\varepsilon - b(a-b+c)+c : \\ (a-1)(a-b-c+1) \end{bmatrix}$$
$$c_1 = C_1^{\perp} = \begin{bmatrix} (a+1)\varepsilon - c(a+b+c)+b : \\ c-(a+1)\varepsilon - b(a-b-c) : \\ (a+1)(a-b+c-1) \end{bmatrix}$$
$$c_2 = C_2^{\perp} = \begin{bmatrix} b-(a+1)\varepsilon - c(a-b-c) : \\ (a+1)\varepsilon - b(a+b+c)+c : \\ (a+1)(a+b-c-1) \end{bmatrix}$$
$$c_3 = C_3^{\perp} = \begin{bmatrix} b-(a-1)\varepsilon - c(a-b+c) : \\ c-(a-1)\varepsilon - b(a+b-c) : \\ (a-1)(a+b+c+1) \end{bmatrix}.$$

Proof. The formulas for the Circumlines can be checked immediately, the Circumcenter formulas are computations using duality. □

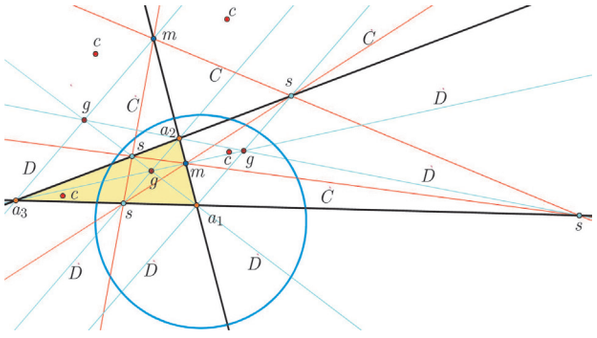

Figure 15: *Circumlines, Circumcenters, Medians and Centroids*

Median lines (or just **medians**) are joins of Points a and Smydpoints n which lie on the opposite lines:

$$D_{1-} \equiv a_1 n_{1-} = \langle 0:1:1\rangle \qquad D_{1+} \equiv a_1 n_{1+} = \langle 0:-1:1\rangle$$
$$D_{2+} \equiv a_2 n_{2+} = \langle 1:0:-1\rangle \qquad D_{2-} \equiv a_2 n_{2-} = \langle 1:0:1\rangle$$
$$D_{3-} \equiv a_3 n_{3-} = \langle 1:1:0\rangle \qquad D_{3+} \equiv a_3 n_{3+} = \langle -1:1:0\rangle.$$

Figure 15 shows the six Medians and their meets.

Theorem 9 (Centroids) *The Median lines D are concurrent in threes, meeting at four* ***Centroid points***

$$g_0 \equiv D_{1+}D_{2+}D_{3+} = [1:1:1]$$
$$g_1 \equiv D_{1+}D_{2-}D_{3-} = [-1:1:1]$$
$$g_2 \equiv D_{1-}D_{2+}D_{3-} = [1:-1:1]$$
$$g_3 \equiv D_{1-}D_{2-}D_{3+} = [1:1:-1].$$

The dual ***Centroid lines*** *are*

$$G_0 = \langle a+b+1 : a+c+1 : b+c+\varepsilon\rangle$$
$$G_1 = \langle a+b-1 : c-a+1 : c-b+\varepsilon\rangle$$
$$G_2 = \langle b-a+1 : a+c-1 : b-c+\varepsilon\rangle$$
$$G_3 = \langle a-b+1 : a-c+1 : b+c-\varepsilon\rangle.$$

Proof. Straightforward. □

4.2 CircumCentroids

While many aspects of the Circumcenter hierarchy are independent of ε, there are some that are not. The following is an extension of the similarly named result in [16].

Theorem 10 (CircumCentroid axis) *The meets of corresponding Circumlines and Centroid lines are collinear precisely when either $b = \pm c$ or $\varepsilon = 1$. If $\varepsilon = 1$, the common line is the Z axis $\langle c : b : \varepsilon a\rangle$, and the joins of corresponding Circumcenters and Centroid points meet at the z point. If $b = c$, then the common line is $\langle b : b : a+\varepsilon-1\rangle$, while if $b = -c$, then the common line is $\langle -b : b : a-\varepsilon+1\rangle$.*

Proof. The meets of Circumlines C_0, C_1, C_2, C_3 and corresponding Centroid lines G_0, G_1, G_2, G_3 are the four **CircumCentroid points**

$$z_0 \equiv C_0G_0 = [a-b-\varepsilon+1 : c-a+\varepsilon-1 : b-c]$$
$$z_1 \equiv C_1G_1 = [b-a-\varepsilon+1 : 1-a-c-\varepsilon : b+c]$$
$$z_2 \equiv C_2G_2 = [1-a-b-\varepsilon : c-a-\varepsilon+1 : b+c]$$
$$z_3 \equiv C_3G_3 = [a+b-\varepsilon+1 : \varepsilon-a-c-1 : b-c].$$

The determinants

$$\det \begin{bmatrix} a-b-\varepsilon+1 & c-a+\varepsilon-1 & b-c \\ b-a-\varepsilon+1 & 1-a-c-\varepsilon & b+c \\ 1-a-b-\varepsilon & c-a-\varepsilon+1 & b+c \end{bmatrix} = -4\left(b^2-c^2\right)(\varepsilon-1)$$

$$\det \begin{bmatrix} a-b-\varepsilon+1 & c-a+\varepsilon-1 & b-c \\ 1-a-b-\varepsilon & c-a-\varepsilon+1 & b+c \\ a+b-\varepsilon+1 & \varepsilon-a-c-1 & b-c \end{bmatrix} = 4\left(b^2-c^2\right)(\varepsilon-1)$$

show that the CircumCentroid points are collinear precisely when $\varepsilon = 1$ or $b = \pm c$. If $\varepsilon = 1$ the common line is $\langle c : b : a\rangle$ which in this case agrees with $Z = \langle c : b : \varepsilon a\rangle$. If $b = c$ we can check that the common line is $\langle b : b : a+\varepsilon-1\rangle$, and if $b = -c$ the common line is $\langle -b : b : a-\varepsilon+1\rangle$. □

4.3 Twin Circumcircles of a Triangle

If a triangle has three midsides, then corresponding Circumcenters will be centers of circles which pass through all three points, as in the classical triangle in Figure 1. This situation also holds for a triangle such as $\overline{a_1a_2a_3}$ in Figure 16, lying outside the null circle (still in blue) shown with three of its Midpoints m, (the other three are off the page), six Midlines M, three of the four Circumlines C, the four Circumcenters c, and the corresponding Circumcircles.

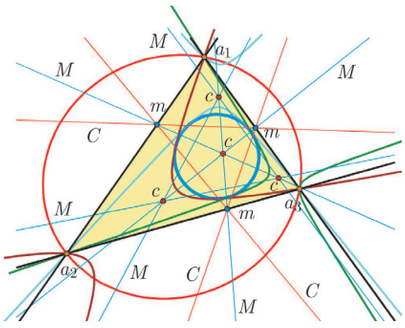

Figure 16: *Circumcenters of a triangle outside the null circle*

But what happens if a triangle has some points inside and some outside the null circle? In that case it turns out that we need to consider special *pairs* of circles, which collectively play the role of circumcircles. We do not know of any classical precedents for this phenomenon.

Definition 6 *Twin circles $\mathcal{C}$ and $\overline{\mathcal{C}}$ are **twin circumcircles** for a triangle $\overline{a_1a_2a_3}$ precisely when each of a_1, a_2, a_3 lie on either $\mathcal{C}$ or $\overline{\mathcal{C}}$.*

Theorem 11 (Twin circumcircles) *If a triangle $\overline{a_1a_2a_3}$ has smydpoints on all three sides, then the four circumcenters c_0, c_1, c_2, c_3 are each the center of twin circumcircles for $\overline{a_1a_2a_3}$.*

Proof. If n is a smydpoint of the side $\overline{a_ka_l}$ then its dual $n^\perp$ passes through two circumcenters, say c_i and c_j. Let's consider just c_i. If n is a sydpoint of $\overline{a_ka_l}$ then the Sydpoint twin circle theorem shows that the circles $\mathcal{C}_{c_i}^{(a_k)}$ and $\mathcal{C}_{c_i}^{(a_l)}$ are twin circles. If n is a midpoint of $\overline{a_ka_l}$ then the reflection r_n interchanges a_k and a_l and fixes both c_i and c_j, so that $\mathcal{C}_{c_i}^{(a_k)}$ and $\mathcal{C}_{c_i}^{(a_l)}$ coincide.

Since c_i is perpendicular to two smydpoints on different lines of the triangle $\overline{a_1a_2a_3}$, the argument can be repeated, so that either there is one circle with center at c_i that passes through all three points, or one of the twin circles $\mathcal{C}_{c_i}^{(a_k)}$ and $\mathcal{C}_{c_i}^{(a_l)}$ also passes through the third point of the triangle, in which case these are twin circumcircles. □

Now let's introduce some labelling and explicit formulas. Consider the circles $\mathcal{C}_i = \mathcal{C}_i^{(a_3)}$ centered at c_i and passing through a_3, for $i = 0,1,2,3$. Their equations $q(p,c_i) = q(c_i,a_3)$ in a variable point $p = [x:y:z]$, can be written, after factoring a common term $-\varepsilon+a^2\varepsilon+b^2+c^2-2abc$, as

$$\mathcal{C}_0\colon (1-\varepsilon)\left(x^2+y^2\right)+2(a-\varepsilon)xy+2(b-\varepsilon)xz+2(c-\varepsilon)yz=0$$
$$\mathcal{C}_1\colon (1-\varepsilon)\left(x^2+y^2\right)+2(a+\varepsilon)xy+2(b+\varepsilon)xz+2(c-\varepsilon)yz=0$$
$$\mathcal{C}_2\colon (1-\varepsilon)\left(x^2+y^2\right)+2(a+\varepsilon)xy+2(b-\varepsilon)xz+2(c+\varepsilon)yz=0$$
$$\mathcal{C}_3\colon (1-\varepsilon)\left(x^2+y^2\right)+2(a-\varepsilon)xy+2(b+\varepsilon)xz+2(c+\varepsilon)yz=0.$$

The respective twin circles $\overline{\mathcal{C}_i}$ with equations $q(p,c_i) = 2-q(c_i,a_3)$ can be written as

$$\overline{\mathcal{C}}_0 : (1+\varepsilon)\left(x^2+y^2\right)+2\varepsilon z^2+2(a+\varepsilon)xy +2(b+\varepsilon)xz+2(c+\varepsilon)yz=0$$
$$\overline{\mathcal{C}}_1 : (1+\varepsilon)\left(x^2+y^2\right)+2\varepsilon z^2+2(a-\varepsilon)xy +2(b-\varepsilon)xz+2(c+\varepsilon)yz=0$$
$$\overline{\mathcal{C}}_2 : (1+\varepsilon)\left(x^2+y^2\right)+2\varepsilon z^2+2(a-\varepsilon)xy +2(b+\varepsilon)xz+2(c-\varepsilon)yz=0$$
$$\overline{\mathcal{C}}_3 : (1+\varepsilon)\left(x^2+y^2\right)+2\varepsilon z^2+2(a+\varepsilon)xy +2(b-\varepsilon)xz+2(c-\varepsilon)yz=0.$$

If $\varepsilon = 1$, then each of the four circumcircles $\mathcal{C}_i$ passes through all three points of the triangle, while their twins $\overline{\mathcal{C}}_i$ pass through none of the points of the triangle; even so, their presence is felt.

In Figure 17 we see a triangle $\overline{a_1a_2a_3}$ with all three points inside the null circle, together with its four pairs of twin circumcircles, each pair with the same colour. The reader might enjoy looking for interesting relations between these circles.

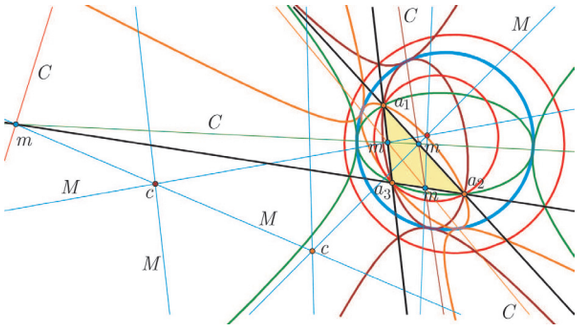

Figure 17: *Twin circumcircles for a classical triangle*

4.4 CircumDual points, Tangent lines and Sound points

If $\varepsilon = -1$, then the circumcircles $\mathcal{C}_i$ pass only through c_3, while the twins $\overline{\mathcal{C}}_i$ pass through c_1 and c_2. In each case we have four twin circumcircle pairs of the Triangle**.** These eight circles are shown for our standard example Triangle in Figure 18, along with the Tangent lines, which we now introduce.

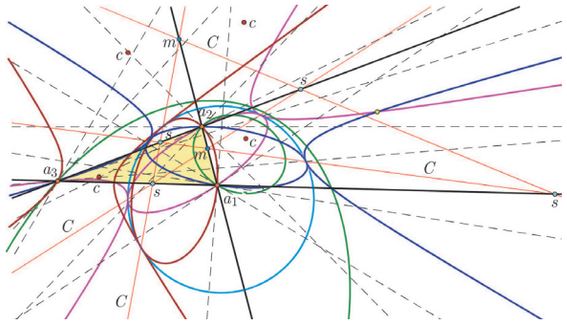

Figure 18: *Twin Circumcircles and Tangent lines*

The **CircumDual point** p_{ij} is the meet of the Dual line A_i and the Circumline C_j, for $i = 1,2,3$ and $j = 0,1,2,3$. Then

$$p_{10} = [a-b : b-1 : -a+1] \qquad p_{20} = [c-1 : a-c : -a+1]$$
$$p_{11} = [a-b : -b-1 : a+1] \qquad p_{21} = [1-c : -a-c : a+1]$$
$$p_{12} = [a+b : b-1 : -a-1] \qquad p_{22} = [c+1 : c-a : -a-1]$$
$$p_{13} = [-a-b : b+1 : 1-a] \qquad p_{23} = [-c-1 : a+c : a-1]$$

$$p_{30} = [\varepsilon - c : b-\varepsilon : -b+c]$$
$$p_{31} = [c-\varepsilon : -b-\varepsilon : b+c]$$
$$p_{32} = [-c-\varepsilon : b-\varepsilon : b+c]$$
$$p_{33} = [-c-\varepsilon : b+\varepsilon : b-c].$$

The **Tangent line** T_{ij} is the join of the CircumDual point p_{ij} and the point a_i. This line is indeed tangent to the circumcircle $\mathcal{C}_i$ at the point a_i if this circle passes through a_i. The twelve Tangent lines are:

$$T_{10} = \langle 0 : a-1 : b-1 \rangle \qquad T_{20} = \langle a-1 : 0 : c-1 \rangle$$
$$T_{11} = \langle 0 : a+1 : b+1 \rangle \qquad T_{21} = \langle a+1 : 0 : c-1 \rangle$$
$$T_{12} = \langle 0 : a+1 : b-1 \rangle \qquad T_{22} = \langle a+1 : 0 : c+1 \rangle$$
$$T_{13} = \langle 0 : a-1 : b+1 \rangle \qquad T_{23} = \langle a-1 : 0 : c+1 \rangle$$

$$T_{30} = \langle b-\varepsilon : c-\varepsilon : 0 \rangle$$
$$T_{31} = \langle b+\varepsilon : c-\varepsilon : 0 \rangle$$
$$T_{32} = \langle b-\varepsilon : c+\varepsilon : 0 \rangle$$
$$T_{33} = \langle b+\varepsilon : c+\varepsilon : 0 \rangle.$$

The **Sound point** s_{ij} is the meet of the Tangent line T_{ij} with the opposite Line L_i. The twelve Sound points are:

$$s_{10} = [0 : 1-b : a-1] \qquad s_{20} = [1-c : 0 : a-1]$$
$$s_{11} = [0 : -b-1 : a+1] \qquad s_{21} = [1-c : 0 : a+1]$$
$$s_{12} = [0 : 1-b : a+1] \qquad s_{22} = [-1-c : 0 : a+1]$$
$$s_{13} = [0 : b+1 : 1-a] \qquad s_{23} = [1+c : 0 : 1-a]$$

$$s_{30} = [\varepsilon - c : b-\varepsilon : 0]$$
$$s_{31} = [\varepsilon - c : b+\varepsilon : 0]$$
$$s_{32} = [c+\varepsilon : \varepsilon - b : 0]$$
$$s_{33} = [-c-\varepsilon : b+\varepsilon : 0].$$

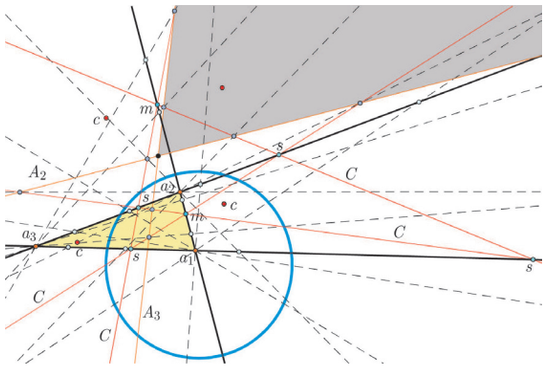

Figure 19: *CircumDual points and Sound points*

4.5 Jay and Wren lines

In this section we begin to see more divergence between the $\varepsilon = 1$ and $\varepsilon = -1$ cases. In the latter case a symmetry emerges between the Circumcenters c_0 and c_3, and between c_1 and c_2.

Theorem 12 (Jay lines) *If $\varepsilon = 1$ then the sets of Sound points $\{s_{10}, s_{20}, s_{30}\}$, $\{s_{11}, s_{21}, s_{31}\}$, $\{s_{12}, s_{22}, s_{32}\}$ and $\{s_{13}, s_{23}, s_{33}\}$ are each collinear, while if $\varepsilon = -1$ then the sets of Sound points $\{s_{10}, s_{20}, s_{33}\}$, $\{s_{11}, s_{21}, s_{32}\}$, $\{s_{12}, s_{22}, s_{31}\}$ and $\{s_{13}, s_{23}, s_{30}\}$ are each collinear. In both cases the common lines are respectively the four **Jay lines***

$$J_0 = \langle (a-1)(b-1) : (a-1)(c-1) : (c-1)(b-1) \rangle$$
$$J_1 = \langle (a+1)(b+1) : (a+1)(c-1) : (c-1)(b+1) \rangle$$
$$J_2 = \langle (a+1)(b-1) : (a+1)(c+1) : (c+1)(b-1) \rangle$$
$$J_3 = \langle (a-1)(b+1) : (a-1)(c+1) : (c+1)(b+1) \rangle.$$

Proof. The forms of the Sound points and Jay lines make verifying these incidences almost trivial. Note that changing the sign of ε interchanges s_{30} with s_{33}, and s_{31} with s_{32}. This explains why the two lists appear different in these two cases. □

In the case of $\varepsilon = 1$ we associate each triple of Sound points to the Circumline which is involved in each term. In the case of $\varepsilon = -1$ we associate each triple to the Circumline which is involved in *two* of the three elements of the triple.

There are four meets of Circumlines and associated Jay lines called **CircumJay points**, namely

$$t_0 \equiv C_0J_0 = [(c-1)(a-b) : (-b+1)(a-c) : (a-1)(b-c)]$$
$$t_1 \equiv C_1J_1 = [(c-1)(a-b) : -(b+1)(a+c) : (a+1)(b+c)]$$
$$t_2 \equiv C_2J_2 = [(c+1)(a+b) : (1-b)(a-c) : -(a+1)(b+c)]$$
$$t_3 \equiv C_3J_3 = [-(c+1)(a+b) : (b+1)(a+c) : (a-1)(b-c)].$$

Note that these formulas are independent of ε.

Theorem 13 (CircumJay) *The four CircumJay points t_0, t_1, t_2, t_3 are collinear and lie on the line*

$$T = \langle c+ab : b+ac : a+bc \rangle.$$

*When $\varepsilon = 1$ this coincides with the Base axis B. When $\varepsilon = -1$, this is a new line which we call the T **axis**. In the case of $\varepsilon = -1$, T, B and L_3 are concurrent at a new point*

$$\overline{t} = [-(b+ac) : c+ab : 0].$$

Proof. The CircumJay point t_0 lies on T since

$$(c-1)(a-b)(c+ab) + (-b+1)(a-c)(b+ac) + (a-1)(b-c)(a+bc) = 0$$

and similarly for the other points. The T axis agrees with the Base axis $B = \langle c+ab : b+ac : \varepsilon a+bc \rangle$ if $\varepsilon = 1$. For $\varepsilon = -1$, the verification of $\overline{t} = TB$ is also straightforward, and clearly it lies on L_3. □

Theorem 14 (Wren lines) *If $\varepsilon = 1$ then the sets of Sound points $\{s_{11}, s_{22}, s_{33}\}$, $\{s_{10}, s_{32}, s_{23}\}$, $\{s_{31}, s_{20}, s_{13}\}$ and $\{s_{21}, s_{12}, s_{30}\}$ are each collinear, while if $\varepsilon = -1$ then the sets of Sound points $\{s_{11}, s_{22}, s_{30}\}$, $\{s_{10}, s_{23}, s_{31}\}$, $\{s_{13}, s_{20}, s_{32}\}$ and $\{s_{12}, s_{21}, s_{33}\}$ are each collinear. In both cases the common lines are respectively the four **Wren lines***

$$W_0 = \langle (a+1)(b+1) : (a+1)(c+1) : (b+1)(c+1) \rangle$$
$$W_1 = \langle (a-1)(b-1) : (c+1)(a-1) : (c+1)(b-1) \rangle$$
$$W_2 = \langle (b+1)(a-1) : (a-1)(c-1) : (b+1)(c-1) \rangle$$
$$W_3 = \langle (a+1)(b-1) : (a+1)(c-1) : (b-1)(c-1) \rangle.$$

Proof. Again, with the formulas for Sound points and Wren lines, it is straightforward to check incidences. As with the Jay lines, changing the sign of ε interchanges s_{03} with s_{33}, and s_{13} with s_{23}. □

Notice that each set of collinear Sound points is associated to the Circumcenter which is not involved in the indices of that group. **CircumWren points** are the meets of Circumlines and associated Wren lines. These points are

$$u_0 \equiv C_0W_0 = [(c+1)(a-b) : -(b+1)(a-c) : (a+1)(b-c)]$$
$$u_1 \equiv C_1W_1 = [(c+1)(a-b) : (-b+1)(a+c) : (a-1)(b+c)]$$
$$u_2 \equiv C_2W_2 = [(c-1)(a+b) : -(b+1)(a-c) : (-a+1)(b+c)]$$
$$u_3 \equiv C_3W_3 = [(-c+1)(a+b) : (b-1)(a+c) : (a+1)(b-c)].$$

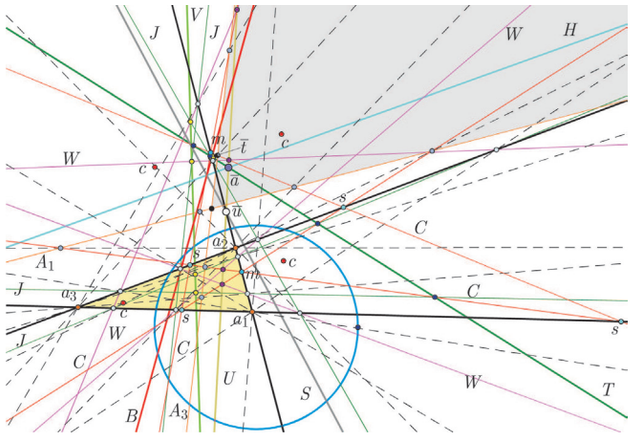

Figure 20: *Jay lines J, Wren lines W, T, U, V axes and new points $\overline{a}, \overline{u}, \overline{t}$*

Theorem 15 (CircumWren) *The four CircumWren points u_0, u_1, u_2, u_3 are collinear and lie on the line*

$$U \equiv \langle ab-c : ac-b : bc-a \rangle.$$

*When $\varepsilon = 1$ this coincides with the Orthic axis S. When $\varepsilon = -1$, this is a new line which we call the U **axis**. In case $\varepsilon = -1$, S, U and L_3 are concurrent in a new point*

$$\overline{u} = [ac-b : c-ab : 0].$$

Proof. We may compute that v_0 lies on U since

$$(c+1)(a-b)(ab-c) - (b+1)(a-c)(ac-b) + (a+1)(b-c)(bc-a) = 0.$$

The other incidences are similar. From (12) we recall that the Orthic axis has equation $S = \langle ab-c : ac-b : bc-a\varepsilon \rangle$ which agrees with U precisely when $\varepsilon = 1$. Again the formula for $\overline{u}$ is easy. □

In Figure 20 we see the CircumJay points t_j (dark blue) on T, the CircumWren points u_j (purple) on U, and the JayWren points v_j (yellow) on V.

Theorem 16 (CircumJayWren) *The lines U, T and H are concurrent, and pass through*

$$\overline{a} \equiv \left[c\left(a^2-b^2\right) : b\left(c^2-a^2\right) : a\left(b^2-c^2\right)\right]. \qquad (13)$$

If $\varepsilon = 1$ then $\overline{a}$ agrees with the Orthoaxis point $a = \left[c\left(a^2\varepsilon-b^2\right) : b\left(c^2-\varepsilon a^2\right) : a\left(b^2-c^2\right)\right]$.

Proof. The concurrence of these lines follows from

$$\det\begin{bmatrix} ab-c & ac-b & bc-a \\ c+ab & b+ac & a+bc \\ ab & ac & bc \end{bmatrix} = 0.$$

The common incidence with (13) is also readily checked. The last statement is self-evident. □

There are four **JayWren points** which are the meets of associated Jay lines and Wren lines:

$$\begin{aligned} v_0 &= J_0W_0 = \left[\left(c^2-1\right)(a-b) : \left(b^2-1\right)(c-a) : \left(a^2-1\right)(b-c)\right] \\ v_1 &= J_1W_1 = \left[\left(c^2-1\right)(a-b) : \left(b^2-1\right)(a+c) : \left(1-a^2\right)(b+c)\right] \\ v_2 &= J_2W_2 = \left[\left(c^2-1\right)(a+b) : \left(b^2-1\right)(a-c) : \left(1-a^2\right)(b+c)\right] \\ v_3 &= J_3W_3 = \left[\left(c^2-1\right)(a+b) : \left(1-b^2\right)(a+c) : \left(a^2-1\right)(b-c)\right]. \end{aligned}$$

Theorem 17 (JayWren) *The four JayWren points v_0, v_1, v_2, v_3 are collinear and lie on the **JayWren axis**, or the V line*

$$V = \left\langle c\left(b^2-1\right)\left(a^2-1\right) : b\left(c^2-1\right)\left(a^2-1\right) : a\left(c^2-1\right)\left(b^2-1\right)\right\rangle.$$

Proof. The JayWren point v_0 lies on V since

$$\begin{aligned} &\left(c^2-1\right)(a-b)c\left(b^2-1\right)\left(a^2-1\right) \\ &\quad - \left(b^2-1\right)(a-c)b\left(c^2-1\right)\left(a^2-1\right) \\ &\quad + \left(a^2-1\right)(b-c)a\left(c^2-1\right)\left(b^2-1\right) = 0. \end{aligned}$$

Checking the other incidences is similar. □

4.6 CircumMeets and reflections

One of the interesting features of this situation concerns the meets of the eight **generalized circumcircles** forming the four twin circumcircles of a triangle with six smydpoints. We establish easily a basic fact.

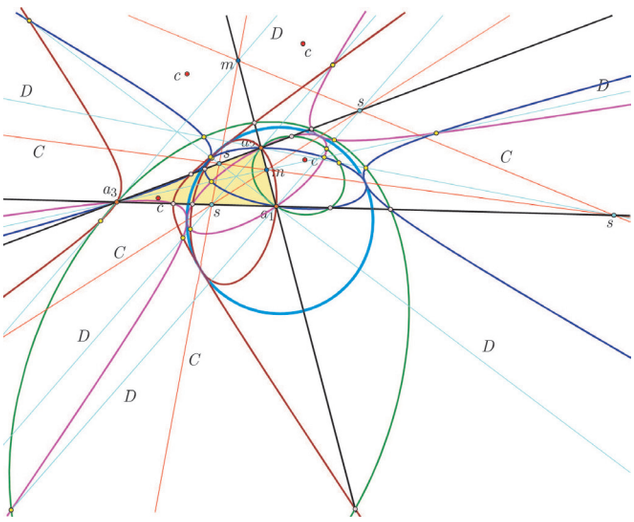

Figure 21: *Circumcircles and CircumMeet points*

Theorem 18 (Smydpoint reflection) *Suppose that a generalized circumcircle $\mathcal{C}$ has center c_j perpendicular to a smydpoint n. If $\mathcal{C}$ passes through a point a_k of the Triangle, then it also passes through the reflection $r_n(a_k)$.*

Proof. If n is perpendicular to c_j, then the reflection r_n in n fixes the center c_j of $\mathcal{C}$, and so fixes $\mathcal{C}$. Thus if $\mathcal{C}$ passes through a_k, it also passes through $r_n(a_k)$. □

This theorem helps explain why in Figure 21 the meets of the generalized circumcircles lie either on the lines of the Triangle, or on the Medians. We see that reflections of Points in Sydpoints are also interesting points of the Triangle—in fact somewhat surprisingly these CircumMeet points are independent of the third Point of the Triangle, and depend only on the particular side on which they lie. The reader can verify with a dynamic geometry package that as we vary one point of the Triangle, the generalized circumcircles move, but their meets on the opposite Line do not.

In general meets of circles are complicated by number-theoretical issues (circles do not have to meet, after all). We conjecture that whenever generalized Circumcircles meet, they do so either on Lines or Medians. We hope to explain the more detailed structure of these CircumMeet points in a future paper.

4.7 Sound conics

The twelve sound points are quite interesting, supporting the linear structures of Jay and Wren lines. They also are connected with four special conics in an interesting way, each conic naturally also associated with a circumcenter.

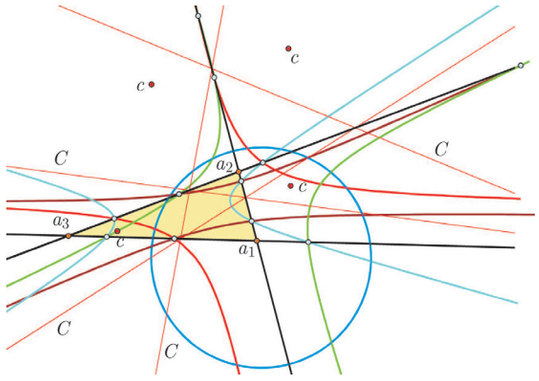

Figure 22: *Sound conics*

Theorem 19 *The sextuples* $\{s_{12},s_{13},s_{21},s_{23},s_{31},s_{32}\}$, $\{s_{12},s_{13},s_{20},s_{22},s_{30},s_{33}\}$, $\{s_{10},s_{11},s_{21},s_{23},s_{30},s_{33}\}$ *and* $\{s_{10},s_{11},s_{20},s_{22},s_{31},s_{32}\}$ *of sound points all lie on conics. Each of these four* ***Sound conics*** $\mathcal{K}_j$ *is associated to a Circumcenter* c_j.

Proof. We compute the coefficients of the equation of the (blue) conic

$$\mathcal{K}_0 : a_1x^2 + a_2y^2 + a_3z^2 + a_4xy + a_5xz + a_6yz = 0$$

passing through points $s_{12},s_{13},s_{21},s_{23},s_{31}$ by solving the linear system

$$\begin{aligned}
(1-b)^2a_2 + (a+1)^2a_3 + (1-b)(a+1)a_6 &= 0\\
(1+b)^2a_2 + (1-a)^2a_3 + (1+b)(1-a)a_6 &= 0\\
(1-c)^2a_1 + (a+1)^2a_3 + (1-c)(a+1)a_5 &= 0\\
(1+c)^2a_1 + (1-a)^2a_3 + (1+c)(1-a)a_5 &= 0\\
(\varepsilon-c)^2a_1 + (b+\varepsilon)^2a_2 + (\varepsilon-c)(b+\varepsilon)a_4 &= 0
\end{aligned}$$

This results in the values

$$\begin{aligned}
a_1 &= (c+\varepsilon)(b-\varepsilon)\left(b^2-1\right)\left(a^2-1\right)\\
a_2 &= (c+\varepsilon)(b-\varepsilon)\left(c^2-1\right)\left(a^2-1\right)\\
a_3 &= (c+\varepsilon)(b-\varepsilon)\left(c^2-1\right)\left(b^2-1\right)\\
a_4 &= 2\left(a^2-1\right)(bc+1)(b\varepsilon-c\varepsilon+bc-1)\\
a_5 &= 2(c+\varepsilon)(b-\varepsilon)\left(b^2-1\right)(ac+1)\\
a_6 &= 2(c+\varepsilon)(b-\varepsilon)(ab+1)\left(c^2-1\right).
\end{aligned}$$

When substituting the coordinates of s_{32} in the above equation with these coefficients, we obtain equality precisely when

$$\left(\varepsilon^2-1\right)\left(a^2-1\right)\left((b-c)\left(4bc+b^2+c^2+2\right)\varepsilon + (bc-1)\left(b^2+c^2-2\right)\right) = 0$$

which is true since $\varepsilon^2 = 1$.

By following the same argument, we can obtain the equations of the (red) conic

$$\mathcal{K}_1 : b_1x^2 + b_2y^2 + b_3z^2 + b_4xy + b_5xz + b_6yz = 0$$

through $s_{12},s_{13},s_{20},s_{22},s_{30},s_{33}$ with coefficients

$$\begin{aligned}
b_1 &= (b+\varepsilon)(c+\varepsilon)\left(b^2-1\right)\left(a^2-1\right)\\
b_2 &= (b+\varepsilon)(c+\varepsilon)\left(c^2-1\right)\left(a^2-1\right)\\
b_3 &= (b+\varepsilon)(c+\varepsilon)\left(c^2-1\right)\left(b^2-1\right)\\
b_4 &= 2(bc-1)\left(a^2-1\right)(b\varepsilon+c\varepsilon+bc+1)\\
b_5 &= 2(b+\varepsilon)(c+\varepsilon)(ac-1)\left(b^2-1\right)\\
b_6 &= 2(b+\varepsilon)(c+\varepsilon)(ab+1)\left(c^2-1\right),
\end{aligned}$$

the (green) conic

$$\mathcal{K}_2 : c_1x^2 + c_2y^2 + c_3z^2 + c_4xy + c_5xz + c_6yz = 0$$

through $s_{10},s_{11},s_{21},s_{23},s_{30},s_{33}$ with coefficients

$$\begin{aligned}
c_1 &= (c+\varepsilon)(b+\varepsilon)\left(b^2-1\right)\left(a^2-1\right)\\
c_2 &= (c+\varepsilon)(b+\varepsilon)\left(c^2-1\right)\left(a^2-1\right)\\
c_3 &= (c+\varepsilon)(b+\varepsilon)\left(c^2-1\right)\left(b^2-1\right)\\
c_4 &= 2(bc-1)(b\varepsilon+c\varepsilon+bc+1)\left(a^2-1\right)\\
c_5 &= 2(c+\varepsilon)(b+\varepsilon)(ac+1)\left(b^2-1\right)\\
c_6 &= 2(c+\varepsilon)(b+\varepsilon)(ab-1)\left(c^2-1\right),
\end{aligned}$$

and the (brown) conic

$$\mathcal{K}_3 : d_1x^2 + d_2y^2 + d_3z^2 + d_4xy + d_5xz + d_6yz = 0$$

through $s_{10},s_{11},s_{20},s_{22},s_{31},s_{32}$ with coefficients

$$\begin{aligned}
d_1 &= (c+\varepsilon)(b-\varepsilon)\left(b^2-1\right)\left(a^2-1\right)\\
d_2 &= (c+\varepsilon)(b-\varepsilon)\left(c^2-1\right)\left(a^2-1\right)\\
d_3 &= (c+\varepsilon)(b-\varepsilon)\left(c^2-1\right)\left(b^2-1\right)\\
d_4 &= 2(bc+1)(b\varepsilon-c\varepsilon+bc-1)\left(a^2-1\right)\\
d_5 &= 2(c+\varepsilon)(b-\varepsilon)(ac-1)\left(b^2-1\right)\\
d_6 &= 2(c+\varepsilon)(b-\varepsilon)(ab-1)\left(c^2-1\right).
\end{aligned}$$

We associate each Sound conic $\mathcal{K}_j$ to the Circumcenter c_j not involved in any of the six Sound points lying on it. □

5 Further directions

We can now extend hyperbolic triangle geometry from classical triangles to more general ones. Taking duals we get also analogous results for the Incenter hierarchy, and it is worthwhile to elaborate these and then investigate further the links between Incenter and Circumcenter hierarchies.

The close relations between twin circles ought to have consequences for relativistic physics, as points inside the null circle correspond to time-like lines and points outside to space-like lines. The geometry we are investigating suggests these two aspects of relativistic geometry ought to be much more closely linked.

Another direction is that over certain finite fields, we can expect some sides to have both midpoints and sydpoints! This is an interesting aspect for those with a number theoretical or combinatorial bend. It turns out that sydpoints play a big role in the theory of conics in UHG as well, as we will explain in a future paper.

Acknowledgements

Ali Alkhaldi would like to thank the University of King Khalid in Saudi Arabia for financial support for his PhD studies at UNSW.

References

[1] J. W. ANDERSON, *Hyperbolic Geometry*, second edition, Springer 2005.

[2] O. BOTTEMA, On the medians of a triangle in hyperbolic geometry, *Can. J. Math.* **10** (1958), 502–506.

[3] H. S. M. COXETER, *Non-Euclidean Geometry*, 6th ed., Mathematical Association of America, Washington D. C., 1998.

[4] M. J. GREENBERG, *Euclidean and Non-Euclidean Geometries: Development and History*, 4th ed., W. H. Freeman and Co., San Francisco, 2007.

[5] C. KIMBERLING, *Triangle Centers and Central Triangles*, vol. 129 Congressus Numerantium, Utilitas Mathematica Publishing, Winnepeg, MA, 1998.

[6] C. KIMBERLING, *Encyclopedia of Triangle Centers*, `http://faculty.evansville.edu/ck6/encyclopedia/ETC.html`.

[7] N. LE, N. J. WILDBERGER, *Universal Affine Triangle Geometry*, *KoG* **16** (2012)

[8] A. PRÉKOPA and E. MOLNAR, eds., *Non-Euclidean Geometries: János Bolyai Memorial Volume*, Springer, New York, 2005.

[9] A. A. UNGAR, Hyperbolic barycentric coordinates, *Aust. J. Math. Anal. Appl.* **6**(1) (2009), 1–35.

[10] A. A. UNGAR, Barycentric calculus in *Euclidean and Hyperbolic Geometry; A comparative introduction*, World Scientific Publishing, Singapore, 2010.

[11] A. A. UNGAR, *Hyperbolic Triangle Centers: The Special Relativistic Approach*, FTP 166, Springer Dordrecht, 2010.

[12] N. J. WILDBERGER, *Divine Proportions: Rational Trigonometry to Universal Geometry*, Wild Egg Books, Sydney, 2005. `http://wildegg.com`.

[13] N. J. WILDBERGER, Affine and projective metrical geometry, *arXiv: math/0612499v1*, (2006), to appear, *J. of Geometry*.

[14] N. J. WILDBERGER, Universal Hyperbolic Geometry I: Trigonometry, *Geometriae Dedicata*, (2012), to appear.

[15] N. J. WILDBERGER, Universal Hyperbolic Geometry II: A pictorial overview, *KoG* **14** (2010), 3–24.

[16] N. J. WILDBERGER, Universal Hyperbolic Geometry III: First steps in projective triangle geometry, *KoG* **15** (2011), 25–49.

Norman John Wildberger
e-mail: n.wildberger@unsw.edu.au

Ali Alkhaldi
e-mail: aalkaldy@hotmail.com

School of Mathematics and Statistics UNSW
Sydney 2052 Australia

Original scientific paper
Accepted 31. 12. 2012.

NGUYEN LE
NORMAN JOHN WILDBERGER

Universal Affine Triangle Geometry and Four-fold Incenter Symmetry

Universal Affine Triangle Geometry and Four-fold Incenter Symmetry

ABSTRACT

We develop a generalized triangle geometry, using an arbitrary bilinear form in an affine plane over a general field. By introducing standardized coordinates we find canonical forms for some basic centers and lines. Strong concurrencies formed by quadruples of lines from the Incenter hierarchy are investigated, including joins of corresponding Incenters, Gergonne, Nagel, Spieker points, Mittenpunkts and the New points we introduce. The diagrams are taken from relativistic (green) geometry.

Key words: Triangle geometry, affine geometry, Rational trigonometry, bilinear form, incenter hierarchy, Euler line, Gergonne, Nagel, Mittenpunkt, chromogeometry

MSC 2000: 51M05, 51M10, 51N10

Univerzalna afina geometrija trokuta i četverostruka simetrija središta upisane kružnice

SAŽETAK

Razvijamo opću geometriju trokuta koristeći proizvoljnu bilinearnu formu u afinoj ravnini nad općim poljem. Uvodeći standardizirane koordinate pronalazimo kanonske oblike nekih osnovnih središta i pravaca. Proučavamo snažnu konkurentnost četvorki pravaca koji pripadaju "hijerarhiji središta upisane kružnice" uključujući i spojnice odgovarajućih sjecišta simetrala kutova trokuta, Georgonnovih točaka, Nagelovih točaka, Mittenpunkova (imenovano sa strane autora, op. ur.) te Novih točaka koje se uvode u članku. Slike su prikazane u tzv. zelenoj geometriji.

Ključne riječi: geometrija trokuta, afina geometrija, racionalna trigonometrija, bilinearna forma, hijerarhija središta upisane kružnice, Eulerov pravac, Georgonnova točka, Nagelova točka, Mittenpunkt, kromogeometrija

1 Introduction

This paper *repositions and extends triangle geometry* by developing it in the wider framework of Rational Trigonometry and Universal Geometry ([10], [11]), valid over arbitrary fields and with general quadratic forms. Our main focus is on strong concurrency results for quadruples of lines associated to the Incenter hierarchy.

Triangle geometry has a long and cyclical history ([1], [3], [16], [17]). The centroid $G = X_2$, circumcenter $C = X_3$, orthocenter $H = X_4$ and incenter $I = X_1$ were known to the ancient Greeks. Prominent mathematicians like Euler and Gauss contributed to the subject, but it took off mostly in the latter part of the 19th century and the first part of the 20th century, when many new centers, lines, conics, and cubics associated to a triangle were discovered and investigated. Then there was a period when the subject languished; and now it flourishes once more—spurred by the power of dynamic geometry packages like GSP, C.a.R., Cabri, GeoGebra, and Cinderella; by the heroic efforts of Clark Kimberling in organizing the massive amount of information on Triangle Centers in his Online Encyclopedia ([5], [6], [7]); and by the explorations and discussions of the Hyacinthos Yahoo group ([4]).

The increased interest in this rich and fascinating subject is to be applauded, but there are also mounting concerns about the consistency and accessibility of *proofs*, which have not kept up with the greater pace of *discoveries*. Another difficulty is that the current framework is modelled on the continuum as "real numbers", which often leads synthetic treatments to finesse number-theoretical issues.

One of our goals is to provide explicit algebraic formulas for points, lines and transformations of triangle geometry which hold in great generality, over the rational numbers, finite fields, and even the field of complex rational numbers, and with different bilinear forms determining the metrical structure without any recourse to transcendental quantities or "real numbers". Of course we proceed only a very small way down this road, but far enough to establish some analogs of results that have appeared first in Universal Hyperbolic Geometry ([14]); namely the con-

currency of some *quadruples* of lines associated to the classical Incenters, Gergonne points, Nagel points, Mittenpunkts, Spieker points as well as the *New points* which we introduce here. We identify the resulting centers in Kimberling's list.

Our basic technology is simple but powerful: we propose to replace the affine study of a *general triangle under a particular bilinear form* with the study of a *particular triangle under a general bilinear form*—analogous to the projective situation as in ([14]), and using the framework of Rational Trigonometry ([10], [11]). By choosing a very elementary standard Triangle—with vertices the origin and the two standard basis vectors—we get reasonably pleasant and simple formulas for various points, lines and constructions. An affine change of coordinates changes any triangle under any bilinear form to the one we are studying, so our results are in fact very general.

Our principle results center around the classical four points, but a big difference with our treatment is that we acknowledge from the start that the very existence of the *Incenter hierarchy* is dependent on number-theoretical conditions which end up playing an intimate and ultimately rather interesting role in the theory. Algebraically it becomes difficult to separate the classical incenter from the three closely related excenters, and the quadratic relations that govern the existence of these carry a natural four-fold symmetry between them. This symmetry becomes crucial to simplifying formulas and establishing theorems. So in our framework, *there are four Incenters I_0, I_1, I_2 and I_3, not one*.

To showcase the generality of our results, we illustrate theorems not over the Euclidean plane, but in the *Minkowski plane* coming from *Einstein's special theory of relativity in null coordinates,* where the metrical structure is determined by the bilinear form

$$(x_1, y_1) \cdot (x_2, y_2) \equiv x_1 y_2 + y_1 x_2.$$

In the language of Chromogeometry ([12] , [13]), this is *green geometry*, with circles appearing as rectangular hyperbolas with asymptotes parallel to the coordinate axes. Green perpendicularity amounts to vectors being Euclidean reflections in these axes, while null vectors are parallel to the axes. It is eye-opening to see that triangle geometry is just as rich in such a relativistic setting as it is in the Euclidean one!

1.1 Summary of results

We summarize the main results of this paper using Figure 1 from green geometry. As established in ([13]), the triangle $\overline{A_1A_2A_3}$ has a *green Euler line CHG* just as in the Euclidean setting, where $C = X_3$ is the Circumcenter, $G = X_2$ is the Centroid, and $H = X_4$ is the Orthocenter, with the affine ratio $\overrightarrow{CG} : \overrightarrow{GH} = 1 : 2$, which we may express as $G = \frac{2}{3}C + \frac{1}{3}H$. The reader might like to check that using the green notation of perpendicularity, the green altitudes really do meet at H, and the green midlines/perpendicular bisectors really do meet at C.

In the general situation there are *four* Incenters/Excenters I_0, I_1, I_2 and I_3 which algebraically are naturally viewed symmetrically. Associated to any one Incenter I_j is a *Gergonne point* $G_j = X_7$ (not to be confused with the centroid also labelled G), a *Nagel point* $N_j = X_8$, a *Mittenpunkt* $D_j = X_9$, a *Spieker point* $S_j = X_{10}$ and most notably a *New point* L_j. It is not at all obvious that these various points can be defined for a general affine geometry, but this is the case, as we shall show. The New points L_0, L_1, L_2, L_3 are a particularly novel feature of this paper. They really do appear to be new, and it seems remarkable that these important points have not been intensively studied, as they fit naturally and simply into the Incenter hierarchy, as we shall see.

The four-fold symmetry between the four Incenters is maintained by all these points: so in fact there are *four* Gergonne, Nagel, Mittenpunkt, Spieker and New points, each associated to a particular Incenter, as also pointed out in ([8]). Figure 1 shows just one Incenter and its related hierarchy: as we proceed in this paper the reader will meet the other Incenters and hierarchies as well.

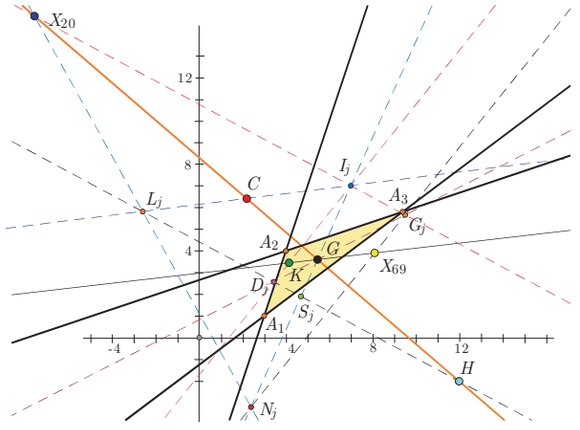

Figure 1: *Aspects of the Incenter hierarchy in green geometry*

The main aims of the paper are to set-up a coordinate system for triangle geometry that incorporates the number-theoretical aspects of the Incenter hierarchy, and respects the four-fold symmetry inherent in it, and then to use this to catalogue existing as well as new points and phenomenon. Kimberling's Triangle Center Encyclopedia ([6]) distinguishes the classical Incenter X_1 as the first and perhaps most important triangle center. Our embrace of the four-fold symmetry between incenters and excenters implies something of a re-evaluation of some aspects of classical

triangle geometry; instead of certain distinguished centers we have rather distinguished quadruples of related points. Somewhat surprisingly, this point of view makes visible a number of remarkable *strong concurrences*—-where four symmetrically-defined lines meet in a center. The proofs of these relations are reasonably straight-forward but not automatic, as in general certain important quadratic relations are needed to simplify expressions for incidence. Here is a summary of our main results.

Main Results

i) The four lines I_jG_j, $j = 0,1,2,3$, meet in the De Longchamps point X_{20} (orthocenter of the Double triangle) — these are the Soddy lines ([9]).

ii) The four lines I_jN_j meet in the Centroid $G = X_2$, and in fact $G = \frac{2}{3}I_j + \frac{1}{3}N_j$ — these are the Nagel lines. The Spieker points S_j also lie on the Nagel lines, and in fact $S_j = \frac{1}{2}I_j + \frac{1}{2}N_j$.

iii) The four lines I_jD_j meet in the Symmedian point $K = X_6$ (isogonal conjugate of the Centroid G) — the standard such line is labelled $L_{1,6}$ in [6].

iv) The four lines I_jL_j meet in the Circumcenter C, and in fact $C = \frac{1}{2}I_j + \frac{1}{2}L_j$ — the standard such line is labelled $L_{1,3}$.

v) The four lines G_jN_j meet in the point X_{69} (isotomic conjugate of the Orthocenter H) — these lines are labelled $L_{7,8}$.

vi) The four lines G_jD_j meet in the Centroid $G = X_2$, and in fact $G = \frac{2}{3}D_j + \frac{1}{3}G_j$ — the standard such line is labelled $L_{2,7}$.

vii) The four lines D_jS_j meet in the Orthocenter $H = X_4$ — the standard such line is labelled $L_{4,7}$.

viii) The four lines N_jL_j meet in the point X_{20} (orthocenter of the Double triangle), and in fact $L_j = \frac{1}{2}X_{20} + \frac{1}{2}N_j$ — the standard such line is labelled $L_{1,3}$.

ix) The New point L_j lies on the line D_jS_j which also passes through the Orthocenter H, and in fact $S_j = \frac{1}{2}H + \frac{1}{2}L_j$.

In particular the various points alluded to here have *consistent definitions over general fields and with arbitrary bilinear forms*! The New points are the meets of the lines $L_{1,3}$ and $L_{4,7}$, they are the reflections of the Incenters I_j in the Circumcenter C, and they are the reflections of the Orthocenter H in the Spieker points S_j.

It is also worth pointing out a few additional relations between the triangle centers that appear here: the point X_{69}, defined as the Isogonal conjugate of the Orthocenter H, is also the central dilation in the Centroid of the Symmedian point K; in our notation $X_{69} = \delta_{-1/2}(K)$. This implies that $G = \frac{2}{3}K + \frac{1}{3}X_{69}$. In addition the De Longchamps point X_{20}, defined as the orthocenter of the Double (or anti-medial) triangle is also the reflection of the Orthocenter H in the Circumcenter C. These relations continue to hold in the general situation.

Table 1 summarizes the various strong concurrences we have found. Note however that not all pairings yield concurrent quadruples: for example the lines joining corresponding Nagel points and Mittenpunkts are *not* in general concurrent.

In the final section of the paper, we give some further results and directions involving chromogeometry.

1.2 Affine structure and vectors

We begin with some terminology and concepts for elementary affine geometry in a linear algebra setting, following [10]. Fix a field F, of characteristic not two, whose elements will be called **numbers**. We work in a two-dimensional affine space $\mathbb{A}^2$ over F, with $\mathbb{V}^2$ the associated two-dimensional vector space. A **point** is then an ordered pair $A \equiv [x,y]$ of numbers enclosed in square brackets, typically denoted by capital letters, such as A, B, C etc. A **vector** of $\mathbb{V}^2$ is an ordered pair $v \equiv (x,y)$ of numbers enclosed in round brackets, typically u, v, w etc. Any pair of points A and B determines a vector $v = \overrightarrow{AB}$; so for example if $A \equiv [2,-1]$ and $B \equiv [5,1]$, then $v = \overrightarrow{AB} = (3,2)$, and this is the same vector $v = \overrightarrow{CD}$ determined by $C \equiv [4,1]$ and $D \equiv [7,3]$.

	Incenter I	Gergonne G	Nagel N	Mittenpunkt D	Spieker S	New L
Incenter I	–	X_{20}	$G = X_2$	$K = X_6$	$G = X_2$	$C = X_3$
Gergonne G	X_{20}	–	X_{69}	$G = X_2$	–	–
Nagel N	$G = X_2$	X_{69}	–	–	$G = X_2$	X_{20}
Mittenpunkt D	$K = X_6$	$G = X_2$	–	–	$H = X_4$	$H = X_4$
Spieker S	$G = X_2$	–	$G = X_2$	$H = X_4$	–	$H = X_4$
New L	$C = X_3$	–	X_{20}	$H = X_4$	$H = X_4$	–

Table 1

The non-zero vectors $v_1 \equiv (x_1, y_1)$ and $v_2 \equiv (x_2, y_2)$ are **parallel** precisely when one is a non-zero multiple of the other, this happens precisely when

$$x_1 y_2 - x_2 y_1 = 0.$$

Vectors may be scalar-multiplied and added componentwise, so that if v and w are vectors and α, β are numbers, the **linear combination** $\alpha v + \beta w$ is defined. For points A and B and a number λ, we may define the **affine combination** $C = (1-\lambda)A + \lambda B$ either by coordinates or by interpreting it as the sum $A + \lambda\overrightarrow{AB}$. An important special case is when $\lambda = 1/2$; in that case the point $C \equiv A/2 + B/2$ is the **midpoint** of $\overline{AB}$, a purely affine notion independent of any metrical framework.
Once we fix an origin $O \equiv [0,0]$, the affine space $\mathbb{A}^2$ and the associated vector space $\mathbb{V}^2$ are naturally identified: to every point $A \equiv [x,y]$ there is an associated position vector $a = \overrightarrow{OA} = (x,y)$. So points and vectors are almost the same thing, but not quite. The choice of distinguished point also allows us a useful notational shortcut: we agree that for a point $A \equiv [x,y]$ and a number λ we write

$$\lambda\,[x,y] \equiv (1-\lambda)\,O + \lambda A = [\lambda x, \lambda y]\,. \tag{1}$$

A **line** is a proportion $l \equiv \langle a : b : c \rangle$ where a and b are not both zero. The point $A \equiv [x,y]$ **lies on** the line $l \equiv \langle a : b : c \rangle$, or equivalently the line l **passes through** the point A, precisely when

$$ax + by + c = 0.$$

For any two distinct points $A_1 \equiv [x_1, y_1]$ and $A_2 \equiv [x_2, y_2]$, there is a unique line $l \equiv A_1A_2$ which passes through them both; namely the **join**

$$A_1A_2 = \langle y_1 - y_2 : x_2 - x_1 : x_1y_2 - x_2y_1 \rangle\,. \tag{2}$$

In vector form, this line has parametric equation $l : A_1 + \lambda v$, where $v = \overrightarrow{A_1A_2} = (x_2 - x_1, y_2 - y_1)$ is a **direction vector** for the line, and λ is a parameter. The direction vector of a line is unique up to a non-zero multiple. The line $l \equiv \langle a : b : c \rangle$ has a direction vector $v = (-b, a)$.
Two lines are **parallel** precisely when they have parallel direction vectors. For every point P and line l, there is then precisely one line m through P parallel to l, namely $m : P + \lambda v$, where v is any direction vector for l. For any two lines $l_1 \equiv \langle a_1 : b_1 : c_1 \rangle$ and $l_2 \equiv \langle a_2 : b_2 : c_2 \rangle$ which are not parallel, there is a unique point $A \equiv l_1 l_2$ which lies on them both; using (1) we can write this **meet** as

$$\begin{aligned} A \equiv l_1 l_2 &= \left[\frac{b_1c_2 - b_2c_1}{a_1b_2 - a_2b_1}, \frac{c_1a_2 - c_2a_1}{a_1b_2 - a_2b_1} \right] \\ &= (a_1b_2 - a_2b_1)^{-1}\,[b_1c_2 - b_2c_1, c_1a_2 - c_2a_1]\,. \end{aligned} \tag{3}$$

Three points $A_1 = [x_1, y_1], A_2 = [x_2, y_2], A_3 = [x_3, y_3]$ are **collinear** precisely when they lie on a common line, which amounts to the condition

$$x_1y_2 - x_1y_3 + x_2y_3 - x_3y_2 + x_3y_1 - x_2y_1 = 0.$$

Three lines $\langle a_1 : b_1 : c_1 \rangle$, $\langle a_2 : b_2 : c_2 \rangle$ and $\langle a_3 : b_3 : c_3 \rangle$ are **concurrent** precisely when they pass through the same point, which amounts to the condition

$$a_1b_2c_3 - a_1b_3c_2 + a_2b_3c_1 - a_3b_2c_1 + a_3b_1c_2 - a_2b_1c_3 = 0.$$

1.3 Metrical structure: quadrance and spread

We now introduce a metrical structure, which is determined by a non-degenerate symmetric 2×2 matrix C, with entries in the fixed field $\mathbb{F}$ over which we work. This matrix defines a symmetric bilinear form on vectors, regarded as row matrices, by the formula

$$v \cdot u = vu = vCu^T\,.$$

Here non-degenerate means $\det C \neq 0$, and implies that if $v \cdot u = 0$ for all vectors u then $v = 0$.
Note our introduction of the simpler notation $v \cdot u = vu$, so that also $v \cdot v = v^2$. There should be no confusion with matrix multiplication, even if v and u are viewed as 1×2 matrices. Since C is symmetric, $v \cdot u = vu = uv = u \cdot v$.
Two vectors v and u are **perpendicular** precisely when $v \cdot u = 0$. Since the matrix C is non-degenerate, for any vector v there is, up to a scalar, exactly one vector u which is perpendicular to v.
The bilinear form determines the main metrical quantity: the **quadrance** of a vector v is the number

$$Q_v \equiv v \cdot v = v^2.$$

A vector v is **null** precisely when $Q_v = v \cdot v = v^2 = 0$, in other words precisely when v is perpendicular to itself.
The **quadrance** between the points A and B is

$$Q(A,B) \equiv Q_{\overrightarrow{AB}}.$$

In the Euclidean case, this is of course the square of the usual distance. But quadrance is a more elementary and fundamental notion than distance, and its algebraic nature makes it ideal for metrical geometry using other bilinear forms (as Einstein and Minkowski tried to teach us a century ago!)
Two lines l and m are **perpendicular** precisely when they have perpendicular direction vectors. A line is **null** precisely when it has a null direction vector (in which case all direction vectors are null).
We now make the important observation that the affine notion of parallelism may also be recaptured via the bilinear form. (This result also appears with the same title in [15].)

Theorem 1 (Parallel vectors) *Vectors v and u are parallel precisely when*

$$Q_v Q_u = (vu)^2 .$$

Proof. If $C = \begin{pmatrix} a & b \\ b & c \end{pmatrix}$, $v = (x,y)$ and $u = (z,w)$, then an explicit computation shows that

$$Q_v Q_u - (vu)^2 = -\frac{(xw-yz)^4 \left(ac-b^2\right)^2}{\left(ax^2+2bxy+cy^2\right)^2 \left(az^2+2bzw+cw^2\right)^2}.$$

Since the quadratic form is non-degenerate, $ac - b^2 \neq 0$, so we see that the left hand side is zero precisely when $xw - yz = 0$, in other words precisely when v and u are parallel. □

This motivates the following measure of the non-parallelism of two vectors; the **spread** between non-null vectors v and u is the number

$$s(v,u) \equiv 1 - \frac{(vu)^2}{Q_v Q_u}.$$

This is the replacement in rational trigonometry for the transcendental notion of angle θ, and in the Euclidean case it has the value $\sin^2\theta$. Spread is a more algebraic, logical, general and powerful notion than that of angle, and together quadrance and spread provide the foundation for *Rational Trigonometry*, a new approach to trigonometry developed in [10]. The current pre-occupation with distance and angle as the basis for Euclidean geometry is a historical aberration contrary to the explicit orientation of Euclid himself, and is a key obstacle to appreciating and understanding the relativistic geometry introduced by Einstein and Minkowski.

The spread $s(v,u)$ is unchanged if either v or u are multiplied by a non-zero number, and so we define the **spread** between any non-null lines l and m with direction vectors v and u to be $s(l,m) \equiv s(v,u)$. From the Parallel vectors theorem, the spread between parallel lines is 0. Two non-null lines l and m are perpendicular precisely when the spread between them is 1.

1.4 Triple spread formula

We now derive one of the basic formulas in the subject: the relation between the three spreads made by three (coplanar) vectors, and give a linear algebra proof, following the same lines as the papers [11] and [15].

Theorem 2 (Triple spread formula) *Suppose that v_1, v_2, v_3 are (planar) non-null vectors with respective spreads $s_1 \equiv s(v_2,v_3)$, $s_2 \equiv s(v_1,v_3)$ and $s_3 \equiv s(v_1,v_2)$. Then*

$$(s_1+s_2+s_3)^2 = 2\left(s_1^2+s_2^2+s_3^2\right) + 4s_1s_2s_3. \qquad (4)$$

Proof. We may that assume at least two of the vectors are linear independent, as otherwise all spreads are zero and the relation is trivial. So suppose that v_1 and v_2 linearly independent, and $v_3 = kv_1 + lv_2$. Suppose the bilinear form is given by the matrix

$$C = \begin{pmatrix} a & b \\ b & c \end{pmatrix}$$

with respect to the ordered basis v_1, v_2. Then in this basis $v_1 = (1,0), v_2 = (0,1)$ and $v_3 = (k,l)$ and we may compute that

$$s_3 = \frac{ac-b^2}{ac} \qquad s_2 = \frac{l^2\left(ac-b^2\right)}{a\left(ak^2+2bkl+cl^2\right)}$$

$$s_1 = \frac{k^2\left(ac-b^2\right)}{b\left(ak^2+2bkl+cl^2\right)}.$$

Then (4) is an identity, satisfied for all a, b, c, k and l. □

We now mention three consequences of the Triple spread formula, taken from [10]. The *Equal spreads theorem* asserts that if $s_1 = s_2 = s$, then $s_3 = 0$ or $s_3 = 4s(1-s)$. This follows from the identity $(s+s+s_3)^2 - 2\left(s^2+s^2+s_3^2\right) - 4s^2s_3 = -s_3\left(s_3 - 4s + 4s^2\right)$. The *Complementary spreads theorem* asserts that if $s_3 = 1$ then $s_1 + s_2 = 1$. This follows by rewriting the Triple spread formula in the form $(s_3 - s_1 - s_2)^2 = 4s_1s_2(1-s_3)$.

And the *Perpendicular spreads theorem* asserts that if v and u are non-null planar vectors with perpendicular vectors $v^\perp$ and $u^\perp$, then $s(v,u) = s\left(v^\perp, u^\perp\right)$. This follows from the Complementary spreads theorem, since if $s\left(v,v^\perp\right) = s\left(u,u^\perp\right) = 1$, then $s\left(v^\perp,u^\perp\right) = 1 - s\left(v^\perp,u\right) = 1 - (1 - s(v,u)) = s(v,u)$.

1.5 Altitudes and orthocenters

Given a line l and a point P, there is a unique line n through P which is perpendicular to the line l; it is the line $n : P + \lambda w$, where w is a perpendicular vector to the direction vector v of l. We call n the **altitude to** l **through** P. Note that this holds true even if l is a null line; in this case a direction vector v of l is null, so the altitude to l through P agrees with the parallel to l through P.

We use the following conventions: a set $\{A,B\}$ of two distinct points is a **side** and is denoted $\overline{AB}$, and a set $\{l,m\}$ of two distinct lines is a **vertex** and is denoted $\overline{lm}$. A set $\{A_1,A_2,A_3\}$ of three distinct non-collinear points is a **triangle** and is denoted $\overline{A_1A_2A_3}$. The triangle $\overline{A_1A_2A_3}$ has lines $l_3 \equiv A_1A_2$, $l_2 \equiv A_1A_3$ and $l_1 \equiv A_2A_3$ (by assumption no two of these are parallel), sides $\overline{A_1A_2}, \overline{A_1A_3}$ and $\overline{A_2A_3}$, and vertices $\overline{l_1l_2}, \overline{l_1l_3}$ and $\overline{l_2l_3}$.

The triangle $\overline{A_1A_2A_3}$ also has three **altitudes** n_1, n_2, n_3 passing through A_1, A_2, A_3 and perpendicular to the opposite lines A_2A_3, A_1A_3, A_1A_2 respectively. The following

holds both for affine and projective geometries: we give a short and novel proof here for the general affine case.

Theorem 3 (Orthocenter) *For any triangle $\overline{A_1A_2A_3}$ the three altitudes n_1, n_2, n_3 are concurrent at a point H.*

Proof. Suppose that a_1, a_2, a_3 are the associated position vectors to A_1, A_2, A_3 respectively. Since no two of the lines of the triangle $\overline{A_1A_2A_3}$ are parallel, the Perpendicular spreads corollary implies that no two of the three altitude lines are parallel. Define H to be the meet of n_1 and n_2, with h the associated position vector. In the identity

$$(h-a_1)(a_3-a_2)+(h-a_2)(a_1-a_3)=(h-a_3)(a_1-a_2)$$

the left hand side equals 0 by assumption, so the right hand is also equal to 0, implying that $h-a_3$ is perpendicular to the line a_1a_2. Therefore, the three altitude lines n_1, n_2, n_3 are concurrent at the point H. □

We call H the **orthocenter** of the triangle $\overline{A_1A_2A_3}$.

1.6 Change of coordinates and an explicit example

If we change coordinates via either an affine transformation in the original affine space $\mathbb{A}^2$, or equivalently a linear transformation in the associated vector space $\mathbb{V}^2$, then the matrix for the form changes in the familiar fashion. Suppose $\phi : V \to V$ is a linear transformation given by an invertible 2×2 matrix M, so that $\phi(v) = vM = w$, with inverse matrix N, so that $wN = v$. Define a new bilinear form $\circ$ by

$$\begin{aligned} w_1 \circ w_2 &\equiv (w_1N)\cdot(w_2N) = (w_1N)C(w_2N)^T \\ &= w_1(NCN^T)w_2^T. \end{aligned} \tag{5}$$

So the matrix C for the original bilinear form $\cdot$ becomes the matrix $D \equiv NCN^T$ for the new bilinear form $\circ$.

Example 1 *We illustrate these abstractions in a concrete example that will be used throughout in our diagrams. Our basic Triangle shown in Figure 2 has points $A_1 \equiv [3,1]$, $A_2 \equiv [4,4]$ and $A_3 \equiv [47/5, 29/5]$, and lines $A_1A_2 = \langle -3:1:8\rangle$, $A_1A_3 = \langle -3:4:5\rangle$ and $A_2A_3 = \langle 1:-3:8\rangle$. The bilinear form we will consider is that of green geometry in the language of chromogeometry ([12], [13]), determined by the symmetric matrix $C_g = \begin{pmatrix} 0 & 1 \\ 1 & 0 \end{pmatrix}$ and corresponding quadrance $Q_{(x,y)} = 2xy$. After translation by $(-3,-1)$ we obtain $\widetilde{A}_1 = [0,0]$, $\widetilde{A}_2 = [1,3]$, $\widetilde{A}_3 = [32/5, 24/5]$. The matrix N and its inverse M*

$$N = \begin{pmatrix} 1 & 3 \\ \frac{32}{5} & \frac{24}{5} \end{pmatrix} \qquad M = N^{-1} = \begin{pmatrix} -\frac{1}{3} & \frac{5}{24} \\ \frac{4}{9} & -\frac{5}{72} \end{pmatrix}$$

*send $[1,0]$ and $[0,1]$ to $\widetilde{A}_2$ and $\widetilde{A}_3$, and $\widetilde{A}_2$ and $\widetilde{A}_3$ to $[1,0]$ and $[0,1]$ respectively. So the effect of translation followed by multiplication by M is to send the original triangle to the **standard triangle** with points $[0,0]$, $[1,0]$ and $[0,1]$. The bilinear form in these new standard coordinates is given by the matrix $N\mathbf{C}_gN^T$ which is, up to a multiple,*

$$C = \begin{pmatrix} \frac{1}{4} & 1 \\ 1 & \frac{64}{25} \end{pmatrix} = \begin{pmatrix} a & b \\ b & c \end{pmatrix}.$$

We will shortly see that the Orthocenter in standard coordinates is $(ac-b^2)^{-1}[b(c-b), b(a-b)]$. In our example this would be the point $\left[-\frac{13}{3}, \frac{25}{12}\right]$, and to convert that back into the original coordinates, we would multiply by N to get

$$\left[-\tfrac{13}{3} \quad \tfrac{25}{12}\right] N = \begin{bmatrix} 9 & -3 \end{bmatrix}$$

and translate by $(3,1)$ to get the original orthocenter $H = [12,-2]$. This is shown in Figure 2, along with the Centroid $G = [82/15, 18/5]$ and the Circumcenter $C = [11/5, 32/5]$—we will meet these points shortly.

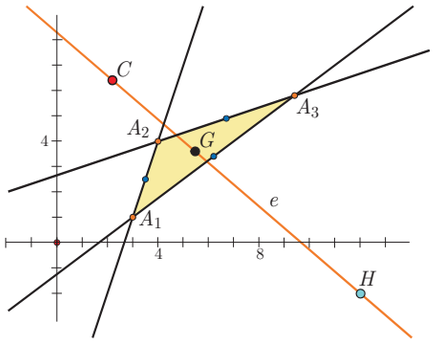

Figure 2: *Euler line in green geometry*

1.7 Bilines

A **biline** of the non-null vertex $\overline{l_1l_2}$ is a line b which passes through l_1l_2 and satisfies $s(l_1,b) = s(l_2,b)$. The existence of bilines depends on number-theoretical considerations of a particularly simple kind.

Theorem 4 (Vertex bilines) *If v and u are linearly independent non-null vectors, then there is a non-zero vector w with $s(v,w) = s(u,w)$ precisely when $1-s(v,u)$ is a square. In this case we may renormalize v and u so that $Q_v = Q_u$, and then there are exactly two possibilities for w up to a multiple, namely $v+u$ and $v-u$, and these are perpendicular.*

Proof. Since v and u are linearly independent, any vector can be written uniquely as $w = kv + lu$ for some numbers

k and l. The condition $s(v,w) = s(u,w)$ amounts to

$$\frac{(vw)^2}{Q_v Q_w} = \frac{(uw)^2}{Q_u Q_w} \Longleftrightarrow u^2\left(kv^2 + lvu\right)^2 = v^2\left(kvu + lu^2\right)^2$$
$$\Longleftrightarrow u^2\left(k^2\left(v^2\right)^2 + 2lkv^2(vu) + l^2(vu)^2\right) =$$
$$= v^2\left(k^2(vu)^2 + 2lku^2(vu) + l^2\left(u^2\right)^2\right)$$
$$\Longleftrightarrow k^2u^2\left(v^2\right)^2 + l^2u^2(vu)^2 = k^2v^2(vu)^2 + l^2v^2\left(u^2\right)^2$$
$$\Longleftrightarrow \left(v^2u^2 - (vu)^2\right)\left(k^2v^2 - l^2u^2\right) = 0.$$

Since v and u are by assumption not parallel, the first term is non-zero by the Parallel vectors theorem, and so the condition $s(v,w) = s(u,w)$ is equivalent to $k^2v^2 = l^2u^2$. Since v,u are non-null, v^2 and u^2 are non-zero, so k and l are also, since by assumption $w = kv + lu$ is non-zero.
So if $s(v,w) = s(u,w)$ then we may renormalize v and u so that $v^2 = u^2$ (by for example setting $\widetilde{v} = kv$ and $\widetilde{u} = lu$, and then replacing $\widetilde{v}, \widetilde{u}$ by v,u again), and then $1 - s(v,u) = (vu)^2 / \left(v^2\right)^2$ is a square. There are then two solutions: $w = v + u$ and $w = v - u$, corresponding to $l = \pm k$. Since $(v+u)(v-u) = v^2 - u^2 = 0$, these vectors are perpendicular. The converse is straightforward along the same lines. □

Example 2 *In our example triangle of Figure 2,* $v_1 = \overrightarrow{A_2A_3} = (27/5, 9/5)$, $v_2 = \overrightarrow{A_1A_3} = (32/5, 24/5)$ *and* $v_3 = \overrightarrow{A_1A_2} = (1,3)$, *so*

$$s(v_2, v_3) = 1 - \frac{\left(v_2 C_g v_3^T\right)^2}{\left(v_2 C_g v_2^T\right)\left(v_3 C_g v_3^T\right)} = \frac{25}{16}$$

is a square, so the vertex at A_1 *has bilines. Since* $Q_{v_2} = v_2 C_g v_2^T = 1536/25$ *and* $Q_{v_3} = v_3 C_g v_3^T = 6$, *we can renormalize* v_2 *by scaling it by* $5/16$ *to get* $u_2 = \overrightarrow{A_1B} = (2, 3/2)$ *so that now* $Q_{u_2} = Q_{v_3}$. *This means that* $u_2 + v_3 = \overrightarrow{A_1C_1}$ *and* $u_2 - v_3 = \overrightarrow{A_1C_2}$ *are the direction vectors for the bilines of the vertex at* A_1.

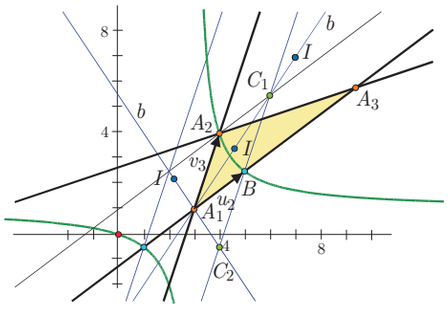

Figure 3 : *Green bilines b at* A_1

These are shown in Figure 3, along with three of the four Incenters I (the other two vertices also have bilines, and they are mutually concurrent). Naturally this triangle has been chosen carefully to ensure that Incenters do exist. In green geometry, a vertex formed from a light-like line and a time-like line will not have bislines, not even approximately over the rational numbers.

2 Standard coordinates and triangle geometry

Our principle strategy to study triangle geometry is to apply an affine transformation to move a general triangle to *standard position*:

$$A_1 = [0,0] \qquad A_2 = [1,0] \qquad \text{and} \qquad A_3 = [0,1]. \tag{6}$$

With this convention, $\overline{A_1A_2A_3}$ will be called the (standard) **Triangle**, with **Points** A_1, A_2, A_3. The **Lines** of the Triangle are then

$$l_1 \equiv A_2A_3 = \langle 1:1:-1\rangle \qquad l_2 \equiv A_1A_3 = \langle 1:0:0\rangle$$

$$l_3 \equiv A_2A_1 = \langle 0:1:0\rangle.$$

All further objects that we define with capital letters refer to this standard Triangle, and coordinates in this framework are called *standard coordinates*. In general the standard coordinates of points and lines in the plane of the original triangle depend on the choice of affine transformation—we are in principle free to permute the vertices—but triangle centers and central lines will have well-defined standard coordinates independent of such permutations.
Since we have performed an affine transformation, whatever metrical structure we started with has changed as in (5). So we will assume that the new metrical structure, in standard coordinates, is determined by a bilinear form with generic symmetric matrix

$$C \equiv \begin{pmatrix} a & b \\ b & c \end{pmatrix}. \tag{7}$$

We assume that the form is non-degenerate, so that the **determinant**

$$\Delta \equiv \det C = ac - b^2$$

is non-zero. Another important number is the **mixed trace**

$$d \equiv a + c - 2b.$$

It will also be useful to introduce the closely related secondary quantities

$$\overline{a} \equiv c - b \qquad \overline{b} \equiv a - c \qquad \overline{c} \equiv a - b$$

to simplify formulas. For example $d = \overline{a} + \overline{c}$.

Theorem 5 (Standard triangle quadrances and spreads) *The quadrances and spreads of* $\overline{A_1A_2A_3}$ *are*

$$Q_1 \equiv Q(A_2,A_3) = d \qquad Q_2 \equiv Q(A_1,A_3) = c$$
$$Q_3 \equiv Q(A_1,A_2) = a$$

and

$$s_1 \equiv s(A_1A_2,A_1A_3) = \frac{\Delta}{ac} \qquad s_2 \equiv s(A_2A_3,A_2A_1) = \frac{\Delta}{ad}$$
$$s_3 \equiv s(A_3A_1,A_3A_2) = \frac{\Delta}{cd}.$$

Furthermore

$$1-s_1 = \frac{b^2}{ac} \qquad 1-s_2 = \frac{(\overline{c})^2}{ad} \qquad 1-s_3 = \frac{(\overline{a})^2}{cd}.$$

Proof. Using the definition of quadrance,

$$Q_1 \equiv Q(A_2,A_3) = Q_{\overrightarrow{A_2A_3}} = (-1,1)C(-1,1)^T$$
$$= a+c-2b = d$$

and similarly for Q_2 and Q_3. Using the definition of spread,

$$s_1 \equiv s(A_1A_2,A_1A_3) = s((1,0),(0,1))$$
$$= 1 - \frac{\left((1,0)C(0,1)^T\right)^2}{\left((1,0)C(1,0)^T\right)\left((0,1)C(0,1)^T\right)}$$
$$= 1 - \frac{1}{ac}b^2 = \frac{\Delta}{ac}$$

and similarly for s_2 and s_3. □

2.1 Basic affine objects in triangle geometry

We now write down some basic central objects which figure prominently in triangle geometry, all with reference to the standard triangle $\overline{A_1A_2A_3}$ in the form (6). The derivations of these formulas are mostly immediate using the two basic operations of joins (2) and meets (3). We begin with some purely affine notions, independent of the bilinear form.

The **Midpoints** of the Triangle are

$$M_1 = \left[\frac{1}{2},\frac{1}{2}\right] \qquad M_2 = \left[0,\frac{1}{2}\right] \qquad M_3 = \left[\frac{1}{2},0\right].$$

The **Medians** are

$$d_1 \equiv A_1M_1 = \langle 1:-1:0\rangle \qquad d_2 \equiv A_2M_2 = \langle 1:2:-1\rangle$$
$$d_3 \equiv A_3M_3 = \langle 2:1:-1\rangle.$$

The **Centroid** is the common meet of the Medians

$$G = \left[\frac{1}{3},\frac{1}{3}\right].$$

The **Circumlines** are the lines of the **Medial triangle** $\overline{M_1M_2M_3}$, these are

$$b_1 \equiv M_2M_3 = \langle 2:2:-1\rangle \qquad b_2 \equiv M_3M_1 = \langle 2:0:-1\rangle$$
$$b_3 \equiv M_1M_2 = \langle 0:2:-1\rangle.$$

The **Double triangle** of $\overline{A_1A_2A_3}$ (usually called the **anti-medial triangle**) is formed from lines through the Points parallel to the opposite Lines. This is $\overline{D_1D_2D_3}$ where

$$D_1 = [1,1] \qquad D_2 = [-1,1] \qquad D_3 = [1,-1].$$

The lines of $\overline{D_1D_2D_3}$ are

$$D_2D_3 = \langle 1:1:0\rangle \qquad D_1D_3 = \langle 1:0:-1\rangle$$
$$D_1D_2 = \langle 0:1:-1\rangle.$$

Figure 4 shows these objects for our example Triangle.

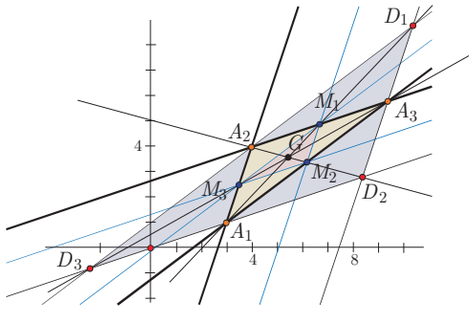

Figure 4: *The Medial triangle* $\overline{M_1M_2M_3}$ *and Double triangle* $\overline{D_1D_2D_3}$

2.2 The Orthocenter hierarchy

We now introduce some objects involving the metrical structure, and so the entries a,b,c of C from (7). Recall that $\overline{a} \equiv c-b$ and $\overline{c} = a-b$.

The **Altitudes** of $\overline{A_1A_2A_3}$ are the lines

$$n_1 = \langle \overline{c} : -\overline{a} : 0\rangle \qquad n_2 = \langle b : c : -b\rangle \qquad n_3 = \langle a : b : -b\rangle.$$

Theorem 6 (Orthocenter formula) *The three Altitudes meet at the* ***Orthocenter***

$$H = \frac{b}{\Delta}[\overline{a},\overline{c}].$$

Proof. We know that the altitudes meet from the Orthocenter theorem. We check that n_1 passes through H by computing $b\Delta^{-1}(\overline{ac}-\overline{ac}) = 0$.

Also n_2 passes through H since

$$\frac{b}{\Delta}(b\overline{a}+c\overline{c})-b = \frac{b}{\Delta}\left(b(c-b)+c(a-b)-ac+b^2\right) = 0$$

and similarly for n_3. □

The **Midlines** m_1, m_2 and m_3 are the lines through the midpoints M_1, M_2 and M_3 perpendicular to the respective sides— these are usually called **perpendicular bisectors**. They are also the altitudes of $\overline{M_1M_2M_3}$:

$$m_1 = \langle -2\overline{c} : 2\overline{a} : \overline{b} \rangle \qquad m_2 = \langle 2b : 2c : -c \rangle$$
$$m_3 = \langle 2a : 2b : -a \rangle .$$

Theorem 7 (Circumcenter) *The Midlines m_1, m_2, m_3 meet at the* ***Circumcenter***

$$C = \frac{1}{2\Delta} [c\overline{c}, a\overline{a}] .$$

Proof. We check that m_1 passes through C by computing

$$\frac{1}{2\Delta} \left(-2\overline{c}^2 c + 2\overline{a}^2 a\right) + \overline{b}$$
$$= \frac{1}{2(ac-b^2)} \left(-2(a-b)^2 c + 2(c-b)^2 a\right) + (a-c) = 0$$

and similarly for m_2 and m_3. □

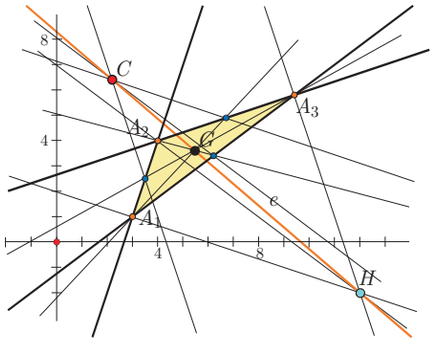

Figure 5: *The Euler line of a triangle*

As Gauss realized, this is also a consequence of the Orthocenter theorem applied to the Medial triangle $\overline{M_1M_2M_3}$, since the altitudes of the Medial triangle are the Midlines of the original Triangle.
The three altitudes of the Double triangle $\overline{D_1D_2D_3}$ are

$$t_1 = \langle \overline{c} : -\overline{a} : -\overline{b} \rangle \quad t_2 = \langle b : c : -\overline{a} \rangle \quad t_3 = \langle a : b : -\overline{c} \rangle .$$

Theorem 8 (Double orthocenter formula) *The three altitudes of the Double triangle meet in the De Longchamps point*

$$X_{20} \equiv \frac{1}{\Delta} \left[b^2 - 2bc + ac, b^2 - 2ab + ac\right] .$$

Proof. We check that t_1 passes through X_{20} by computing

$$\frac{1}{\Delta} \left(\overline{c}\left(b^2 - 2bc + ac\right) - \overline{a}\left(b^2 - 2ab + ac\right)\right) - \overline{b}$$
$$= \frac{1}{\Delta}((a-b)\left(b^2 - 2bc + ac\right) - (c-b)\left(b^2 - 2ab + ac\right)$$
$$- (a-c)\left(ac - b^2\right)) = 0$$

and similarly for t_2 and t_3. □

The existence of an Euler line in relativistic geometries was established in [13], here we extend this to the general case.

Theorem 9 (Euler line) *The points H, C and G are concurrent, and satisfy $G = \frac{1}{3}H + \frac{2}{3}C$. The Euler line $e \equiv CH$ is*

$$e = \left\langle \Delta - 3b\overline{c} : -\Delta + 3b\overline{a} : b\overline{b} \right\rangle .$$

Proof. Using the formulas above for H and C, we see that

$$\frac{1}{3}H + \frac{2}{3}C = \left(\frac{1}{3}\right)\frac{1}{\Delta}[b\overline{a}, b\overline{c}] + \left(\frac{2}{3}\right)\frac{1}{2\Delta}[c\overline{c}, a\overline{a}]$$
$$= \frac{1}{3\Delta}\left[ac - b^2, ac - b^2\right] = \frac{1}{3}[1,1] = G.$$

Computing the equation for the Euler line CH is straightforward. □

In Figure 5 we illustrate the situation with our basic example triangle with the Altitudes, Medians and Midlines meeting to form the Orthocenter H, Centroid G and Circumcenter C respectively on the Euler line e.
The **bases of altitudes** of $\overline{M_1M_2M_3}$ are:

$$E_1 = \frac{1}{2d}[\overline{c}, \overline{a}] \qquad E_2 = \frac{1}{2c}[c, \overline{a}] \qquad E_3 = \frac{1}{2a}[\overline{c}, a] .$$

The joins of Points and corresponding bases of altitudes of $\overline{M_1M_2M_3}$ are

$$A_1E_1 = \langle \overline{a} : -\overline{c} : 0 \rangle \qquad A_2E_2 = \langle \overline{a} : c : -\overline{a} \rangle$$
$$A_3E_3 = \langle a : \overline{c} : -\overline{c} \rangle .$$

Theorem 10 (Medial base perspectivity) *The three lines A_1E_1, A_2E_2, A_3E_3 meet at the point*

$$X_{69} = \frac{1}{a + c - b} [\overline{c}, \overline{a}] .$$

Proof. Straightforward. □

2.3 Bilines and Incenters

We now introduce the *Incenter hierarchy*. Unlike the Orthocenter hierarchy, this depends on number-theoretical conditions. Recall that $d \equiv a + c - 2b$.

Theorem 11 (Existence of Triangle bilines) *The Triangle $\overline{A_1A_2A_3}$ has Bilines at each vertex precisely when we can find numbers u, v, w in the field satisfying*

$$ac = u^2 \qquad ad = v^2 \qquad cd = w^2. \tag{8}$$

Proof. From the Vertex bilines theorem, bilines exist precisely when the spreads s_1, s_2, s_3 of the Triangle have the property that $1-s_1, 1-s_2, 1-s_3$ are all squares. From the Standard triangle quadrances and spreads theorem, this occurs for our standard triangle $\overline{A_1A_2A_3}$ precisely when we can find u, v, w satisfying (8). □

There is an important flexibility here: the three **Incenter constants** u, v, w are only determined up to a sign. The relations imply that

$$d^2u^2 = v^2w^2 \qquad c^2v^2 = u^2w^2 \qquad a^2w^2 = u^2v^2.$$

So we may choose the sign of u so that $du = vw$, and multiplying by u we get

$$acd = uvw.$$

From this we deduce that

$$du = vw \qquad cv = uw \qquad \text{and} \qquad aw = uv. \tag{9}$$

The **quadratic relations** (8) and (9) will be very important for us, for they reveal that the existence of the Incenter hierarchy is a number-theoretical issue which depends not only on the given triangle and the bilinear form, but also on the nature of the field over which we work, and they allow us to simplify many formulas involving u, v and w. Because only quadratic conditions are involved, we may always extend our field by adjoining (algebraic!) square roots to ensure that a given triangle has bilines.

The quadratic relations carry an important symmetry: we may replace any two of u, v and w with their negatives, and the relations remain unchanged. So if we have a formula F_0 involving u, v, w, then we may obtain related formulas F_1, F_2, F_3 by replacing v, w with their negatives, u, w with their negatives, and u, v with their negatives respectively. Adopting this convention allows us to exhibit the single formula F_0, since then F_1, F_2, F_3 are determined—we refer to this as **quadratic symmetry**, and will make frequent use of it in the rest of this paper.

From now on our working assumption is that: *the standard triangle $\overline{A_1A_2A_3}$ has bilines at each vertex, implying that we have Incenter constants u, v and w satisfying* (8) *and* (9). So u, v and w now become ingredients in our formulas for various objects in the Incenter hierarchy, along with the numbers a, b and c (and d) from the bilinear form $C = \begin{pmatrix} a & b \\ b & c \end{pmatrix}$.

Theorem 12 (Bilines) *The Bilines of the Triangle are $b_{1+} \equiv \langle v : w : 0 \rangle$ and $b_{1-} \equiv \langle v : -w : 0 \rangle$ through A_1, $b_{2+} \equiv \langle u : u+w : -u \rangle$ and $b_{2-} \equiv \langle u : u-w : -u \rangle$ through A_2, and $b_{3+} \equiv \langle u-v : u : -u \rangle$ and $b_{3-} \equiv \langle u+v : u : -u \rangle$ through A_3.*

Proof. We use the Bilines theorem to find bilines through $A_1 = [0,0]$. The lines meeting at A_1 have direction vectors $v_1 = (0,1)$ and $v_2 = (1,0)$, with $Q_{v_1} = (0,1)C(0,1)^T = c$ and $Q_{v_2} = (1,0)C(1,0)^T = a$. Now we renormalize and set $u_1 = \frac{v}{w}v_1$ to get $Q_{u_1} = \frac{v^2}{w^2}c = a = Q_{v_2}$. So the biliness at A_1 have direction vectors

$$u_1 + v_2 = \frac{v}{w}(0,1) + (1,0) = \left(1, \frac{v}{w}\right) \qquad \text{and}$$
$$u_1 - v_2 = \frac{v}{w}(0,1) - (1,0) = \left(-1, \frac{v}{w}\right)$$

and the bilines are $b_{1+} \equiv \langle v : w : 0 \rangle$ and $b_{1-} \equiv \langle v : -w : 0 \rangle$. Similarly you may check the other bilines through A_2 and A_3. □

Theorem 13 (Incenters) *The triples $\{b_{1+}, b_{2+}, b_{3+}\}$, $\{b_{1+}, b_{2-}, b_{3-}\}$, $\{b_{1-}, b_{2+}, b_{3-}\}$ and $\{b_{1-}, b_{2-}, b_{3+}\}$ of Bilines are concurrent, meeting respectively at the four* ***Incenters***

$$I_0 = \left[\frac{-uw}{uv-uw+vw}, \frac{uv}{uv-uw+vw}\right] = \frac{1}{(d+v-w)}[-w, v]$$
$$I_1 = \left[\frac{uw}{-uv+uw+vw}, \frac{-uv}{-uv+uw+vw}\right] = \frac{1}{(d-v+w)}[w, -v]$$
$$I_2 = \left[\frac{uw}{uv+uw+vw}, \frac{uv}{uv+uw+vw}\right] = \frac{1}{(d+v+w)}[w, v]$$
$$I_3 = \left[\frac{uw}{uv+uw-vw}, \frac{uv}{uv+uw-vw}\right] = \frac{1}{(d-v-w)}[-w, -v].$$

Proof. We may check concurrency of the various triples by computing

$$\det\begin{bmatrix} v & w & 0 \\ u & u+w & -u \\ u-v & u & -u \end{bmatrix} = \det\begin{bmatrix} v & w & 0 \\ u & u-w & -u \\ u+v & u & -u \end{bmatrix}$$
$$= \det\begin{bmatrix} v & -w & 0 \\ u & u-w & -u \\ u-v & u & -u \end{bmatrix} = \det\begin{bmatrix} v & -w & 0 \\ u & u+w & -u \\ u+v & u & -u \end{bmatrix} = 0.$$

The corresponding meet of $\langle v : w : 0 \rangle$, $\langle u : u+w : -u \rangle$ and $\langle u-v : u : -u \rangle$ is

$$b_{1+}b_{2+}b_{3+} = \left[\frac{-uw}{uv-uw+vw}, \frac{uv}{uv-uw+vw}\right]$$
$$= \frac{u}{aw-cv+du}[-w, v]$$
$$= \frac{1}{(d+v-w)}\ [-w, v] \equiv I_0.$$

We have used the quadratic relations, and the last equality is valid since

$$u(d+v-w) - (aw-cv+du) = cv - aw + uv - uw = 0.$$

The computations are similar for the other Incenters. □

The reader should check that the formulas for I_1, I_2, I_3 may also be obtained from I_0 by the quadratic symmetry rule described above. From now on in such a situation we will only write down the formula corresponding to I_0, and we will also often omit algebraic manipulations involving the quadratic relations.

The **Incenter altitude** t_{ij} is the line through the Incenter I_j and perpendicular to the Line l_i of our Triangle. There are twelve Incenter altitudes; three associated to each Incenter. The Incenter altitudes associated to I_0 are

$$t_{10} = \langle \overline{c}\,(d+v-w) : -\overline{a}\,(d+v-w) : \overline{a}v + \overline{c}w \rangle$$
$$t_{20} = \langle b\,(d+v-w) : c\,(d+v-w) : bw - cv \rangle$$
$$t_{30} = \langle a\,(d+v-w) : b\,(d+v-w) : aw - bv \rangle .$$

The **Contact points** C_{ij} are the meets of corresponding Incenter altitudes t_{ij} and Lines l_i. There are twelve Contact points; three associated to each Incenter. The Contact points associated to the Incenter I_0 are

$$C_{10} = \frac{1}{(d+v-w)}\,[\overline{a} - w, \overline{c} + v]$$
$$C_{20} = \frac{1}{c\,(d+v-w)}\,[0, cv - bw]$$
$$C_{30} = \frac{1}{a\,(d+v-w)}\,[bv - aw, 0] .$$

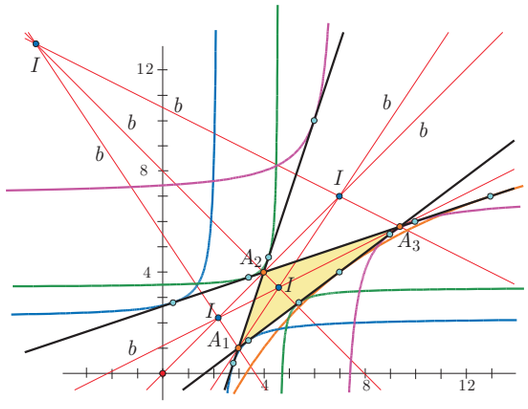

Figure 6: *Green bilines b, Incenters I, Contact points and Incircles*

In Figure 6 we see our standard example Triangle in the green geometry with Bilines b at each vertex, meeting in threes at the Incenters I. The Contact points are also shown, as are the Incircles, which are the circles with respect to the metrical structure centered at the Incenters and passing through the Contact points: they have equations in the variable point X of the form $Q(X,I) = Q(C,I)$ where I is an incenter and C is one of its associated Contact points. In this green geometry such circles appear as rectangular hyperbolas, with axes parallel to the coordinate axes.

2.4 New points

One of the main novelties of this paper is the introduction of the four *New points* L_j associated to each Incenter I_j. It is surprising that these points have seemingly slipped through the radar: they deserve to be among the top twenty in Kimberling's list, in our opinion.

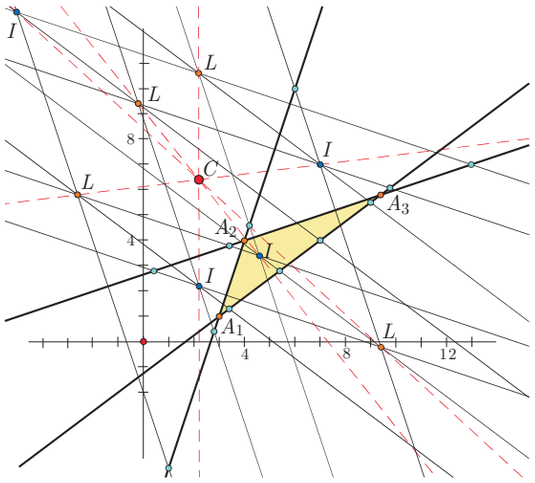

Figure 7: *Green Incenter altitudes, New points L and In-New center C*

Theorem 14 (New points) *The triples* $\{t_{11}, t_{22}, t_{33}\}$, $\{t_{10}, t_{23}, t_{32}\}$, $\{t_{20}, t_{13}, t_{31}\}$ *and* $\{t_{30}, t_{12}, t_{21}\}$ *of Incenter altitudes are concurrent. Each triple is associated to the Incenter which does not lie on any of the lines in that triple. The points where these triples meet are the* ***New points*** L_i*; for example* $\{t_{11}, t_{22}, t_{33}\}$ *meet at*

$$L_0 = \frac{1}{2\Delta}\,[\overline{a}u + cv + bw + c\overline{c}, \overline{c}u - bv - aw + a\overline{a}] .$$

Proof. We check that L_0 as defined is incident with $t_{11} = \langle \overline{c}\,(d - v + w) : -\overline{a}\,(d - v + w) : -\overline{a}v - \overline{c}w \rangle$ by computing

$$\begin{aligned}
&((c-b)u + cv + bw + c(a-b))\,(a-b)\,(a+c-2b-v+w) \\
&+ ((a-b)u - bv - aw + a(c-b))\,(-(c-b)\,(a+c-2b-v+w)) \\
&- 2\,(ac-b^2)\,((c-b)v + (a-b)w) \\
&= a^3c + 2ab^3 - 2a^2cb - a^2b^2 - ac^3 + 2ac^2b + c^2b^2 \\
&- 2cb^3 + b^2v^2 - b^2w^2 - acv^2 + acw^2 \\
&= (ac-b^2)\,(a^2 - c^2 - 2ab + 2cb - v^2 + w^2) = 0
\end{aligned}$$

using the quadratic relations (8). The computations for the other Incenter altitudes and L_1, L_2, L_3 are similar. □

The **In-New lines** are the joins of corresponding Incenter points and New points. The In-New line associated to I_0 is

$$I_0L_0 = \langle -a\overline{a}d + (ac + ab - 2b^2)\,v + a\overline{a}w : \\ c\overline{c}d + c\overline{c}v + (ac + cb - 2b^2)\,w : -a\overline{a}w - c\overline{c}v \rangle .$$

Theorem 15 (In-New center) *The four In-New lines I_jL_j are concurrent and meet at the circumcenter*

$$C = \frac{1}{2\Delta}\left[c\overline{c}, a\overline{a}\right],$$

and in fact C is the midpoint of $\overline{I_jL_j}$.

Proof. We check that C is the midpoint of $\overline{I_jL_j}$ by computing

$$\begin{aligned}
&\frac{1}{2}I_j + \frac{1}{2}L_j = \left(\frac{1}{2}\right)\frac{1}{(d+v-w)}\left[-w, v\right] \\
&+\left(\frac{1}{2}\right)\frac{1}{2\Delta}[(c-b)u+cv+bw+c(a-b),(a-b)u-bv-aw+a(c-b)] \\
&= \frac{1}{4\Delta(d+v-w)}\left[2c(a-b)(d+v-w), 2a(c-b)(d+v-w)\right] \\
&= \frac{1}{2\Delta}\left[c\overline{c}, a\overline{a}\right] = C.
\end{aligned}$$

□

The In-New center theorem shows that what we are calling the In-New lines are also the In-Circumcenter lines, the standard one which is labelled $L_{1,3}$ in [6]. The Incenter altitudes, New points and In-New lines are shown in Figure 7.

The proofs in these two theorems are typical of the ones which appear in the rest of the paper. Algebraic manipulations are combined with the quadratic relations to simplify expressions. Although sometimes long and involved, the verifications are in principle straightforward, and so *from now on we omit the details for results such as these*.

3 Transformations

Important classical transformations of points associated to a triangle include dilations in the centroid, and the isogonal and isotomic conjugates. It is useful to have general formulae for these in our standard coordinates.

3.1 Dilations about the Centroid

The dilation δ of factor λ centered at the origin takes $[x, y]$ to $\lambda[x, y]$. This also acts on vectors by scalar multiplying, and in particular it leaves spreads unchanged and multiplies any quadrance by a factor of λ^2. Similarly the dilation centered at a point A takes a point B to $A + \lambda\overrightarrow{AB}$. Any dilation preserves directions of lines, so preserves spreads, and changes quadrances between points proportionally.

Given our Triangle $\overline{A_1A_2A_3}$ with centroid G, define the **central dilation** $\delta_{-1/2}$ to be the dilation by the factor $-1/2$ centered at G. It takes the three Points of the Triangle to the midpoints M_1, M_2, M_3 of the opposite sides. This medial triangle $\overline{M_1M_2M_3}$ then clearly has lines which are parallel to the original triangle.

Since the central dilation preserves spread, the three altitudes of $\overline{A_1A_2A_3}$ are sent by $\delta_{-1/2}$ to the three altitudes of the medial triangle, which are the midlines/perpendicular bisectors of the original Triangle, showing again that $\delta_{-1/2}$ sends the orthocenter H to the circumcenter C, and as in the Euler line theorem it follows that G lies on $e = HC$, dividing $\overline{HC}$ in the affine ratio $2:1$.

We will see later that the central dilation also explains aspects of the various Nagel lines (there are four), since $\delta_{-1/2}$ takes any Incenter I_i to an incenter of the Medial triangle, called a **Spieker point** S_i. It follows that the four joins of Incenters and corresponding Spieker points all pass through G, and G divides each side $\overline{I_iS_i}$ in the affine ratio $2:1$.

The inverse of the central dilation $\delta_{-1/2}$ is δ_{-2}, which takes the Points of $\overline{A_1A_2A_3}$ to the points of the Double triangle $\overline{D_1D_2D_3}$, which has $\overline{A_1A_2A_3}$ as its medial triangle.

Theorem 16 (Central dilation formula) *The central dilation takes $X = [x, y]$ to*

$$\delta_{-1/2}(X) = \frac{1}{2}\left[1-x, 1-y\right]$$

while the inverse central dilation δ_{-2} takes X to $\delta_{-2}(X) = [1-2x, 1-2y]$.

Proof. If $Y = \delta_{-1/2}(X)$ then affinely $\frac{1}{3}X + \frac{2}{3}Y = G$ so that

$$Y = \frac{3}{2}G - \frac{1}{2}X = \frac{1}{2}\left[1-x, 1-y\right].$$

Inverting, we get the formula for $\delta_{-2}(X)$. □

Example 3 *The central dilation of the Orthocenter is*

$$\begin{aligned}
\delta_{-1/2}(H) &= \frac{1}{2}\left[1 - \frac{b(c-b)}{\Delta}, 1 - \frac{b(a-b)}{\Delta}\right] \\
&= \frac{1}{2\Delta}\left[c(a-b), a(c-b)\right] = \frac{1}{2\Delta}\left[c\overline{c}, a\overline{a}\right] = C
\end{aligned}$$

which is the Circumcenter.

Example 4 *The inverse central dilation of the Orthocenter is the **De Longchamps point** X_{20}—the orthocenter of the Double triangle $\overline{D_1D_2D_3}$*

$$\begin{aligned}
\delta_{-2}(H) = X_{20} &\equiv \left[1 - \frac{2b(c-b)}{\Delta}, 1 - \frac{2b(a-b)}{\Delta}\right] \\
&= \frac{1}{\Delta}\left[b^2 - 2cb + ac, b^2 - 2ab + ac\right].
\end{aligned}$$

3.2 Reflections and Isogonal conjugates

Suppose that v is a non-null vector, so that v is not perpendicular to itself. It means that we can find a perpendicular vector w so that v and w are linearly independent. Now if u is an arbitrary vector, write $u = rv + sw$ for some unique numbers r and s, and define the **reflection of u in v** to be

$$r_v(u) \equiv rv - sw.$$

If we replace v with a multiple, the reflection is unchanged. Now suppose that l and m are lines which meet at a point A, with respective direction vectors v and u. Then the **reflection of m in l** is the line through A with direction vector $r_v(u)$. It is important to note that if n is the perpendicular to l through A, then

$$r_l(m) = r_n(m).$$

Our standard triangle $\overline{A_1A_2A_3}$ determines an important transformation of points.

Theorem 17 (Isogonal conjugate) *If X is a point distinct from A_1, A_2, A_3, then the reflections of the lines A_1X, A_2X, A_3X in the bilines at A_1, A_2, A_3 respectively meet in a point $i(X)$, called the **isogonal conjugate** of X. If $X = [x,y]$ then*

$$i(X) = \frac{x+y-1}{ax^2+2bxy+cy^2-ax-cy}[cy, ax].$$

Proof. First we reflect the vector $a = (x,y)$ in the bilines $\langle v : w : 0\rangle$ and $\langle v : -w : 0\rangle$ through A_1. We do this by writing $(x,y) = r(w,v) + s(w,-v) = (rw+sw, rv-sv)$ and solving to get $r = (2vw)^{-1}(vx+wy)$ and $s = (2vw)^{-1}(vx-wy)$. The reflection is then

$$r(w,v) - s(w,-v) = \frac{1}{2vw}(vx+wy)(w,v) - \frac{1}{2vw}(vx-wy)(w,-v) = \left(\frac{wy}{v}, \frac{vx}{w}\right)$$

which is, up to a multiple and using the quadratic relations,

$$\left(w^2y, v^2x\right) = (cdy, adx) = d(cy, ax).$$

So reflection in the biline at A_1 takes the line A_1X to the line $A_1 + \lambda_1(cy, ax)$. Similarly, by computing the reflections of $(x-1,y)$ and $(x,y-1)$ in the bilines at A_2 and A_3, we find that the lines A_2X and A_3X get sent to the lines $A_2 + \lambda_2(ax + (a-d)y - a, -ax - ay + a)$ and $A_3 + \lambda_3(-cx - cy + c, x(c-d) + cy - c)$ respectively. It is now a computation that these three reflected lines meet at the point $i(X)$ as defined above. □

Example 5 *The isogonal conjugate of the centroid G is the **symmedian point***

$$K \equiv i\left(\left[\frac{1}{3}, \frac{1}{3}\right]\right) = \frac{1}{2(a+c-b)}[c,a] = X_6.$$

Example 6 *The isogonal conjugate of the Orthocenter H is the Circumcenter:*

$$i\left(\left[\frac{b(c-b)}{\Delta}, \frac{b(a-b)}{\Delta}\right]\right) = \frac{1}{2\Delta}[c(a-b), a(c-b)] = C = X_3.$$

3.3 Isotomic conjugates

Theorem 18 (Isotomic conjugates) *If X is a point distinct from A_1, A_2, A_3, then the lines joining the points A_1, A_2, A_3 to the reflections in the midpoints M_1, M_2, M_3 of the meets of A_1X, A_2X, A_3X with the lines of the Triangle are themselves concurrent, meeting in the **isotomic conjugate** of X. If $X = [x,y]$ then*

$$t(X) = \left[\frac{y(x+y-1)}{x^2+xy+y^2-x-y}, \frac{x(x+y-1)}{x^2+xy+y^2-x-y}\right].$$

Proof. The point $X \equiv [x,y]$ has Cevian lines which meet the lines A_2A_3, A_1A_3, A_1A_2 respectively in the points

$$\left[\frac{x}{x+y}, \frac{y}{x+y}\right] \qquad \left[0, \frac{y}{1-x}\right] \qquad \left[\frac{x}{1-y}, 0\right].$$

These three points may be reflected respectively in the midpoints $[1/2, 1/2], [0, 1/2], [1/2, 0]$ to get the points

$$\left[\frac{y}{x+y}, \frac{x}{x+y}\right] \qquad \left[0, \frac{1-x-y}{1-x}\right] \qquad \left[\frac{1-x-y}{1-y}, 0\right].$$

The lines $\langle x : -y : 0\rangle$, $\langle 1-x-y : 1-x : -1+x+y\rangle$ and $\langle 1-y : 1-x-y : -1+x+y\rangle$ joining these points to the original vertices meet at $t(X)$ as defined above. □

Example 7 *The isotomic conjugate of the Orthocenter H is*

$$t\left(\left[\frac{(c-b)b}{ac-b^2}, \frac{(a-b)b}{ac-b^2}\right]\right) = \left[\frac{a-b}{a+c-b}, \frac{c-b}{a+c-b}\right] \equiv X_{69}.$$

4 Strong concurrences

4.1 Sight Lines, Gergonne and Nagel points

We now adopt the principle that algebraic verifications of incidence, using the quadratic relations, will be omitted.

A **Sight line** s_{ij} is the join of a Contact point C_{ij} with the Point A_i opposite to the Line that it lies on, and is naturally associated with the Incenter I_j. There are twelve Sight lines; three associated to each Incenter:

$$\begin{aligned}
s_{10} &= \langle \overline{c} + v : -\overline{a} + w : 0\rangle \\
s_{20} &= \langle cv - bw : c(d+v-w) : -cv + bw\rangle \\
s_{30} &= \langle a(d+v-w) : -aw + bv : aw - bv\rangle \\
s_{11} &= \langle \overline{c} - v : -\overline{a} - w : 0\rangle \\
s_{21} &= \langle -cv + bw : c(d-v+w) : cv - bw\rangle \\
s_{31} &= \langle a(d-v+w) : aw - bv : -aw + bv\rangle \\
s_{12} &= \langle \overline{c} + v : -\overline{a} - w : 0\rangle \\
s_{22} &= \langle cv + bw : c(d+v+w) : -cv - bw\rangle \\
s_{32} &= \langle a(d+v+w) : aw + bv : -aw - bv\rangle \\
s_{13} &= \langle \overline{c} - v : -\overline{a} + w : 0\rangle \\
s_{23} &= \langle -cv - bw : c(d-v-w) : cv + bw\rangle \\
s_{33} &= \langle a(d-v-w) : -aw - bv : aw + bv\rangle.
\end{aligned}$$

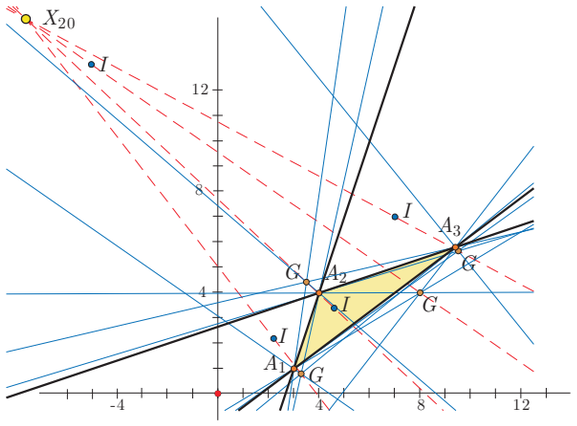

Figure 8: *Green Sight lines, Gergonne points G, In-Gergonne lines and In-Gergonne center X_{20}*

Here we introduce a well-known center of the triangle, the Gergonne point (see for example [2], [9]).

Theorem 19 (Gergonne points) *The triples $\{s_{10}, s_{20}, s_{30}\}$, $\{s_{11}, s_{21}, s_{31}\}$, $\{s_{12}, s_{22}, s_{32}\}$ and $\{s_{13}, s_{23}, s_{33}\}$ of Sight lines are concurrent. Each triple is associated to an Incenter, and the meets of these triples are the **Gergonne points** G_j. The Gergonne point associated to I_0 is*

$$G_0 = \frac{b-u}{2(du-cv+aw)-\Delta}\left[w-\overline{a}, -v-\overline{c}\right].$$

The join of a corresponding Incenter I_j and Gergonne point G_j is an **In-Gergonne line** or **Soddy line**. There are four Soddy lines, and

$$\begin{aligned} I_0G_0 = \langle & 2b\overline{c}v + (\Delta - 2b\overline{c})\,w - (\Delta - 2b\overline{c})\,d : \\ & 2b\overline{a}w + (\Delta - 2b\overline{a})\,v + (\Delta - 2b\overline{a})\,d : \\ & -(\Delta - 2b\overline{a})\,v - (\Delta - 2b\overline{c})\,w\rangle. \end{aligned}$$

Theorem 20 (In-Gergonne center) *The four In-Gergonne/Soddy lines I_jG_j are concurrent, and meet at the De Longchamps point*

$$X_{20} = \frac{1}{\Delta}\left[b^2 - 2cb + ac, b^2 - 2ab + ac\right]$$

which is the orthocenter of the Double triangle. Furthermore the midpoint of $\overline{HX_{20}}$ is the Circumcenter C, so that X_{20} lies on the Euler line.

Proof. The concurrency of the In-Gergonne/Soddy lines I_jG_j is as usual. The equation

$$\begin{aligned} & \frac{1}{2\Delta}\left[b(c-b), b(a-b)\right] + \frac{1}{2\Delta}\left[b^2 - 2cb + ac, b^2 - 2ab + ac\right] \\ & = \frac{1}{2\Delta}\left[c(a-b), a(c-b)\right] = C \end{aligned}$$

shows that $C = \frac{1}{2}H + \frac{1}{2}X_{20}$. Since the Euler line is $e = CH$, X_{20} lies on e. □

Figure 8 shows the Gergonne points G and the In-Gergonne lines meeting at X_{20}.

Theorem 21 (Nagel points) *The triples $\{s_{11}, s_{22}, s_{33}\}$, $\{s_{10}, s_{32}, s_{23}\}$, $\{s_{20}, s_{31}, s_{13}\}$ and $\{s_{30}, s_{21}, s_{12}\}$ of Sight lines are concurrent. Each triple involves one Sight line associated to each of the Incenters, and so is associated to the Incenter with which it does not share a Sight line. The points where these triples meet are the **Nagel points** N_j. For example, $\{s_{11}, s_{22}, s_{33}\}$ meet at*

$$N_0 = \frac{1}{\Delta}\left[(b+u)\overline{a} + cv + bw, (b+u)\overline{c} - bv - aw\right].$$

Proof. We check that N_0 as defined is incident with $\langle \overline{c} - v : -\overline{a} - w : 0\rangle$ by computing

$$\begin{aligned} & \frac{(b+u)\overline{a} + cv + bw}{\Delta}(\overline{c} - v) + \frac{(b+u)\overline{c} - bv - aw}{\Delta}(-\overline{a} - w) \\ & = \frac{-cduv^2 + aduw^2 + c\overline{c}v^2w + a\overline{a}vw^2 - ac\overline{a}dv - ac\overline{c}dw}{\Delta} = 0 \end{aligned}$$

using the quadratic relations, (8) and (9).
The computations for the other Sight lines and N_1, N_2, N_3 are similar. □

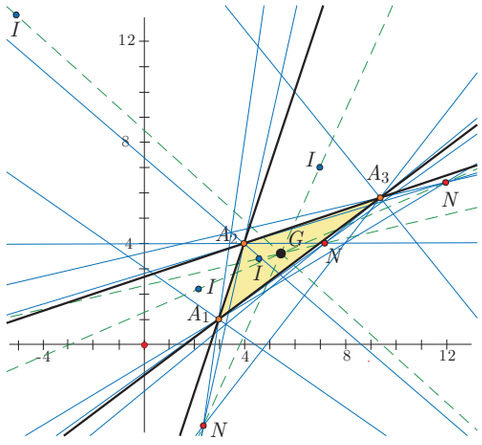

Figure 9: *Green Sight lines, Nagel points N, In-Nagel lines and In-Nagel center $G = X_2$*

The join of a corresponding Incenter and Nagel point is an **In-Nagel line.** There are four In-Nagel lines, and

$$I_0N_0 = \langle 2v + w - d : v + 2w + d : -v - w\rangle.$$

In classical triangle geometry, the line I_0N_0 is called simply the *Nagel line*.

Theorem 22 (In-Nagel center) *The four In-Nagel lines I_jN_j are concurrent, and meet at the Centroid $G = X_2$, and in fact $G = \frac{2}{3}I_j + \frac{1}{3}N_j$.*

Proof. Using the formulas above for I_0 and N_0, we see that

$$\begin{aligned}\frac{2}{3}I_0+\frac{1}{3}N_0 &= \left(\frac{2}{3}\right)\frac{1}{(d+v-w)}\left[-w,v\right]\\ &+\left(\frac{1}{3}\right)\frac{1}{\Delta}\left[(b+u)\overline{a}+cv+bw,(b+u)\overline{c}-bv-aw\right]\\ &= \frac{1}{3\Delta(d+v-w)}\left[\Delta(d+v-w),\Delta(d+v-w)\right]\\ &= \frac{1}{3}\left[1,1\right]=G.\end{aligned}$$

□

The join of a corresponding Gergonne point G_j and Nagel point N_j is a **Gergonne-Nagel line**. There are four Gergonne-Nagel lines, and

$$G_0N_0 = \langle -\overline{a}u+\overline{a}v+aw : \overline{c}u+cv+\overline{c}w : -\overline{c}w-\overline{a}v\rangle\,.$$

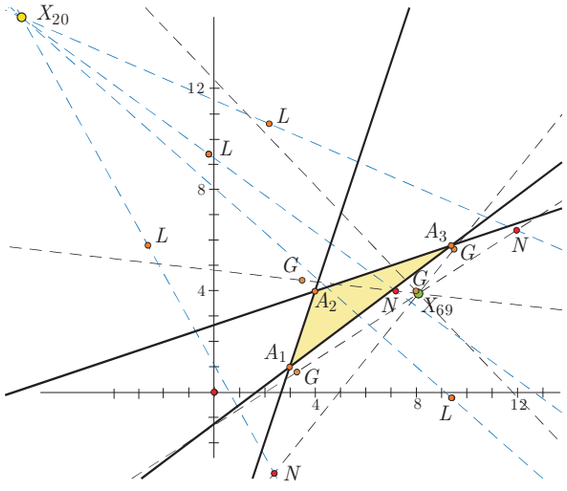

Figure 10: *Green Gergonne-Nagel center X_{69} and Nagel-New center X_{20}*

Theorem 23 (Gergonne-Nagel center) *The four Gergonne-Nagel G_jN_j lines are concurrent, and meet at the isotomic conjugate of the Orthocenter,*

$$X_{69} = \frac{1}{a+c-b}\left[\overline{c},\overline{a}\right].$$

The join of a corresponding New point L_j and Nagel point N_j is a **Nagel-New line**. There are four Nagel-New lines, and the one associated to I_0 is

$$\begin{aligned}L_0N_0 = \langle & ac-3ab+2b^2-\overline{c}u+bv+aw :\\ & 3cb-ac-2b^2+\overline{a}u+cv+bw :\\ & (a-c)b+(a-c)u-\overline{a}v+\overline{c}w\rangle.\end{aligned}$$

Theorem 24 (Nagel-New center) *The four Nagel-New lines N_jL_j meet in the De Longchamps point X_{20}, and in fact $L_j = \frac{1}{2}N_0+\frac{1}{2}X_{20}$.*

Proof. We check that

$$\begin{aligned}\frac{1}{2}X_{20}+\frac{1}{2}N_0 &= \left(\frac{1}{2}\right)\frac{1}{\Delta}\left[b^2-2cb+ac,b^2-2ab+ac\right]\\ &+\left(\frac{1}{2}\right)\frac{1}{\Delta}\left[(b+u)\overline{a}+cv+bw,(b+u)\overline{c}-bv-aw\right]\\ &= \frac{1}{2\Delta}\left[\overline{a}u+cv+bw+c\overline{c},\overline{c}u-bv-aw+a\overline{a}\right]=L_0.\end{aligned}$$

□

4.2 InMid lines and Mittenpunkts

The join of an Incenter I_j with a Midpoint M_i is an **InMid line**. There are twelve InMid lines:

$$\begin{aligned}I_0M_1 &= \langle v+w-d : v+w+d : -v-w\rangle\\ I_0M_2 &= \langle v+w-d : 2w : -w\rangle\\ I_0M_3 &= \langle 2v : v+w+d : -v\rangle\\ I_1M_1 &= \langle v+w+d : v+w-d : -v-w\rangle\\ I_1M_2 &= \langle v+w+d : 2w : -w\rangle\\ I_1M_3 &= \langle 2v : v+w-d : -v\rangle\\ I_2M_1 &= \langle v-w-d : v-w+d : -v+w\rangle\\ I_2M_2 &= \langle v-w-d : -2w : w\rangle\\ I_2M_3 &= \langle 2v : v-w+d : -v\rangle\\ I_3M_1 &= \langle -v+w-d : -v+w+d : v-w\rangle\\ I_3M_2 &= \langle -v+w-d : 2w : -w\rangle\\ I_3M_3 &= \langle -2v : -v+w+d : v\rangle\,.\end{aligned}$$

Theorem 25 (InMid lines) *The triples of InMid lines $\{I_1M_1,I_2M_2,I_3M_3\}$, $\{I_0M_1,I_2M_3,I_3M_2\}$, $\{I_0M_2,I_1M_3,I_3M_1\}$ and $\{I_0M_3,I_1M_2,I_2M_1\}$ are concurrent. Each triple involves one InMid line associated to each of three Incenters, and so is associated to the Incenter which does not appear. The points where these triples meet are the **Mittenpunkts** D_j. For example, $\{I_1M_1,I_2M_2,I_3M_3\}$ meet at*

$$D_0 = \frac{1}{2(a+c-b+u-v+w)}\left[c+u+w,a+u-v\right].$$

The join of a corresponding Incenter I_j and Mittenpunkt D_j is an **In-Mitten line**. There are four In-Mitten lines, and

$$I_0D_0 = \langle (c+d)v+aw-ad : cv+(a+d)w+cd : -aw-cv\rangle\,.$$

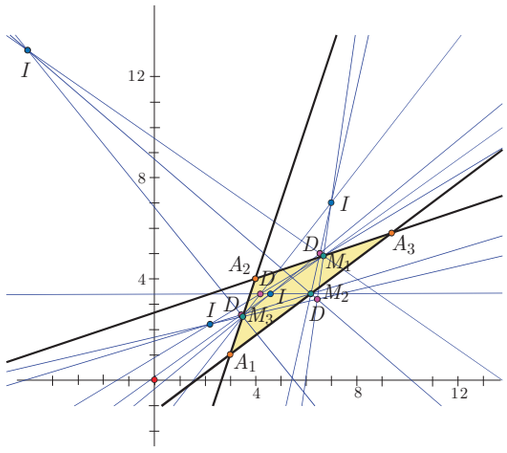

Figure 11: *Green InMid lines and Mittenpunkts D*

Theorem 26 (In-Mitten center) *The four In-Mitten lines are concurrent and meet at the* ***symmedian point*** *(see Example 3)*

$$K = X_6 = \frac{1}{2(a+c-b)}[c,a].$$

The join of a corresponding Gergonne point G_j and Mittenpunkt D_j is a **Gergonne-Mitten** line. There are four Gergonne-Mitten lines and

$$D_0G_0 = \left\langle \begin{array}{c} (\Delta-4bd)u+(4c\overline{c}-\Delta)v+2(4a\overline{a}-\Delta)w+(a-2\overline{a})\Delta : \\ -(\Delta-4bd)u+2(4c\overline{c}-\Delta)v+(4a\overline{a}-\Delta)w-(c-2\overline{c})\Delta : \\ (\Delta-4c\overline{c})v+(\Delta-4a\overline{a})w-\overline{b}\Delta \end{array} \right\rangle.$$

Theorem 27 (Gergonne-Mitten center) *The four Gergonne-Mitten lines G_jD_j meet in the Centroid $G = X_2$, and in fact $G = \frac{2}{3}D_j + \frac{1}{3}G_j$.*

Proof. We use the formulas above for D_0 and G_0 to compute

$$\begin{aligned} &\frac{2}{3}D_0 + \frac{1}{3}G_0 \\ &= \left(\frac{2}{3}\right)\frac{1}{2(a+c-b+u-v+w)}[c+u+w, a+u-v] \\ &+ \left(\frac{1}{3}\right)\frac{b-u}{2(du-cv+aw)-\Delta}[w-(c-b), -v-(a-b)] \\ &= \frac{1}{3}[1,1] = G. \end{aligned}$$

□

The join of a corresponding Mittenpunkt D_j and New point L_j is a **Mitten-New** line. There are four Mitten-New lines and

$$D_0L_0 = \langle av+bw-\overline{c}d : bv+cw+\overline{a}d : -b(v+w)\rangle.$$

Theorem 28 (Mitten-New center) *The four Mitten-New lines D_jL_j are concurrent, and meet at the Orthocenter*

$$H = \frac{1}{\Delta}[b\overline{a}, b\overline{c}].$$

Figure 12 shows the four In-Mitten lines meeting at $K = X_6$, the four Gergonne-Mitten lines meeting at $G = X_2$ and the four Mitten-New lines meeting at $H = X_4$.

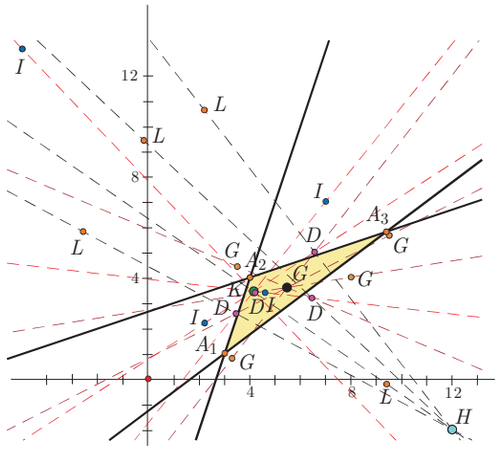

Figure 12: *Green Mitten-New center H, Gergonne-Mitten center G and In-Mitten center K*

4.3 Spieker points

The central dilation of an Incenter is a **Spieker point**. There are four Spieker points S_0, S_1, S_2, S_3 which are central dilations of I_0, I_1, I_2, I_3 respectively.

Theorem 29 (Spieker points) *The four Spieker points are*

$$\begin{aligned} S_0 &= \frac{1}{2}\frac{1}{(d+v-w)}[v+d, -w+d] \\ S_1 &= \frac{1}{2}\frac{1}{(d-v+w)}[-v+d, w+d] \\ S_2 &= \frac{1}{2}\frac{1}{(d+v+w)}[v+d, w+d] \\ S_3 &= \frac{1}{2}\frac{1}{(d-v-w)}[-v+d, -w+d]. \end{aligned}$$

Proof. We use the central dilation formula which takes $I_0 = (d+v-w)^{-1}[-w, v]$ to the point

$$\begin{aligned} S_0 \equiv \delta_{-1/2}(I_0) &= \frac{1}{2}\left[1 - \frac{-w}{d+v-w}, 1 - \frac{v}{d+v-w}\right] \\ &= \frac{1}{2(d+v-w)}[v+d, -w+d] \end{aligned}$$

and similarly for the other Spieker points. □

Theorem 30 (Spieker-Nagel lines) *The Spieker points lie on the corresponding In-Nagel lines, and in particular S_0, S_1, S_2, S_3 are the midpoints of the sides $\overline{I_0N_0}$, $\overline{I_1N_1}$, $\overline{I_2N_2}$, $\overline{I_3N_3}$ respectively.*

Proof. We check that in fact S_0 is the midpoint of $\overline{I_0N_0}$ by computing

$$\begin{aligned}&\frac{1}{2}I_0+\frac{1}{2}N_0=\frac{1}{2}\frac{1}{(d+v-w)}\left[-w,v\right]\\&+\frac{1}{2}\frac{1}{\Delta}\left[(b+u)(c-b)+cv+bw,(b+u)(a-b)-bv-aw\right]\\&=S_0.\end{aligned}$$

The computations for the other In-Nagel lines and S_1, S_2, S_3 are similar. □

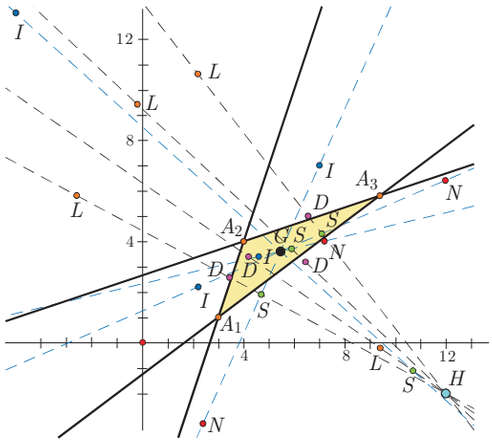

Figure 13: *Green Spieker points S and Mitten-Spieker center H*

The joins of corresponding Mittenpunkts D_j and Spieker points S_j are the **Mitten-Spieker lines**. There are four Mitten-Spieker lines, and

$$D_0S_0=\langle av+bw-\overline{c}d:bv+cw+\overline{a}d:-b(v+w)\rangle.$$

Theorem 31 (Mitten-Spieker center) *The four Mitten-Spieker lines D_jS_j are concurrent and meet at the Orthocenter $H=X_4$.*

Theorem 32 (New Mitten-Spieker) *The Spieker point S_j is the midpoint of $\overline{HL_j}$, so that the corresponding New point L_j also lies on the corresponding Mitten-Spieker line.*

Proof. The midpoint of $\overline{HL_0}$ is

$$\begin{aligned}\frac{1}{2}H+\frac{1}{2}L_0&=\frac{1}{2\Delta}\left[b(c-b),b(a-b)\right]\\&\quad+\frac{1}{4\Delta}[(c-b)u+cv+bw+c(a-b),\\&\qquad(a-b)u-bv-aw+a(c-b)]\\&=\frac{1}{4(ac-b^2)}[ac-b^2+(c-b)(u+b)+cv+bw,\\&\qquad ac-b^2+(a-b)(u+b)-aw-bv]\\&=\frac{1}{4(ac-b^2)}[ac-b^2+(c-b+w)(u+b),\\&\qquad ac-b^2+(a-b-v)(u+b)]\\&=\frac{1}{4}\left[1+\frac{(c-b+w)}{u-b},1+\frac{(a-b-v)}{u-b}\right]\\&=\frac{1}{4(u-b)}\left[c-2b+u+w,a-2b+u-v\right].\end{aligned}$$

Now a judicious use of the quadratic relations, which we leave to the reader, shows that this is S_0. The computations for the other Spieker points are similar. □

The proof shows in fact that there is quite some variety possible in the formulas for the various points and lines in this paper.

5 Future Directions

This paper might easily be the starting point for many more investigations, as there are lots of additional points in the Incenter hierarchy that might lead to similar phenomenon. In a related but slightly different direction, the basic idea of *Chromogeometry* ([12], [13]) is that we can expect wonderful relations between the corresponding geometrical facts in the *blue* (Euclidean bilinear form $x_1x_2+y_1y_2$), *red* (bilinear form $x_1x_2-y_1y_2$) and *green* (bilinear form $x_1y_2+y_1x_2$) geometries.

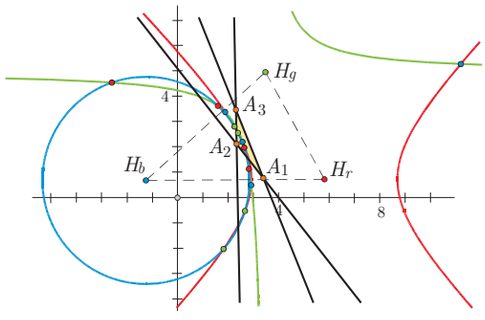

Figure 14: *Blue, red and green Incenter circles*

A spectacular illustration of this is the following, which we will describe in detail in a future work: if we have a triangle

$\overline{A_1A_2A_3}$ that has both blue, red and green Incenters (a rather delicate issue, as it turns out), then remarkably the four red Incenters and four green Incenters lie on a conic, in fact a *blue circle*, as in Figure 14. Similarly, the four red Incenters and four blue Incenters lie on a green circle, and the four green Incenters and four blue Incenters lie on a red circle. The centers of these three coloured Incenter circles are exactly the respective orthocenters H_b, H_r, H_g which form the *Omega triangle* of the given triangle $\overline{A_1A_2A_3}$, introduced in [12].

In particular the four green Incenters I that have appeared in our diagrams are in fact *concyclic in a Euclidean sense, as well as in a red geometry sense*. By applying central dilations, we may conclude similar facts about circles passing through Nagel points and Spieker points. Many more interesting facts wait to be discovered.

References

[1] PHILIP J. DAVIS, The Rise, Fall, and Possible Transfiguration of Triangle Geometry: A Mini-history, *Amer. Math. Monthly* **102** (1995), 204–214.

[2] M. HOFFMANN, S. GORJANC, On the Generalized Gergonne Point and Beyond, *Forum Geom.* **8** (2008), 151–155.

[3] R. HONSBERGER, *Episodes of 19th and 20th Century Euclidean Geometry*, Math. Assoc. America, 1995.

[4] Hyacinthos Yahoo Group `http://tech.groups.yahoo.com/group/hyacinthos`.

[5] C. KIMBERLING, *Triangle Centers and Central Triangles*, vol. 129 Congressus Numerantium, Utilitas Mathematica Publishing, Winnepeg, MA, 1998.

[6] C. KIMBERLING, *Encyclopedia of Triangle Centers*, `http://faculty.evansville.edu/ck6/encyclopedia/ETC.html`.

[7] C. KIMBERLING, Major Centers of Triangles, *Amer. Math. Monthly* **104** (1997), 431–438.

[8] B. ODEHNAL, Generalized Gergonne and Nagel points, *Beiträge Algebra Geom.* **51 (2)** (2010), 477–491.

[9] A. OLDKNOW, The Euler-Gergonne-Soddy Triangle of a Triangle, *Amer. Math. Monthly* **103 (4)** (1996), 319–329.

[10] N. J. WILDBERGER, *Divine Proportions: Rational Trigonometry to Universal Geometry*, Wild Egg Books, Sydney, 2005. `http://wildegg.com`.

[11] N. J. WILDBERGER, Affine and projective metrical geometry, *arXiv: math/0612499v1*, (2006), to appear, *J. of Geometry*.

[12] N. J. WILDBERGER, Chromogeometry, *Mathematical Intelligencer* **32 (1)** (2010), 26–32.

[13] N. J. WILDBERGER, Chromogeometry and Relativistic Conics, *KoG* **13** (2009), 43–50.

[14] N. J. WILDBERGER, Universal Hyperbolic Geometry III: First steps in projective triangle geometry, *KoG* **15** (2011), 25–49.

[15] N. J. WILDBERGER, A. ALKHALDI, Universal Hyperbolic Geometry IV: Sydpoints and twin circles, to appear, *KoG* **16** (2012).

[16] P. Yiu, *Introduction to the Geometry of the Triangle*, Florida Atlantic University lecture notes, 2001.

[17] P. Yiu, *A Tour of Triangle Geometry*, Florida Atlantic University lecture notes, 2004.

Nguyen Le
e-mail: n.h.le@unsw.edu.au

Norman John Wildberger
e-mail: n.wildberger@unsw.edu.au

School of Mathematics and Statistics UNSW
Sydney 2052 Australia

Stručni rad
Prihvaćeno 27. 06. 2012.

TATJANA SLIJEPČEVIĆ - MANGER

Obujam rotacijskog tijela

The Volume of a Solid of Revolution

ABSTRACT

In this paper we present classical methods (disk and shell integration) to compute the volume of a solid of revolution. We also give a method to compute the volume of a solid of revolution as a double integral. In the end we show how Guldin-Pappus' theorem follows from the third method.

Key words: volume, solid of revolution, disk method, shell method, double integral

MSC 2010: 26B15, 28A75, 51M25

Obujam rotacijskog tijela

SAŽETAK

U ovom članku su opisane klasične metode diska i ljuske za računanje volumena rotacijskih tijela. Također je navedena metoda za računanje volumena rotacijskih tijela pomoću dvostrukog integrala, te Guldin-Pappusov poučak kao neposredna posljedica te metode.

Ključne riječi: volumen, rotacijsko tijelo, metoda diska, metoda ljuske, dvostruki integral

1 Uvod

Računanje obujma rotacijskog tijela je uobičajena tema koja se pojavljuje u kolegijima iz matematike na preddiplomskoj razini studiranja [1]. Udžbenici obično sadrže dvije klasične metode izvoda formula za računanje obujma rotacijskog tijela:

- metodu ljuske, gdje se tijelo podijeli vertikalno na tanke koncentrične ljuske oko osi vrtnje,
- metodu diska, koja se sastoji u djeljenju tijela horizontalno na tanke slojeve okomite na os vrtnje.

Metodu odabiremo prema načinu zadavanja područja koje rotira i prema izboru osi rotacije o čemu će biti govora nešto kasnije. U ovom članku su opisane metode ljuske i diska, a također i metoda računanja volumena rotacijskog tijela pomoću dvostrukog integrala. Metode diska i ljuske se mogu izvesti iz spomenutog dvostrukog integrala korištenjem Fubinijevog teorema. Direktna posljedica dvostrukog integrala za računanje volumena rotacijskog tijela je i Guldin-Pappusov poučak. Svi rezultati su bez gubitka općenitosti prikazani za slučaj rotacije oko osi y.

2 Klasične metode

Izvedimo formulu za računanje obujma rotacijskog tijela metodom ljuske. Promotrimo područje Ω koje je omeđeno neprekidnim funkcijama $y = f_1(x)$ i $y = f_2(x)$ između $x = a$ i $x = b$ kao u primjeru na slici 1.

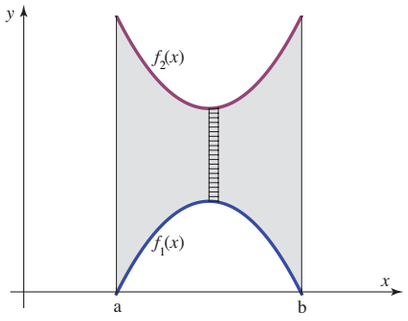

Slika 1: *Područje omeđeno funkcijama $f_1(x)$ i $f_2(x)$ između a i b*

Za svaku točku $T(x,y) \in \Omega$ x-koordinata predstavlja udaljenost točke T od osi rotacije y. Označimo s $V(\Omega, y)$ obujam tijela dobivenog rotacijom područja Ω oko osi y. Odaberemo određeni $x \in [a,b]$. Promotrimo vertikalnu trakicu koja se prostire od donjeg do gornjeg ruba lika Ω širine dx kao na slici 1. Kada vertikalna trakica rotira oko osi y, dobivamo vertikalnu cilindričnu ljusku približnog obujma $2\pi x(f_2(x) - f_1(x))\mathrm{d}x$. Zbrajanjem obujama ljusaka za sve $x \in [a,b]$ dobivamo približni obujam rotacijskog tijela. Prelaskom na limes, kada širina trakice teži prema nuli, zbroj prelazi u integral

$$V(\Omega, y) = \int_a^b 2\pi x(f_2(x) - f_1(x))\mathrm{d}x,$$

koji predstavlja točnu vrijednost obujma rotacijskog tijela dobivenu metodom ljuske (detaljnije obrazloženje pogledajte u [1], točka 7.5.2, stranica 318).

Sada ćemo izvesti formulu za računanje obujma rotacijskog tijela metodom diska. Pretpostavimo da je područje Ω omeđeno funkcijama $x = g_1(y)$ i $x = g_2(y)$ između $y = c$ i $y = d$ kao u primjeru na slici 2.

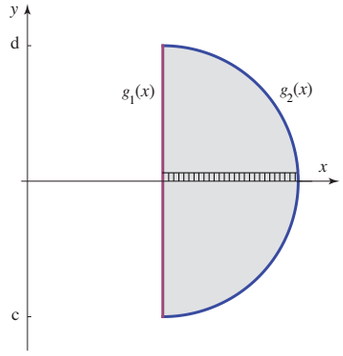

Slika 2: *Područje omeđeno funkcijama $g_1(y)$ i $g_2(y)$ između c i d*

Fiksiramo $y \in [c,d]$ i promotrimo vodoravnu trakicu duž lika Ω visine dy kao na slici 2. Kada trakica rotira oko osi y, dobivamo vodoravni disk približnog obujma $\pi(g_2^2(y) - g_1^2(y))$dy. Zbrajanjem obujama svih diskova za $y \in [c,d]$ dobivamo približni obujam rotacijskog tijela. Prelaskom na limes, kada visina vodoravne trakice teži prema nuli, zbroj postaje integral

$$V(\Omega,y) = \int_c^d \pi(g_2^2(y) - g_1^2(y))\mathrm{d}y,$$

koji predstavlja točnu vrijednost obujma rotacijskog tijela dobivenu metodom diska (detaljnije obrazloženje pogledajte u [1], točka 7.5.2, stranica 318).

3 Obujam kao dvostruki integral

Neka je Ω zatvoreno područje koje se nalazi u ravnini $z = 0$ i ne siječe os y, kao na slici 3.

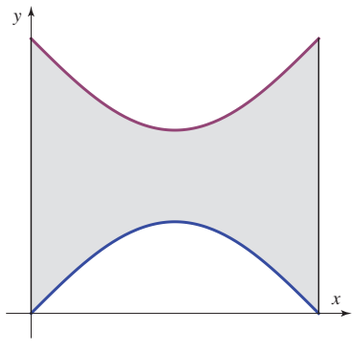

Slika 3: *Zatvoreno područje Ω koje rotiramo oko osi y.*

Kada lik Ω rotiramo oko osi y dobivamo rotacijsko tijelo prikazano na slici 4.

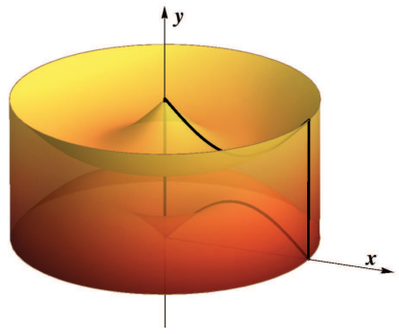

Slika 4: *Rotacijsko tijelo nastalo rotacijom područja Ω sa slike 3.*

Izvedimo formulu za računanje obujma rotacijskog tijela uz pomoć dvostrukog integrala. Za svaku točku $T(x,y) \in \Omega$, promotrimo sitni pravokutnik sa središtem u točki T površine dS. Kada pustimo da pravokutnik rotira oko osi y, dobijemo prstenasti dio rotacijskog valjka obujma $2\pi x\mathrm{d}S$. Zbroj svih takvih prstenastih dijelova daje približnu vrijednost obujma rotacijskog tijela. Ukoliko prijeđemo na limes, kada površina pravokutnika teži prema nuli, dobijemo formulu za obujam rotacijskog tijela pomoću dvostrukog integrala:

$$V(\Omega,y) = \iint_\Omega 2\pi x\mathrm{d}S. \tag{1}$$

Primijetimo da se opisane metode računanja obujma rotacijskog tijela odnose na slučajeve kada os rotacije y ne siječe lik Ω.

Postavlja se pitanje kako odrediti obujam rotacijskog tijela kada os rotacije y siječe lik Ω kao na slici 5.

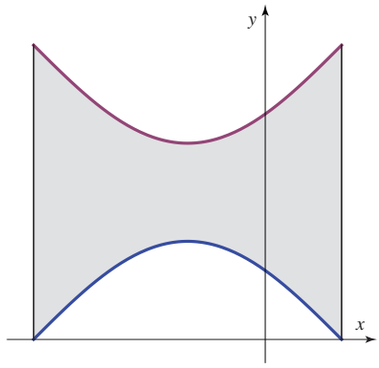

Slika 5: *Os rotacije y siječe područje Ω.*

U tom slučaju potrebno je rotirati lik koji se dobije kao unija dijela područja s desne strane osi y i zrcalne slike područja s lijeve strane osi y kako je prikazano na slici 6.

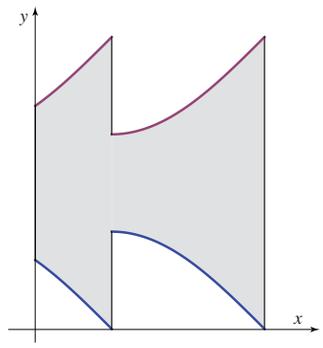

Slika 6: *Unija dijela područja Ω s desne strane osi y i zrcalne slike dijela područja Ω s lijeve strane osi y.*

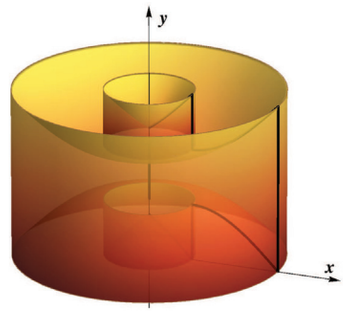

Slika 7: *Rotacijsko tijelo koje nastaje rotacijom područja Ω sa slike 5 oko osi y.*

Primjer koji slijedi pokazuje da prikazani pristup računanja obujma pomoću dvostrukog integrala ima nekih prednosti u odnosu na klasične metode. Naime, prilikom računanja dvostrukog integrala možemo koristiti polarne koordinate u kojima je određivanje integrala u nekim slučajevima jednostavnije nego u Kartezijevim koordinatama.

Neka je Ω područje u ravnini omeđeno jediničnom kružnicom $x^2+y^2=1$ i pravcima $y=\sqrt{3}x$ i $y=-x$ kao na slici 8. Izračunajmo, koristeći integrale, obujam tijela dobivenog rotacijom područja Ω oko osi y.

• Koristeći metodu ljuske dobijemo sljedeću formulu za obujam rotacijskog tijela

$$V(\Omega,y)=\int_0^{\frac{1}{2}}2\pi(\sqrt{3}x+x)\mathrm{d}x+\int_{\frac{1}{2}}^{\frac{\sqrt{2}}{2}}2\pi(\sqrt{1-x^2}+x)\mathrm{d}x$$

$$+\int_{\frac{\sqrt{2}}{2}}^{1}2\pi(2\sqrt{1-x^2})\mathrm{d}x.$$

• Prema metodi diska traženi obujam se računa po formuli

$$V(\Omega,y)=\int_{-\frac{\sqrt{2}}{2}}^{0}\pi(1-y^2-y^2)\mathrm{d}y+\int_0^{\frac{\sqrt{3}}{2}}\pi\left(1-y^2-\frac{y^2}{3}\right)\mathrm{d}y.$$

• Prema formuli (1) obujam rotacijskog tijela možemo izračunati prelaskom na polarne koordinate na sljedeći način

$$V(\Omega,y)=\iint_\Omega 2\pi x\mathrm{d}S=2\pi\int_{-\frac{\pi}{4}}^{\frac{\pi}{3}}\mathrm{d}\phi\int_0^1 r\cdot r\cos\phi\mathrm{d}r$$

$$=2\pi\int_{-\frac{\pi}{4}}^{\frac{\pi}{3}}\cos\phi\mathrm{d}\phi\int_0^1 r^2\mathrm{d}r=2\pi\sin\phi\Big|_{-\frac{\pi}{4}}^{\frac{\pi}{3}}\frac{r^3}{3}\Big|_0^1=\frac{\pi}{3}(\sqrt{3}+\sqrt{2}).$$

Prema tome, obujam rotacijskog tijela se u ovom primjeru izračuna nešto lakše pomoću dvostrukog integrala nego klasičnom metodom ljuske.

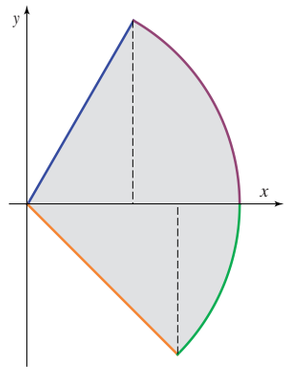

Slika 8: *Područje omeđeno jediničnom kružnicom $x^2+y^2=1$ i pravcima $y=\sqrt{3}x$ i $y=-x$.*

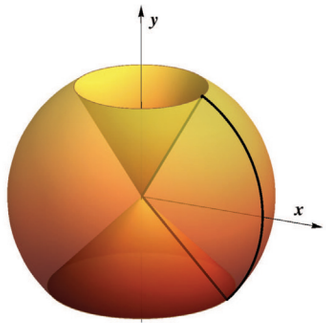

Slika 9: *Rotacijsko tijelo koje nastaje rotacijom područja sa slike 8 oko osi y.*

4 Izvod klasičnih metoda

Sada ćemo pokazati kako možemo dobiti klasične metode diska i ljuske iz formule (1).

Promotrimo najprije područje Ω koje je omeđeno neprekidnim funkcijama $y=f_1(x)$ i $y=f_2(x)$ između $x=a$ i $x=b$ kao u primjeru na slici 1. Prema Fubinijevom teoremu dvostruki integral $I=\iint_\Omega 2\pi x\mathrm{d}S$ možemo izračunati pomoću jednostrukih integrala na sljedeći način

$$I=\int_a^b\left(\int_{f_1(x)}^{f_2(x)}2\pi x\mathrm{d}y\right)\mathrm{d}x=\int_a^b 2\pi x(f_2(x)-f_1(x))\mathrm{d}x,$$

što predstavlja dobro poznatu formulu koja se dobije metodom ljuske.

Pretpostavimo sada da je područje Ω omeđeno funkcijama $x = g_1(y)$ i $x = g_2(y)$ između $y = c$ i $y = d$ kao u primjeru na slici 2. I u ovom slučaju, koristeći Fubinijev teorem, svedemo dvostruki integral I na formulu

$$I = \int_c^d \left(\int_{g_1(y)}^{g_2(y)} 2\pi x \mathrm{d}x \right) \mathrm{d}y = \int_c^d \pi(g_2^2(y) - g_1^2(y)) \mathrm{d}y,$$

koja odgovara metodi diska.

Sada se postavlja pitanje zbog čega su klasične metode za računanje obujma rotacijskog tijela u suštini jednake, iako su na prvi pogled geometrijski posve različite. Odgovor na spomenuto pitanje je vrlo jednostavan. Naime, koristeći formulu $\iint_\Omega 2\pi x \mathrm{d}S$ zapravo zbrajamo obujme prstenastih dijelova rotacijskog valjka dobivene rotiranjem pravokutnika sa središtem u $T(x,y)$ površine dS oko y-osi. Zbrajanje svih obujama možemo provoditi na dva različita načina:

• Odaberemo određeni $x = x_0$. Zbrajanjem obujama prstenastih dijelova rotacijskog valjka koji odgovaraju točkama (x_0, y) za sve y takve da je $(x_0, y) \in \Omega$, dobijemo vertikalnu cilindričnu ljusku. Sada treba samo zbrojiti obujme tih ljusaka da bismo dobili približni obujam rotacijskog tijela. Opisani postupak zapravo predstavlja metodu ljuske.

• Neka je $y = y_0$ fiksan. Zbroj obujama prstenastih dijelova rotacijskog valjka koji odgovaraju točkama (x, y_0) za sve x takve da je $(x, y_0) \in \Omega$ predstavlja vodoravni disk. Sada zbrojimo obujme svih takvih diskova da bismo dobili približni obujam rotacijskog tijela. Opisani postupak nije ništa drugo nego metoda diska.

Dakle, dvije klasične metode slijede iz dvostrukog integrala tako da se prstenasti dijelovi rotacijskog valjka, čiji obujmi se zbrajaju, pažljivo poslože na odgovarajući način.

5 Guldin-Pappusov poučak

Promotrimo zatvoreno područje Ω u ravnini $z = 0$ koje ne siječe os y kao na slici 3. Označimo sa C težište područja Ω, a s $\mathcal{D}$ površinu od Ω. Uz navedene oznake, Guldin-Pappusov poučak u klasičnom obliku kaže da je obujam rotacijskog tijela dobivenog rotacijom područja Ω oko osi y dan formulom:

$$V(\Omega, y) = 2\pi x_C \mathcal{D},$$

gdje je x_C apscisa težišta C područja Ω. Drugim riječima, obujam torusa koji se dobije rotacijom područja Ω oko osi y je jednak obujmu cilindra osnovice Ω i visine $2\pi x_C$.

Izvedimo sada Guldin-Pappusov poučak koristeći dvostruki integral za računanje obujma rotacijskog tijela. Prisjetimo se da se koordinate težista $C(x_C, y_C)$ lika Ω površine $\mathcal{D}$ računaju prema formulama

$$x_C = \frac{\iint_\Omega x \mathrm{d}S}{\mathcal{D}}, \quad y_C = \frac{\iint_\Omega y \mathrm{d}S}{\mathcal{D}}.$$

Sada iz formule (1) slijedi:

$$V(\Omega, y) = \iint_\Omega 2\pi x \mathrm{d}S = 2\pi \iint_\Omega x \mathrm{d}S = 2\pi x_C \mathcal{D},$$

pri čemu smo koristili linearnost integrala i definiciju težišta.

6 Zaključak

Metoda određivanja obujma rotacijskog tijela pomoću dvostrukog integrala je zanimljiva ne samo s matematičkog, nego i sa stanovišta metodike nastave. Ponovimo neke od prednosti opisane metode:

- Metoda predstavlja poopćenje metode diska, metode ljuske i Guldin-Pappusovog poučka. Svi navedeni rezultati slijede neposredno iz formule (1).
- Primjena tehnika računanja dvostrukog integrala, kao što je prelazak na polarne koordinate, u nekim slučajevima pojednostavljuje postupak računanja.
- Odabir klasične metode za računanje obujma rotacijskog tijela ovisi o obliku tijela. Za primjenu metode određivanja obujma pomoću dvostrukog integrala oblik tijela nije bitan.

Literatura

[1] T. DOŠLIĆ, N. SANDRIĆ, *Matematika I*, interna skripta Građevinskog fakulteta Sveučilišta u Zagrebu

[2] P. JAVOR, *Matematička analiza 1*, Element, Zagreb, 2001.

[3] P. JAVOR, *Matematička analiza 2*, Element, Zagreb, 2002.

[4] J. MARTÍN-MORALES, A. M. OLLER-MARCÉN, Volumes of Solids of Revolution. A Unified Approach, arXiv:1205.2204v1 [math.HO] 10 May 2012

Tatjana Slijepčević-Manger
e-mail: tmanger@grad.hr

Građevinski fakultet, Sveučilište u Zagrebu
Fra Andrije Kačića-Miošića 26, 10000 Zagreb

How to get KoG?

The easiest way to get your copy of KoG is by contacting the editor's office:

Marija Šimić Horvath
marija.simic@arhitekt.hr
Faculty of Architecture
Kačićeva 26, 10 000 Zagreb, Croatia
Tel: (+385 1) 4639 176
Fax: (+385 1) 4639 465

The price of the issue is €15 + mailing expenses €5 for European countries and €10 for other parts of the world.

The amount is payable to:

ACCOUNT NAME:	Hrvatsko društvo za geometriju i grafiku Kačićeva 26, 10000 Zagreb, Croatia
IBAN:	HR862360000-1101517436

Kako nabaviti KoG?

KoG je najbolje nabaviti u uredništvu časopisa:

Marija Šimić Horvath
marija.simic@arhitekt.hr
Arhitektonski fakultet
Kačićeva 26, 10 000 Zagreb
Tel: (01) 4639 176
Fax: (01) 4639 465

Za Hrvatsku je cijena primjerka 100 KN + 10 KN za poštarinu.

Nakon uplate za:

HDGG (za KoG), Kačićeva 26, 10000 Zagreb
žiro račun broj **2360000-1101517436**

poslat ćemo časopis na Vašu adresu.

Ako Vas zanima tematika časopisa i rad našeg društva, preporučamo Vam da postanete članom HDGG-a (godišnja članarina iznosi 150 KN). Za članove društva časopis je besplatan.

INSTRUCTIONS FOR AUTHORS

SCOPE. "KoG" publishes scientific and professional papers from the fields of geometry, applied geometry and computer graphics.

SUBMISSION. Scientific papers submitted to this journal should be written in English or German, professional papers should be written in Croatian, English or German. The papers have not been published or submitted for publication elsewere.
The manuscript with wide margines and double spaced should be sent in PDF format via e-mail to one of the editors:

Sonja Gorjanc	Ema Jurkin
sgorjanc@grad.hr	ema.jurkin@rgn.hr

The first page should contain the article title, author and coauthor names, affiliation, a short abstract in English, a list of keywords and the Mathematical subject classification.

UPON ACCEPTANCE. After the manuscript has been accepted for publication authors are requested to send its LaTex file via e-mail to the address:

sgorjanc@grad.hr

Figures should be included in EPS or PS formats.

OFFPRINTS. The corresponding author and coauthors will recieve hard copies of the issue free of charge and a PDF file of the article via e-mail.

UPUTE ZA AUTORE

PODRUČJE. "KoG" objavljuje znanstvene i stručne radove iz područja geometrije, primijenjene geometrije i računalne grafike.

UPUTSTVA ZA PREDAJU RADA. Znanstveni radovi trebalju biti napisani na engleskom ili njemačkom jeziku, a stručni na hrvatskom, engleskom ili njemačkom. Rad ne smije biti objavljen niti predan na recenziju u drugim časopisima.
Rukopis sa širokim marginama i dvostrukim proredom šalje se u PDF formatu elektronskom poštom na adresu jedne od urednica:

Sonja Gorjanc	Ema Jurkin
sgorjanc@grad.hr	ema.jurkin@rgn.hr

Prva stranica treba sadržavati naslov rada, imena autora i koautora, podatke o autoru i koautorima, sažetak na hrvatskom i engleskom, ključne riječi i MSC broj.

PO PRIHVAĆANJU RADA. Tekst prihvaćenog rada autor dostavlja elektronskom poštom kao LaTeX datoteku, a slike u EPS ili PS formatu na adresu:

sgorjanc@grad.hr

POSEBNI OTISCI. Svaki autor i koautor dobiva po jedan primjerak časopisa i PDF datoteku svog članka.

ISSN 1331-1611